

THESIS
GEOLOGY, MINERALIZATION, AND FLUID INCLUSION ANALYSIS
OF THE AJAX VEIN SYSTEM, CRIPPLE CREEK, COLORADO

Submitted by
Peter C. Dwelley
Earth Resources

In partial fulfillment of the requirements
for the Degree of Master of Science
Colorado State University
Fort Collins, Colorado
Fall 1984

ABSTRACT OF THESIS

GEOLOGY, MINERALIZATION, AND FLUID INCLUSION ANALYSIS
OF THE AJAX VEIN SYSTEM, CRIPPLE CREEK, COLORADO

The Ajax mine is located in the Cripple Creek mining district, Teller County, Colorado. Mine workings extend through a vertical range of 3363 feet (1025 m), from 10,105 feet (3081 m) to 6742 feet (2055 m) elevation. Production is from gold-telluride veins hosted in Precambrian granite and Tertiary breccia. Mine production amounts to more than 700,000 oz. of gold at average grades of 0.60 to 1.00 oz. gold per ton. The mine is situated on the southern margin of a Tertiary volcanic complex composed of highly differentiated alkaline rocks that intrude fine-grained breccia and minor sediment. Most of the mineralization in the Ajax is hosted by Precambrian granite which surrounds the complex. Complex formation began about 34 m.y. ago.

Five stages of vein mineralization have been recognized. Vein content is dependent on the relative time at which the structure was receptive to ore-forming fluids. Vein minerals, in order of decreasing volume, consist of quartz, fluorite, pyrite, adularia, dolomite, rutile, sphalerite, hematite, galena, marcasite, calaverite, chalcopyrite, pyrrhotite, and acanthite. The Au/Ag ratio varies from 20:1 to 1:1 and is controlled by grade; higher Au/Ag ratios correspond to greater gold values. No consistent vertical trend in Au/Ag ratio has been

recognized. A subtle increase in base metal content with depth may reflect initial development of a weak zonation pattern.

Vein-related alteration is fracture controlled and poorly developed. Two lateral zones of alteration were defined. Inner zone alteration varies from one to three times vein width and consists of the following: complete replacement of biotite and plagioclase, quartz recrystallization, and microcline rimmed and veined by adularia. Outer-zone alteration varies from two to five times vein width and consists of partial replacement of biotite and plagioclase, unaltered quartz, and mostly unaltered microcline that may be weakly veined by adularia and quartz.

Fluid inclusion analyses of quartz, fluorite, and sphalerite from stages 1 through 4 define a complex fluid evolution. Filling temperatures ranged from 206 to 510°C during stage 1 mineralization and from 123 to 350°C during stage 3. Stage 4 fluid deposited calaverite and quartz at temperatures ranging from 105 to 159°C. Salinity of the ore fluid ranged from 30 to 47 wt% eNaCl during stage 1 and decreased to between 0 and 8.3 wt% eNaCl during stage 3. Stage 4 fluid salinity was approximately equal to stage 3. Initial temperature and salinity decrease was caused by mixing of stage 1 magmatic fluid with meteoric water. Additional temperature decrease resulted from cooling of the magmatic heat source(s). The irregular vertical thermal gradient present in the vein system may be the result of lateral fluid flow caused by intersection of veins with the breccia complex and/or presence of intrusive heat sources within the breccia.

CO₂ has been recognized in the fluids of stages 1, 3, and 4. Subtle boiling occurred in all stages over a great vertical range,

consisting primarily of CO₂ effervescence. The presence of CO₂ greatly increases the estimated maximum depth at which boiling can occur.

Based on stability of alteration minerals, pH is estimated to have a minimum value of 5.5 at 300°C. Opaque mineral relationships indicate oxygen fugacity ranged from -36 to -28.4 log f_{O₂}. The physical-chemical character of the ore fluid indicates the most amenable gold transport mechanism. Base metals and gold were originally transported as chloride complexes. Decreasing salinity lowered chlorine ion activity which, in conjunction with temperature decrease, decomposed the chloride complexes. Gold remained in solution by forming migration complexes with tellurium. Sulfide deposition increased the H₂Te:H₂S ratio, causing greater gold-tellurium complex stability. Gold remained in solution until decreasing temperature in stage 4 deposited calaverite and quartz.

Character of the ore-forming fluid and close relationship of the veins to intrusive activity, among other evidence, indicate a magmatic source for the ore metals.

Peter Campbell Dwelley
Department of Earth Resources
Colorado State University
Fort Collins, Colorado 80523
Spring, 1984

ACKNOWLEDGEMENTS

It is a pleasure to acknowledge the assistance and time provided by the staff of Texasgulf Metals Co. including Charles Brechtel, Alex Paul, Charles Matteson and Steve Peters.

Recent financial assistance provided by Lou Knight of Hecla Mining Corp. is greatly appreciated.

Identification of opaque minerals was facilitated by discussions with Ben Leonard of the U.S. Geological Survey who provided patient guidance and laboratory facilities. Thanks are also due Ralph Christian of the U.S.G.S. who provided electron microprobe analyses.

Sincerest thanks are extended to Doctor Tommy B. Thompson for his continuing interest and great patience. The writer also appreciates the help provided by Doctor Malcolm E. McCallum and Doctor John Vaughan.

This paper has benefited from the helpful discussions and criticisms provided by my fellow graduate students in the Earth Resources department.

Finally, utmost gratitude is extended to my parents whose continuing encouragement and support were greatly appreciated.

TABLE OF CONTENTS

| | |
|--|-------------|
| ABSTRACT | iii |
| ACKNOWLEDGEMENTS | vi |
| <u>Chapter</u> | <u>Page</u> |
| I. INTRODUCTION | 1 |
| A. Purpose | 1 |
| B. Location and Geography | 1 |
| C. History | 4 |
| D. Methods | 5 |
| E. Previous Work | 7 |
| II. REGIONAL GEOLOGY | 9 |
| A. Introduction | 9 |
| B. Pre-Tertiary Rocks | 12 |
| C. Tertiary Rocks | 13 |
| 1. Breccia | 13 |
| 2. Volcanic and plutonic rocks | 14 |
| 3. Basaltic breccia | 14 |
| D. Structural Geology | 15 |
| 1. Regional tectonics | 15 |
| 2. District structural geology | 15 |
| E. District Mineralization | 20 |
| III. AJAX MINE GEOLOGY | 21 |
| A. General | 21 |
| B. Rock Types | 21 |
| 1. Ajax granite | 21 |
| 2. Phonolite dikes | 22 |

Table of Contents (cont')

| <u>Chapter</u> | <u>Page</u> |
|---|-------------|
| 3. Basalt dikes | 22 |
| 4. Breccia | 23 |
| C. Structural Geology | 23 |
| 1. General | 23 |
| 2. North-south veins | 47 |
| 3. North-northwest veins | 54 |
| 4. West-northwest veins | 57 |
| IV. VEIN MINERALOGY AND PARAGENESIS | 63 |
| A. General | 63 |
| B. Paragenesis and Mineralogy | 66 |
| 1. Stage 1 | 66 |
| 2. Stage 2 | 66 |
| 3. Stage 3 | 69 |
| 4. Stage 4 | 78 |
| 5. Stage 5 | 83 |
| C. Vein Morphology | 83 |
| 1. Bobtail vein | 83 |
| 2. Newmarket vein | 88 |
| 3. Other veins | 91 |
| D. Vertical Metal Zonation | 91 |
| V. VEIN-RELATED ALTERATION | 99 |
| A. Introduction | 99 |
| B. Lateral Zonation | 104 |
| 1. Inner zone | 104 |
| 2. Outer zone | 108 |
| 3. Deuteric zone | 108 |
| C. Alteration of Phonolite and Basalt Dikes | 108 |
| D. Chemical Changes | 111 |
| E. Alteration Controls | 111 |
| 1. Bobtail vein | 113 |
| 2. Newmarket vein | 114 |
| 3. Breccia | 115 |

Table of Contents (cont')

| <u>Chapter</u> | <u>Page</u> |
|---|-------------|
| VI. FLUID INCLUSION ANALYSIS | 116 |
| A. Introduction and Methods | 116 |
| B. General Characteristics | 117 |
| C. Fluid Temperature | 125 |
| 1. Stage 1 | 125 |
| 2. Stage 2 | 126 |
| 3. Stage 3 | 126 |
| 4. Stage 4 | 131 |
| D. Fluid Salinity | 131 |
| 1. CO ₂ effect | 131 |
| 2. Stage 1 | 132 |
| 3. Stages 3 and 4 | 134 |
| E. Additional Fluid Parameters | 135 |
| 1. Fluid density | 135 |
| 2. Trapping pressure | 136 |
| 3. CO ₂ content | 137 |
| 4. Boiling level | 138 |
| a. Evidence for boiling | 138 |
| b. Boiling depth | 139 |
| F. Ajax Fluid Evolution | 140 |
| VII. CONTROLS ON ORE DEPOSITION | 146 |
| A. Introduction | 146 |
| B. Structural Control | 146 |
| C. Gold Transport | 148 |
| 1. pH | 149 |
| 2. Temperature and pressure | 151 |
| 3. Salinity | 151 |
| 4. Oxygen fugacity | 152 |
| 5. Mechanism of gold transport | 152 |
| VIII. SUMMARY AND CONCLUSIONS | 155 |
| A. General Summary | 155 |
| B. Metal Source | 159 |

Table of Contents (cont')

| <u>Chapter</u> | <u>Page</u> |
|--|-------------|
| C. Recommendations for Exploration | 160 |
| D. Recommended Reading | 161 |
| REFERENCES | 162 |

LIST OF FIGURES

| <u>Figure</u> | <u>Page</u> |
|---|-------------|
| 1. Location map, Cripple Creek | 3 |
| 2. Geologic map, Cripple Creek complex | 11 |
| 3. Map showing Rio Grande rift-related faults in Colorado | 16 |
| 4. Plan map, Ajax mine, 400 level | 25 |
| 5. Plan map, Ajax mine, 700 level | 27 |
| 6. Plan map, Ajax mine, 1000 level | 29 |
| 7. Plan map, Ajax mine, 1400 level | 31 |
| 8. Plan map, Ajax mine, 1600 level | 33 |
| 9. Plan map, Ajax mine, 2000 level | 35 |
| 10. Plan map, Ajax mine, 2300 level | 37 |
| 11. Plan map, Ajax mine, 2600 level | 39 |
| 12. Plan map, Ajax mine, 3000 level | 41 |
| 13. Plan map, Ajax mine, 3100 level | 43 |
| 14. Plan map, Ajax mine, 3350 level | 45 |
| 15. Cross section, Bobtail vein | 49 |
| 16. Cross section, Newmarket vein | 51 |
| 17. Schematic drawing, Newmarket and Breccia-hosted veins | 53 |
| 18. Long section, Newmarket vein | 56 |
| 19. Schematic drawing, Bobtail vein | 59 |
| 20. Long section, Bobtail vein | 62 |
| 21. Paragenetic diagram, Ajax mineralization | 65 |
| 22. A. Photograph of Bobtail vein, hand specimen | |

List of Figures (cont')

| <u>Figure</u> | <u>Page</u> |
|--|-------------|
| B. Photomicrograph, thin-section from Bobtail vein showing first and fourth stage mineralization | 68 |
| 23. A. Photomicrograph, polished-section from Bobtail vein showing pyrrhotite-chalcopyrite inclusion in pyrite | |
| B. Photomicrograph, polished-section from Newmarket vein showing magnetite partially replaced by quartz and late replacement of both by pyrite-marcasite | 71 |
| 24. A. Photomicrograph, polished-section from Bobtail vein showing partial replacement of pyrite by sphalerite and galena | |
| B. Photomicrograph, polished-section from 1000 level vein showing partial replacement of sphalerite by galena | 73 |
| 25. A. Photomicrograph, thin-section from Bobtail vein showing stage 2 and 3 mineralization | |
| B. Photograph of Bobtail vein, hand specimen, showing stage 3 quartz-fluorite | 75 |
| 26. A. Photomicrograph, polished-section from Bobtail vein showing specular hematite inclusions in pyrite | |
| B. Photomicrograph, polished-section from Christensen vein showing rutile overgrowths on pyrite | 77 |
| 27. A. Photomicrograph, polished-section from Bobtail vein showing stage 4 calaverite | |
| B. Photomicrograph, polished-section from Newmarket vein showing calaverite replacing earlier pyrite | 80 |
| 28. A. Photomicrograph, polished-section from Bobtail vein showing gold-tellurite rim on calaverite | |
| B. Photomicrograph, polished-section from Bobtail vein showing multiple stage pyrite | 82 |
| 29. A. Photograph of Bobtail vein, hand specimen, showing stage 5 euhedral dolomite | |
| B. Photograph of Bobtail vein, same as above, cut slab, showing roscoelite alteration of granite overgrown by minerals of stages 1, 4, and 5 | 85 |
| 30. A. Photograph of Bobtail vein, hand specimen, showing phonolite-hosted stage 3 mineralization | |
| B. Photograph of Bobtail vein, hand specimen, showing multiple repetition of stage 3 mineralization | 87 |
| 31. A. Photograph of Newmarket vein, hand specimen, showing stage 4 quartz and characteristic weak alteration | |
| B. Photograph of Newmarket vein, hand specimen, showing "bughole" granite | 90 |

List of Figures (cont')

| <u>Figure</u> | <u>Page</u> |
|---|-------------|
| 32. A. Photograph of Mohican vein, hand specimen, showing stage 3 quartz-fluorite and weak alteration | |
| B. Photograph of breccia-hosted mineralization, hand specimen, showing intense alteration and stage 3 fluorite | 96 |
| 33. Diagram showing vein-related alteration | 101 |
| 34. A. Photomicrograph, thin-section from Bobtail vein, showing biotite pseudomorphically replaced by dolomite, secondary orthoclase, roscoelite-sericite, pyrite | |
| B. Photomicrograph, thin-section from Bobtail vein, showing inner zone alteration | 103 |
| 35. A. Photomicrograph, thin-section from Bobtail vein, showing inner zone alteration | |
| B. Photomicrograph, thin-section from X-10-U-8 vein, showing outer zone alteration | 106 |
| 36. A. Photomicrograph, thin-section from Bobtail vein (phonolite-hosted), showing alteration of phonolite | |
| B. Photomicrograph, thin-section from Newmarket vein, showing stage 1 veinlet and weak alteration | 110 |
| 37. A. Photomicrograph, doubly polished plate from Bobtail vein, showing stage 1 fluid inclusions with halite daughter minerals | |
| B. Photomicrograph, doubly polished plate from Mohican vein, showing stage 1 fluid inclusions with halite, hematite, and sylvite(?) daughter minerals. | 122 |
| 38. A. Photomicrograph, doubly polished plate from Bobtail vein, showing stage 3 fluid inclusion with double meniscus (CO ₂) | |
| B. Photomicrograph, doubly polished plate from Bobtail vein, showing stage 4 fluid inclusion | 124 |
| 39. Fluid inclusion homogenization temperature range diagram for Ajax vein system | 128 |
| 40. A. Photomicrograph, doubly polished plate from Mohican vein, showing CO ₂ double meniscus and variable liquid to vapor ratios | |
| B. Photomicrograph, doubly polished plate from Christensen vein, showing vapor-dominated fluid inclusion beside liquid-dominated inclusion | 130 |
| 41. Plot of mean and minimum homogenization temperatures for Ajax vein system | 144 |

CHAPTER I

INTRODUCTION

A. Purpose

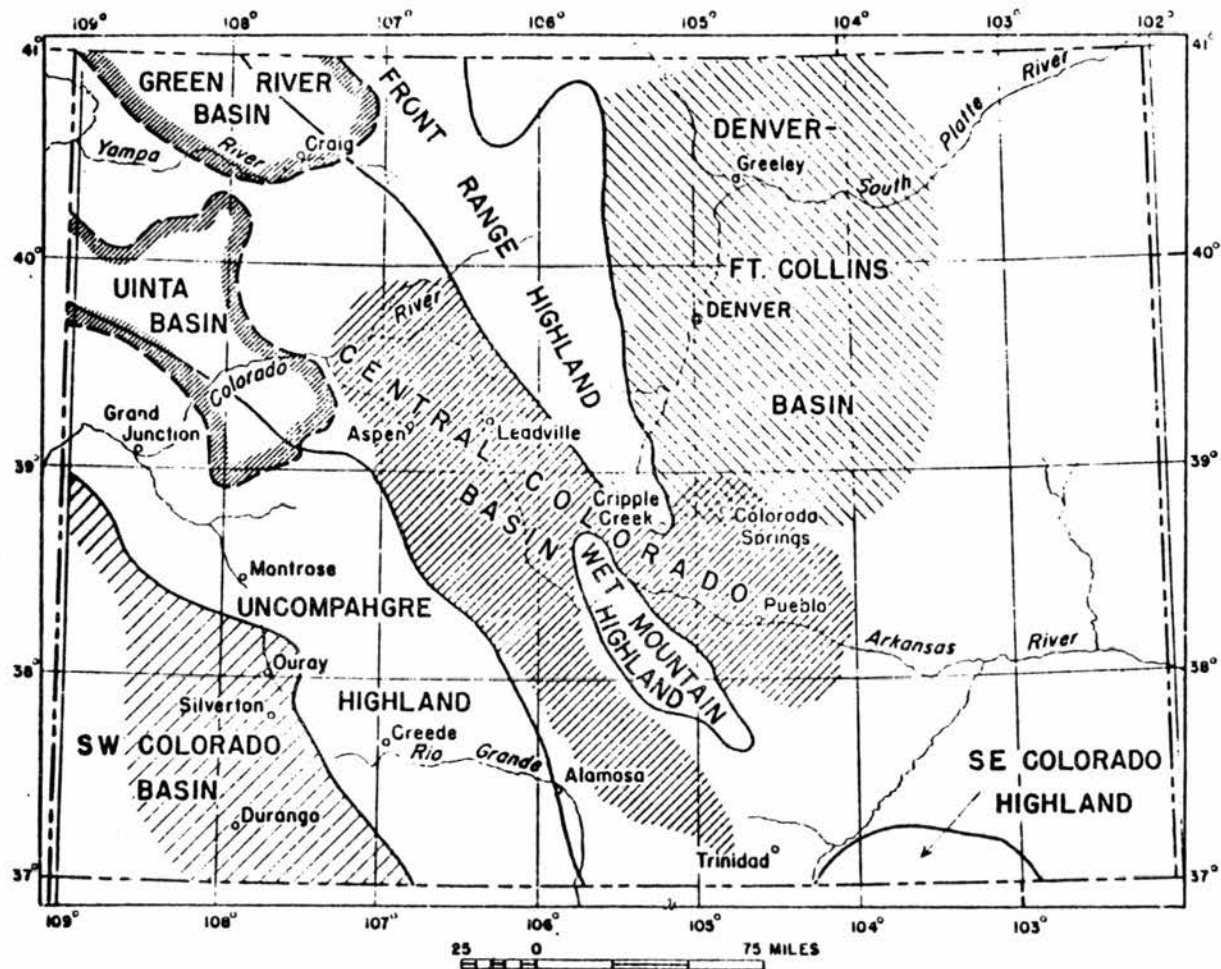
The purpose of this thesis project was to examine in detail the nature of the ore-forming system responsible for the unique and prolific mineralization of the Ajax vein system. The vein system is exposed over a vertical distance of 3363 feet (1025 m) providing an ideal opportunity to study the effect of depth on ore fluid composition and temperature, ore and gangue mineralogy, and wall-rock alteration. Additional aspects of the study include an attempt to explain the great vertical extent of mineralization, and the apparent lack of vertical zonation of both the alteration and ore mineral assemblages.

The depth extent and possible limits of mineralization are important factors influencing future economic potential of the Cripple Creek district. This thesis will attempt to elucidate these factors.

B. Location and Geography

The Cripple Creek district encompasses approximately 15 sq mi (39 sq km) and is located 21 mi (34 km) southwest of Colorado Springs, in south-central Teller County, Colorado (Fig. 1). The district is approximately 10 mi (16 km) southwest of Pikes Peak near the southern border of the Front Range, and is topographically characterized by rounded hills of moderate relief. Elevations in the district range from 9000 ft (2744 m) to 10,800 ft (3293 m). In general, the district is

Figure 1. Location map of Cripple Creek showing relationship to major tectonic features of Colorado (from Epis and Chapin, 1964).



sparsely vegetated with various range grasses and aspen trees. Spruce and aspen trees are the dominant vegetation types at higher elevations and generally are confined to north-facing slopes. Climate in the area is semi-arid; the summer months are characterized by afternoon thunderstorms. The winter months are unusually mild for the elevation and a permanent snowpack is only rarely developed, although erratic heavy snowstorms do occur. The town of Cripple Creek lies on the western edge of the district at an elevation of 9500 ft (2896 m); and the town of Victor is situated near the southern edge of the district at an elevation of 9750 ft (2973 m).

The Ajax mine is located just north of Victor and has a shaft collar elevation of 10,105 ft (3081 m).

C. Mining History

Excellent historical reviews of the Cripple Creek district with details on district discovery and individual mine production have been published (Cross and Penrose, 1895, Lindgren and Ransome, 1906, Loughlin and Koschmann, 1935).

The district as a whole has produced in excess of 19 million ounces of gold. 18,572,899 ounces were extracted during the period from 1891 to 1946. In excess of 450,000 ounces were mined during the period from 1946 to 1983 with most of the production coming from the Ajax mine.

Mining operations at the Ajax began in 1895 and, from 1895 to 1921, 247,917 ounces of gold were produced (Henderson, 1926). No production data are available for 1922, 1923, 1933, and 1934. From 1924 to 1932, 101,765 tons were mined at an average grade of 1.04 oz Au/ton or a total of 105,784 ounces of gold (Loughlin and Koschmann, 1935). From 1935 to 1961, 360,000 ounces of gold at an average grade of 0.60 oz Au/ton were

extracted. During this period the Ajax mine was the largest producer in the district and, from 1952 to 1960, it was the leading gold producer in the state (Minerals Yearbook, 1934-1961). In summary, from 1895 to 1961, the Ajax produced in excess of 700,000 ounces of gold at grades ranging from 0.60 to 1.04 oz Au/ton with an approximate average grade of 0.80 oz Au/ton. The Ajax closed in 1961 and remained inoperative until 1972. At that time Golden Cycle Corporation, former operators of the Ajax, spurred by the increase in the price of gold (58.60 dollars/oz), announced plans to renovate the mine. In 1975 after gold reached 161.50 dollars/oz, Golden Cycle formed a partnership with Texasgulf Metals Corp.. The partnership announced plans to rehabilitate the Ajax and re-evaluate a large part of the district. Texasgulf withdrew from the partnership in 1979, but rejoined following the dramatic increase in gold prices later in 1979 (Minerals Yearbook, 1961-1979). The mine was operated on a restricted basis by Texasgulf until September, 1983 at which time Hecla Mining Corp. bought out the Texasgulf interest in the partnership.

D. Methods

Field work for this thesis was carried out during the summer of 1982 and consisted of sampling and large-scale cross sectional mapping of veins on 12 different levels of the Ajax mine. The levels sampled are: 400, 700, 1000, 1400, 1600, 2000, 2300, 2600, 2800, 3000, 3100, and 3350. Two of the largest and most consistent veins, the Bobtail and the Newmarket, were chosen as representatives of the Ajax system. The Bobtail was sampled from the 3350 level to the 2000 level; and the Newmarket was sampled from the 3100 level to the 2000 level. Above the 2000 level, access to the Newmarket was restricted by caved ground; and

the dip of the Bobtail is such that it is no longer enclosed within the Ajax workings. Veins sampled above the 2000 level were the Apex, Christensen, Mohican, and several unnamed veins. Underground sampling was hampered by inaccessibility of the workings, intense iron-oxide staining of the rock walls, and the extremely resistant and unaltered nature of the veins.

Literature research consisted of compiling a series of plan maps of the Ajax mine and locating the few and relatively obscure references on Cripple Creek.

Laboratory work involved an in-depth study of the underground samples and consisted of fluid inclusion analysis, petrographic and X-ray diffraction analysis, ore microscopy and electron microprobe analysis, and preparation of samples for geochemical analysis.

Fluid inclusions were analyzed using a heating-freezing stage and involved measurement of the temperatures of homogenization, freezing, clathrate melting, and NaCl dissolution. Prior to heating-freezing stage analysis, a visual study of the fluid inclusions was carried out to determine their general nature.

Thin section and X-ray diffraction analyses were used to identify and characterize the vein-related alteration assemblages and the gangue minerals.

Ore microscopy and follow up electron microprobe analyses were performed to identify and characterize the opaque minerals present in the vein system.

The vein and wallrock samples were halved and analyzed for Au, Ag, Cd, Co, Cu, Mo, Ni, Pb, Te, V, and Zn by Texasgulf Metals Corp. laboratory at the Carlton mill.

E. Previous Work

Cross and Penrose (1895) conducted the initial geologic survey of the Cripple Creek district and were the first to publish a geologic map of the district. They believed the complex to be a product of explosive volcanic activity. Upon request of the mine owners, Lindgren and Ransome (1906) resurveyed the district in 1903, further delineating the petrology and structure of the district and remapping the area in detail. Loughlin (1927) studied the deeper vein systems of the district and noted an apparent lack of vertical zonation of the ore minerals. In 1933 Koschmann and Loughlin (1935) examined the district to determine depth potential of the mineralization and the best location for a deep drainage tunnel. They were the first to report the presence of stratified "sedimentary" rocks within the complex. Based on the presence of stratified sediments exposed in the newer workings, Koschmann (1949) proposed that the complex had been formed as a result of intermittent subsidence and the bulk of the volcanic breccia was waterlain. A detailed structural analysis by Koschmann (1949) indicates that the vein systems are related to major structural features of the basin floor and walls. Since 1949, no regional geologic work has been done in the district. Lovering and Goddard (1950) re-evaluated early literature and concluded that the Cripple Creek complex was the result of both explosive volcanic activity and subsidence. They were the first to use the term "caldera" in reference to the complex. The regional geochemical trends have been defined by Gott, McCarthy Jr., Van Sickle, and McHugh (1969). They identified northwest-trending Au-Ag-Te anomalies and regarded them as potentially favorable zones for large

tonnage, low grade gold deposits. They also examined the major element and trace element changes in response to hydrothermal alteration. The regional geophysical characteristics of the Cripple Creek complex have been indentified by Kleinkopf, Peterson, and Gott (1970). They recognized two gravity and magnetic lows, one directly over the complex and a similar feature immediately east of the complex. The only recent geologic study in the Cripple Creek area is a M.Sc. thesis by Lane (1976) on the El Paso mine, in which fluid inclusion homogenization temperatures are reported from vein fluorite and barite. Lane (1976) also performed the first detailed ore mineral study of a Cripple Creek vein system.

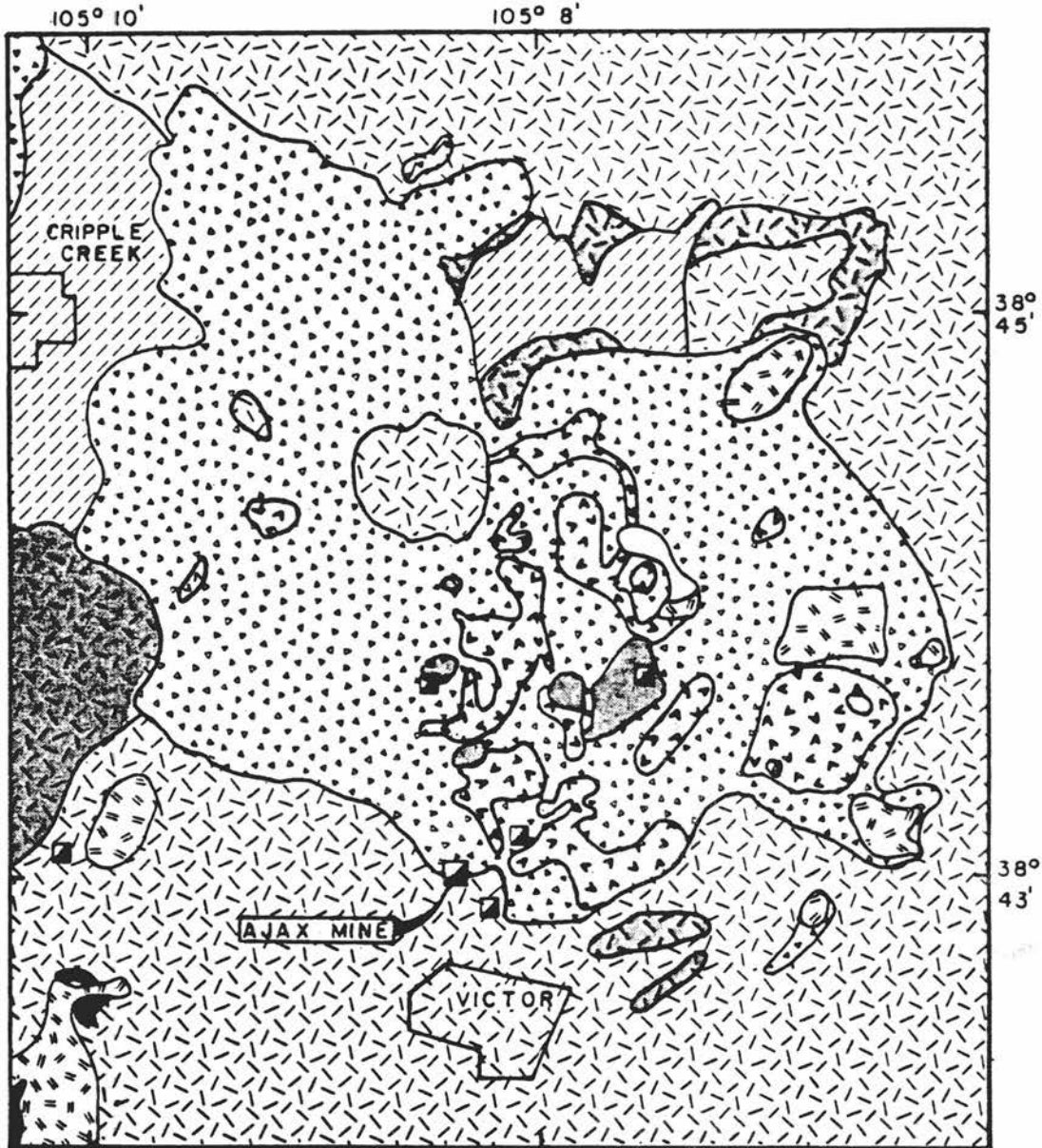
CHAPTER II
REGIONAL GEOLOGY

A. Introduction

This chapter is intended to provide the reader with a general overview of the district geology and to elucidate more recent data. For detailed descriptions of the regional geology, the reader is referred to earlier literature: Cross and Penrose (1895), Lindgren and Ransome (1906), and Loughlin and Koschmann (1935). It is apparent to this writer, in light of recent mining activity, that a re-evaluation of areas currently identified as breccia and stratified sediment is necessary to fully comprehend the processes responsible for formation of the Cripple Creek complex.

The Cripple Creek district is located on the boundary between the Front Range highland (Fig. 1) and the Central Colorado basin. The volcanic complex (Fig. 2) consists of a sequence of Tertiary intrusions, flows, and breccias, filling an elliptical-shaped crater approximately 4 mi (6.4 km) long and 2 mi (3.2 km) wide. Granitic and schistose rocks of Precambrian age surround the crater. Numerous dikes and small stocks of Tertiary age intrude the surrounding granite and schist and are genetically related to Tertiary rocks of the central complex. Graton (1905) first postulated that the Tertiary rock units were differentiation products of a single parent magma based on their constant silica to alumina ratio. A small phonolite stock to the west

Figure 2. Geologic map of Cripple Creek complex. Note location of Ajax mine on the southern margin of the complex (modified from Koschmann, 1949).














GEOLOGIC MAP OF THE CRIPPLE CREEK COMPLEX

0 4000 8000 Feet

Scale 1: 48000

EXPLANATION

| | | | | | |
|---|---------------------|---|-----------------------|---|---------------|
|  | Basalt breccia |  | Breccia |  | Mine Shaft |
|  | Trachydolerite sill |  | Rhyolite | | |
|  | Phonolite |  | Pikes Peak Granite | } TERTIARY | } PRECAMBRIAN |
|  | Syenite |  | Cripple Creek Granite | | |
|  | Latite-phonolite |  | Gneiss and schist | | |

of the complex has been dated at 27.9-29.3 million years (Obradovich, 1973). The syenite intrusive near the center of the complex has an age of 33.4-33.8 million years (McDowell, 1971).

B. Pre-Tertiary Rocks

Precambrian rocks present in the Cripple Creek district consist of three distinct units into which the Tertiary sequence has been intruded. The Idaho Springs Formation is comprised of an interlayered quartz-biotite-feldspar gneiss and quartz-sillimanite schist, cropping out to the north and west of the complex. Pikes Peak Granite is the predominant Precambrian rock present in the area. It is a typical coarse-grained granite consisting of pink microcline, orthoclase, quartz, plagioclase, and biotite. The granite surrounds the complex on the north, east, and south, and is part of the Pikes Peak batholith. Locally, the granite has a gneissic texture which becomes more prevalent along contacts with the gneiss-schist. Pegmatitic and aplitic dike phases are common within the granite and generally have a composition similar to their host rock. Cripple Creek Granite is medium grained and slightly porphyritic in nature. Similar in appearance to the Pikes Peak variety, it is generally darker and finer grained. Variations of the two can be indistinguishable. Cripple Creek Granite is correlated with the Silver Plume granite (Lovering and Goddard, 1950); it crops out to the west of the complex and as an isolated island within the complex. No major Paleozoic or Mesozoic rock units have been recognized within the Cripple Creek district.

C. Tertiary Rocks

1. Cripple Creek breccia

The term "breccia" has been the subject of much misinterpretation and is one aspect of the district geology in need of redefinition. Breccia is volumetrically the most abundant rock within the complex. In general, the term "breccia" implies a fragmental rock composed of latite-phonolite, phonolite, and lesser amounts of granite and syenite, all of which have been altered by hypogene and supergene processes. The breccia matrix is composed of dolomitic carbonate, varying amounts of pyrite, and rock flour. The structure of the breccia is extremely variable, ranging from well stratified, coarse to fine grained material on the eastern side of the complex to the fragmental, angular, and unsorted material of the Globe Hill area. Fluidized channelways have been recognized in association with hydrothermal breccias of the Ironclad mine south of Globe Hill (oral communication, Thompson, T. B., 1982). Carbonized tree fragments have been identified from several locations in the breccia at depths greater than 800 ft (244 m) (Lindgren and Ransome, 1906). Rickard (1900) reported the presence of a silicified tree stump on the 500 level of the Independence mine. The presence of mud cracks, raindrop impressions, cross bedding, and fossil bird tracks within the breccia have been documented by Koschmann (1949). It is apparent that the breccia is a complex unit formed by a combination of processes. High permeability of the breccia during early stage mineralization is evidenced by pervasive alteration present throughout the unit. This early stage fluid interaction served to lithify the breccia, rendering it impermeable to later stage, precious-

metal-bearing fluids. Subsequent mineralization was confined to structural openings with only minor dissemination into the wallrock.

2. Volcanic and plutonic rocks

Latite-phonolite is present within the district as the predominant constituent of the breccia and as small stocks, numerous dikes, and minor flows, all of which intrude the breccia. Latite-phonolite commonly is light grey to yellowish grey with a porphyritic texture. Syenite is volumetrically the least abundant rock type within the complex. It is a dark grey, medium-to fine-grained rock that is extremely resistant to erosion. It occurs as small stocks and dikes intruding the breccia. Phonolite is the most abundant Tertiary rock in the district. It forms small stocks and dikes both within the complex and in the surrounding area. It is light to dark grey, fine grained, and intrudes both the breccia and the Precambrian rocks. Four types of alkaline basalts have been recognized by previous workers in the Cripple Creek district (Lindgren and Ransome, 1906). All four types are dark grey to black, fine grained, and occur as thin dikes intruding both the breccia, and to a lesser extent, the Precambrian rocks.

3. Basaltic breccia

A circular shaped basaltic breccia pipe is exposed near the center of the district at what is now known as the Cresson mine. The pipe is composed of angular fragments of basalt, minor latite-phonolite, phonolite, Cripple Creek breccia, and granite, cemented by a matrix of basalt and basaltic rock flour impregnated with dolomitic carbonate and pyrite. In the northern part of the district a similar pipe of basaltic breccia occurs outside of the complex.

D. Structural Geology

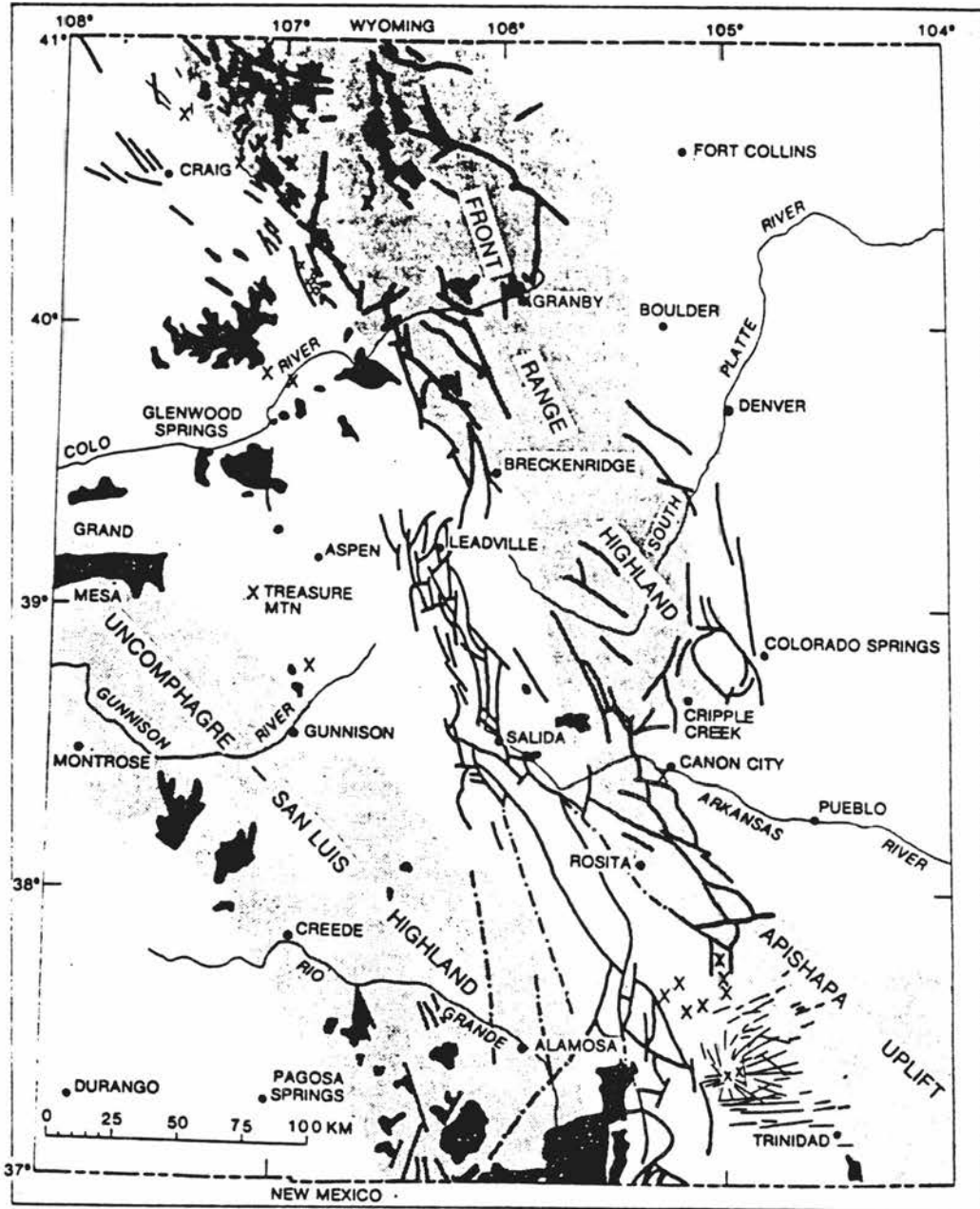
1. Regional tectonics

The Cripple Creek district is situated near the eastern boundary of the Rio Grande rift system (Fig. 3). The highly alkaline rocks of the Cripple Creek district correlate well with the theory that off-rift sequences tend to be alkaline in nature. It is probable that the structural and igneous events of the Cripple Creek region during the Tertiary were related to Rio Grande rift movement. Chapin and Epis (1964) postulate that Cripple Creek is a member of a northeast-trending, middle to late Tertiary volcanic belt which includes Silverton, Lake City, Bonanza, and Guffey. The belt is thought to be a structurally positive hinge area marked by Laramide thrusting in opposite directions and is characterized by explosive, post-Laramide volcanism. A gravity and magnetic low associated with the Cripple Creek complex has been delineated by Kleinkopf et al. (1970). The negative gravity anomaly is a result of density differences between the Tertiary breccia-volcanic sequence and the Precambrian crystalline rocks. An additional inference is that a large intrusive body is present at depth. The magnetic low is caused by hydrothermal alteration, resulting in the remobilization of the iron contained in magnetite to form pyrite (Kleinkopf et al., 1970).

2. District structural geology

Detailed descriptions of the structural history of the Cripple Creek district are provided by Loughlin and Koschmann (1935), and Lovering and Goddard (1950). This section is intended to briefly review their interpretations and present evidence in favor of a more diverse structural history.

Figure 3. Map showing relationship of Cripple Creek to major Rio Grande rift-related structures (from Tweto, 1979).



During the Laramide revolution, Precambrian shear zones were reactivated and the Cripple Creek-Pikes Peak region was domed in response to a regional compression from the south. Fracture systems trending northwest, northeast, north-northeast, and east-southeast, formed in response to compression and shearing. Intermittent subsidence along the fracture systems coupled with often explosive volcanic activity characterized early stage development of the complex. Between eruptions the volcanic material was reworked and stratified, forming sedimentary deposits interlayered with the volcanic rocks. In later complex development, explosive activity ceased and small stocks and dikes intruded the consolidated breccia and surrounding Precambrian rock. Late stage explosive brecciation occurred in the area of what is now the Cresson mine. Subsequent weak compression and shearing with minor settling reopened fracture zones and provided favorable sites for ore deposition. The theory that, during and subsequent to ore deposition, movement had essentially ceased is well illustrated by the general lack of structural dislocation or brecciation of the veins. Small-scale spreading of the fissures during mineralization is evident in the Ajax vein system; post-mineral faulting, although rare, has occurred with a maximum vertical displacement of 120 ft (37 m). These movements were minor and further exemplify the relatively stable conditions present during and after mineralization.

Recent mining activity has exposed mineralized hydrothermal breccias in the Globe Hill area. These appear to reflect late stage explosive events; mineralization occurs as low grade, microscopic, free gold. Features that characterize the pipes are: fluidized channelways, angular fragments, increase in fragment size outward from the pipe

center, silicification, and open voids in the matrix. Whether mineralization is the result of primary native gold deposition or the alteration of earlier formed gold-tellurides by hypogene or supergene processes is currently unknown. Clearly these breccias, in addition to the basaltic breccia pipes, represent a later stage of explosive brecciation subsequent to the initial breccia development of the Cripple Creek complex. The presence of carbonized wood (Lindgren and Ransome, 1906) and the multiple stages of brecciation and volcanism occurring at Cripple Creek are similar to features recognized in the gold-telluride-bearing precious metal systems of the Baguio district, Philippines (Callow and Worley, 1965; Bryner, 1969). Mineralization at the Acupan mine in the Philippines consists of both gold- and silver-telluride-bearing veins and native gold mineralized breccia pipes (Callow and Worley, 1965). Significant similarities exist between the Cripple Creek complex and breccias of the Acupan mine in which convective movement of rock fragments has been documented (Sawkins, O'Neil, and Thompson, 1979). Flared nature of the granite-breccia contact at Cripple Creek supports the idea that the complex was formed primarily by forces acting in an upward direction as opposed to downward subsidence (Lindgren, 1906). The work of Cloos (Mayo, 1976, after Cloos, 1941) on formation processes of breccia pipes is applicable to Cripple Creek. The tectonic setting and mechanism of emplacement involving a combination of intrusive, extrusive, and gravitational processes as documented by Cloos, appears to closely parallel the situation present during the formation of the Cripple Creek complex. Although conclusive evidence has not yet been presented, this writer believes that the Cripple Creek complex is the result of an unusually long lived and complex interplay

of "Cloos-model" breccia pipe development, intrusive volcanism, and hydrothermal brecciation, culminated by precious metal mineralization.

E. District Mineralization

Gold-telluride mineralization in the Cripple Creek district occurs as open-space filling in narrow fissures hosted by Tertiary breccia and Precambrian granite. The most common telluride is calaverite, but sylvanite and krennerite are also present. Minor amounts of other tellurides are present but are insignificant in terms of gold production. The average Au:Ag ratio in the ores is 10:1. Vertical dimension of the ore-hosting structures is generally extensive with some veins having dip lengths of over 3500 ft (1067 m). Gold values within the fissures are irregular, controlled by the time at which each structure was receptive to ore fluids.

Narrow bodies of replacement ore occur where fissures coalesce. This type of occurrence is most common in breccia-hosted mineralization on upper mine levels.

Recent mining in the district has been from native gold-bearing silificied and argillized, angular fragment breccias. Formation processes of these breccias are currently unknown.

CHAPTER III

AJAX MINE GEOLOGY

A. General

The Ajax shaft collar is located within the breccia near the granite contact on the south-central boundary of the complex (Fig. 2). The mine has a surface elevation of 10,105 ft (3081 m) and is developed on 25 levels with a minimum elevation of 6742 ft (2055 m). Vertical extent of the Ajax from the surface to the 3350 level is 3363 ft (1025 m). Mineralization consists of narrow, open-space filling veins and small, pod-like replacement bodies. The predominant ore host is Pikes Peak Granite, although some veins do extend into the breccia and locally the veins cross phonolite dikes.

B. Rock Types

1. Ajax Granite

Primary focus of the sampling program was on veins hosted by Pikes Peak Granite. Within the Ajax mine area, the rock is referred to as Ajax Granite. This term is primarily for convenience, as no distinct variation from the "normal" Pikes Peak granite exists within the mine area. The Ajax Granite is a pink, medium-to coarse-grained, hypidiomorphic granular rock composed of 35-45% microcline (1-10 mm), 15-25% quartz (2-5 mm), 10-20% oligoclase (0.5-2 mm), 10-20% biotite (0.5-1.5 mm), and 1-5% accessory minerals consisting of apatite, magnetite, zircon, and sphene. Commonly the granite occurs as coarse,

even grained masses; locally gneissic, aplitic, and pegmatitic features are present. The quartz in the granite contains abundant small (15 μ m) fluid inclusions that are three phase, liquid dominated, and contain NaCl daughter minerals.

2. Phonolite dikes

All phonolite dikes examined on the levels sampled were altered to some extent as they are commonly associated with a mineralized vein. The phonolite is a grey to greenish-grey, fragmental porphyritic rock with a glassy, trachytic groundmass. It is composed of 10-20% granite wallrock xenocrysts (0.25-9 mm) consisting of 80-90% microcline and 10-20% quartz. The groundmass (80-90%) is vuggy and consists of alkali feldspar laths and devitrified glass. Feldspathoid minerals probably originally occupied the vugs, which comprise up to 25% of the groundmass. They are the most readily altered mineral in the phonolite and only a few nepheline phenocrysts were observed in the petrographic analysis. The dikes vary in width from 1 to 35 ft (0.3-4.6 m) and although many of the dikes do not appear to follow any consistent trend, generally they are more prevalent along the major shear zone trends in the granite.

3. Basalt dikes

Basalt dikes are intensely altered by supergene and, to a lesser degree, hypogene processes. Fresh basalt was observed in a dike paralleling the Newmarket vein on the 3100 level. It is a porphyritic dark grey to black rock with a sub-trachytic, glassy groundmass. The dike consists of 25-35% phenocrysts and 65-75% groundmass. The phenocrysts are composed of 55-65% analcite (0.1-0.5 mm), 15-25% biotite

(0.5-9 mm), 10-20% olivine (0.5-4 mm), and minor quartz and microcline fragments. The groundmass is very fine grained and consists of plagioclase laths, devitrified glass, and minor alkali feldspar laths. The basalt dikes vary from 1.5 to 15 ft (0.5-4.6 m) in width, are younger than the phonolites and predate mineralization.

4. Cripple Creek breccia

Breccia was observed at two locations on the 1600 level. It consists of fragmented clasts of granite, latite-phonolite, and phonolite ranging in size from less than an inch to several feet in diameter. As a result of good permeability allowing interaction with the hydrothermal fluids, rocks that compose the breccia were intensely altered and subsequently lithified by secondary quartz. Good permeability of the breccia was present only during early stage mineralization. Processes of alteration and lithification served to render the unit impermeable, and confined precious-metal mineralization to open structures.

C. Structural Geology

1. General

Most of the mineralization in the Ajax mine is hosted by Ajax Granite (Pikes Peak). The granite-breccia contact slopes steeply away from the Ajax shaft in a northerly direction; the shaft passes through the contact and into granite near the 200 level. A series of modified plan maps of levels sampled (Figs. 4-14) adapted from a computer generated compilation of previous work (Texasgulf Metals Corp.) serve to illustrate the nature of the granite-breccia contact and general trends of the veins and dikes. The mineralized structures of the Ajax vein

Figure 4. Plan map of Ajax 400 level. Note granite-breccia contact just north of the shaft. Location of sample 4-B-1 is shown. Long section and cross section lines (N and B) are also shown.

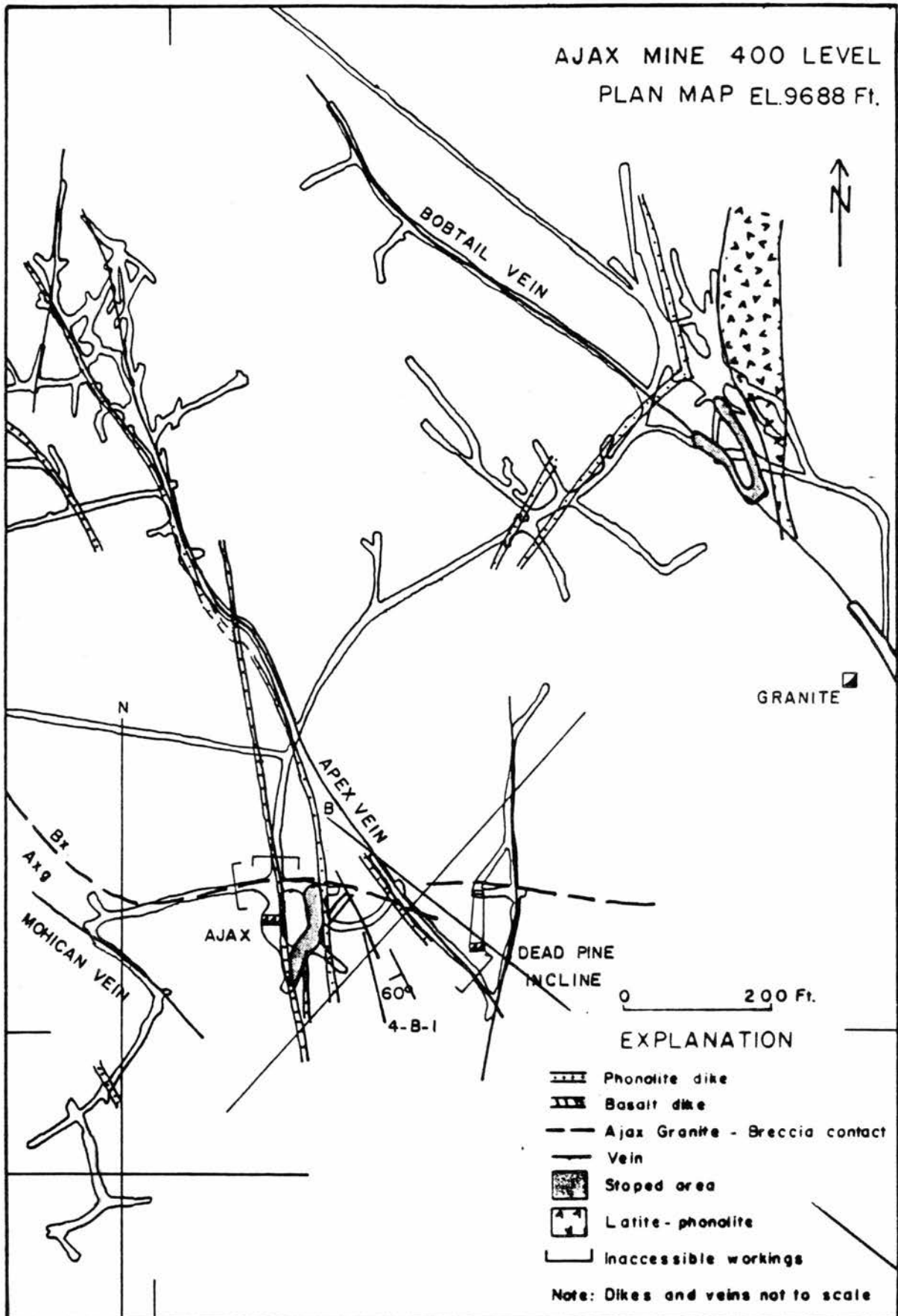


Figure 5. Plan map of Ajax 700 level. Locations of samples 7-M-B and 7-M-2f are shown.

AJAX MINE PLAN MAP
700 LEVEL EL. 9414 Ft.

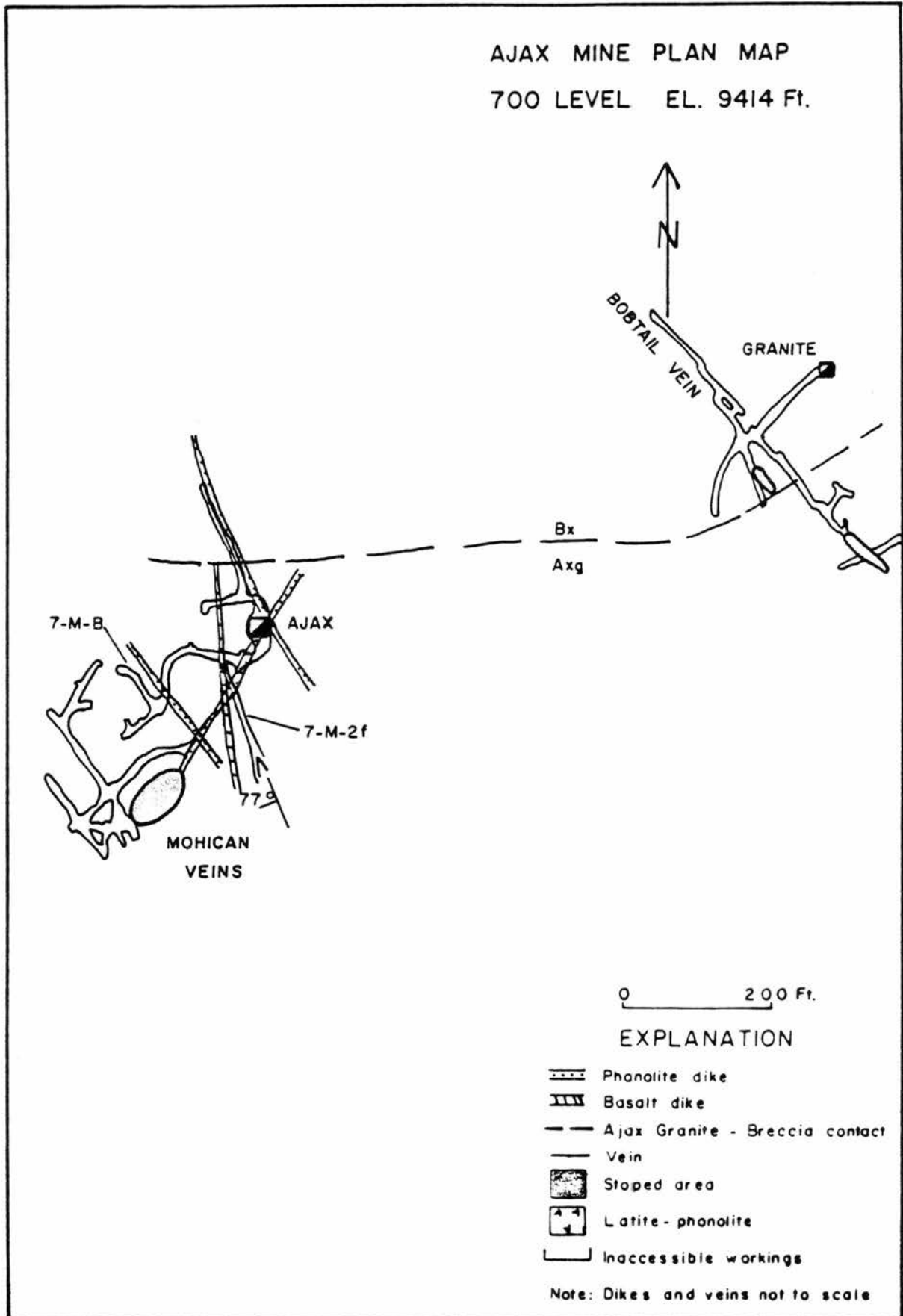


Figure 6. Plan map of Ajax 1000 level. Note first appearance of Newmarket vein. Granite-breccia contact moving away from shaft to the north. Locations of samples 10-A-1, 10-M-1, 10-NM-2 are shown.

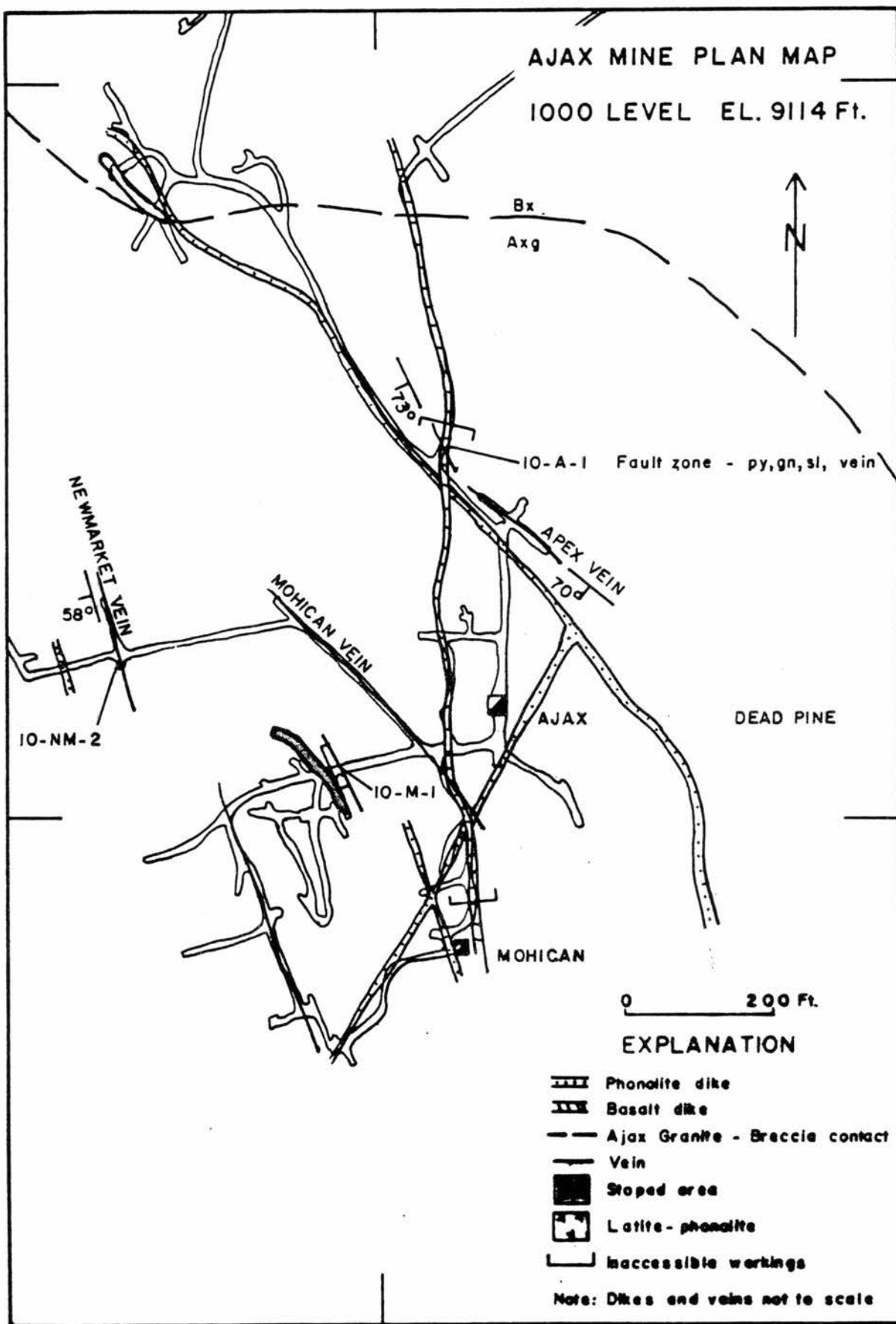
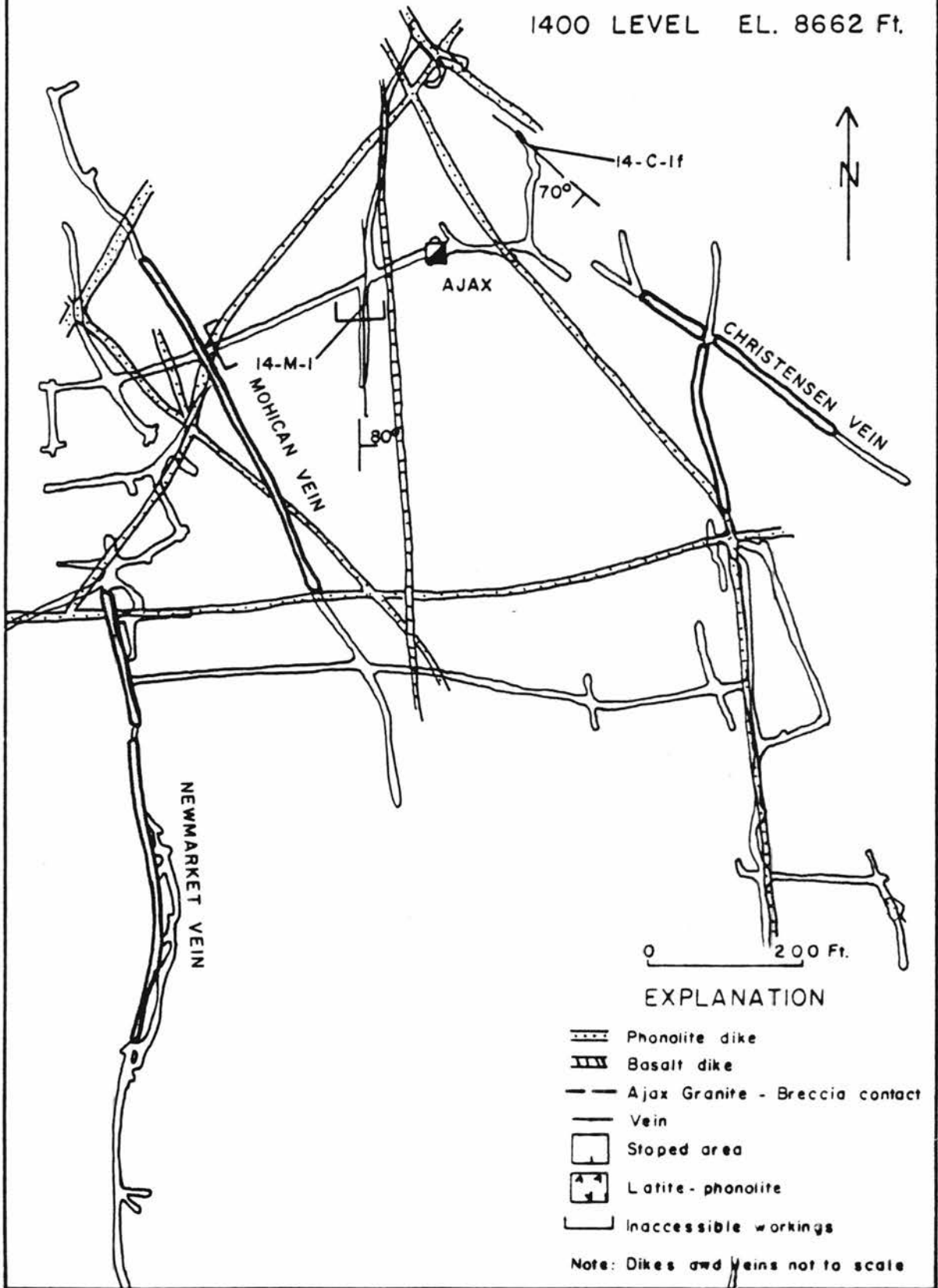


Figure 7. Plan map of Ajax 1400 level. Sample locations 14-C-1f
and 14-M-1 are shown.

AJAX MINE PLAN MAP

1400 LEVEL EL. 8662 Ft.



EXPLANATION

-  Phonolite dike
-  Basalt dike
-  Ajax Granite - Breccia contact
-  Vein
-  Stoped area
-  Latite-phonolite
-  Inaccessible workings

Note: Dikes and veins not to scale

Figure 8. Plan map of Ajax 1600 level. Note position of granite-breccia contact nearer shaft. Note location of breccia-hosted samples 16-Z, and 16-X. Sample locations 16-M and 16-C are also shown.

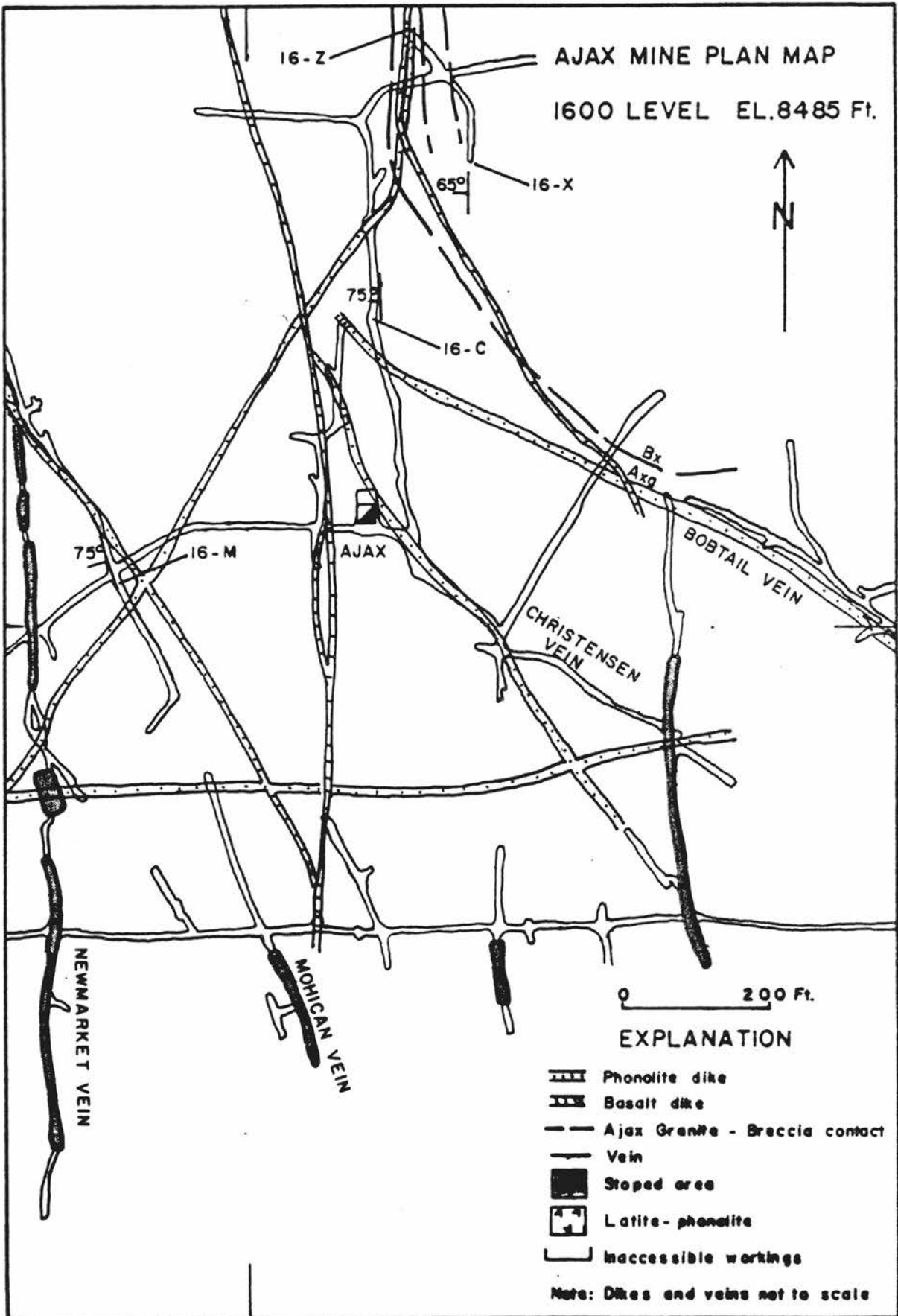


Figure 9. Plan map of Ajax 2000 level. Note position of granite-breccia contact. Bobtail vein is part of Ajax workings. Sample locations 20-BTS-1, 20-U-1, 20-NM-1, and 20-NM-2 are shown. Locations of long section and cross section lines are also shown.

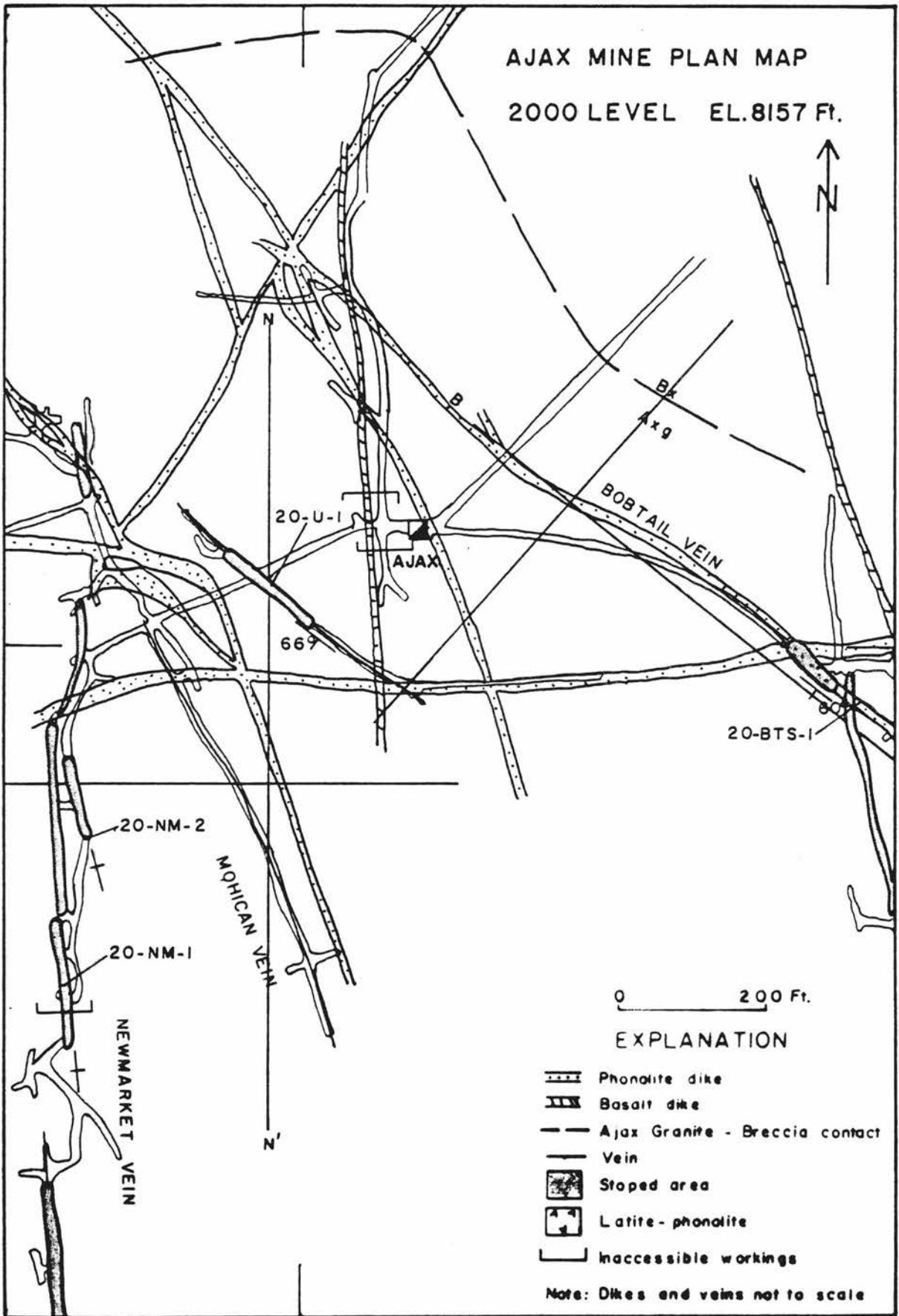


Figure 10. Plan map of Ajax 2300 level. Note granite-breccia contact is no longer near shaft. Sample locations 23-BTS-1f and 23-M-1f are shown.

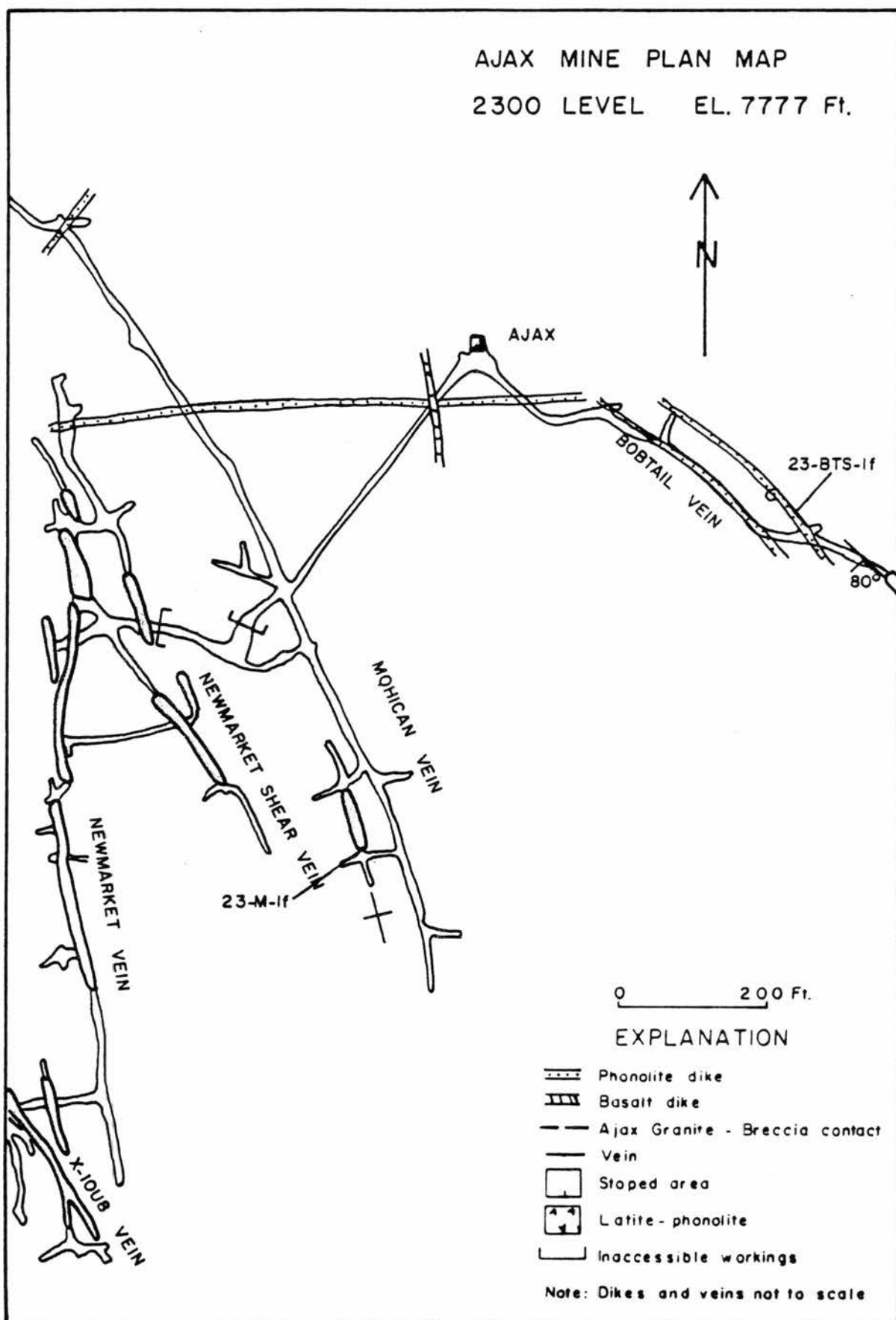


Figure 11. Plan map of Ajax 2600 level. Workings are entirely granite-hosted. Bobtail vein lies on the south side of the shaft. Sample locations 26-BTS-1, 26-NMS-1, and 26-NM-1 are shown.

AJAX MINE PLAN MAP

2600 LEVEL EL. 7537 Ft.

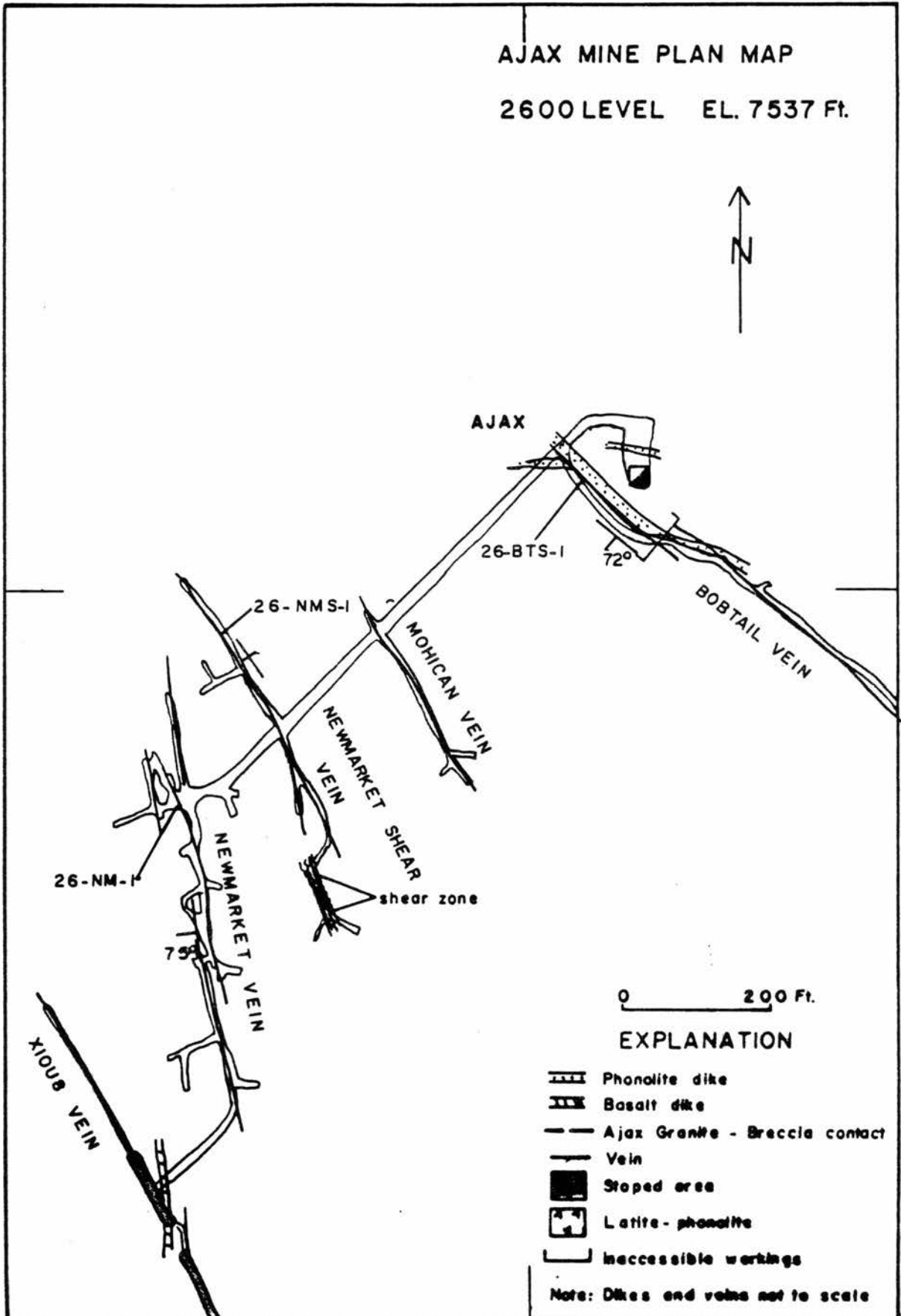
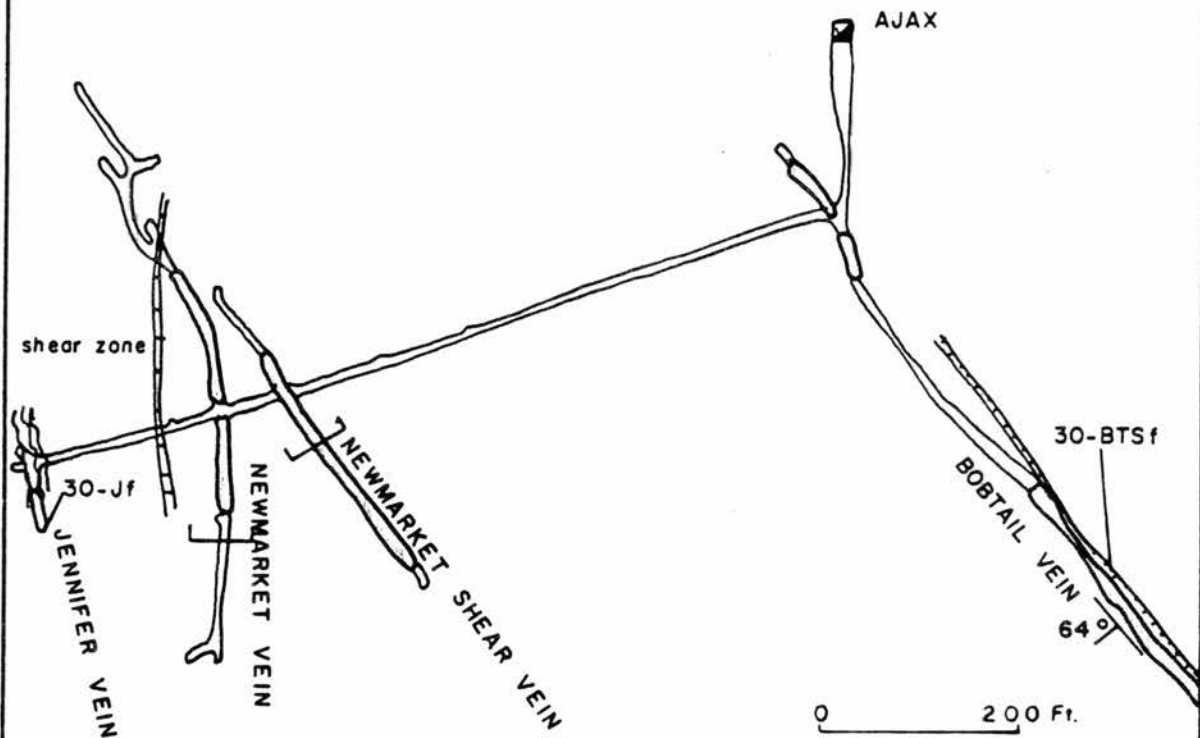






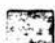
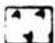

Figure 12. Plan map of Ajax 3000 level. Sample locations 30-BTSf and 30-Jf are shown.

AJAX MINE PLAN MAP
3000 LEVEL EL. 7137 Ft.



0 200 Ft.

EXPLANATION

-  Phonolite dike
-  Basalt dike
-  Ajax Granite - Breccia contact
-  Vein
-  Stoped area
-  Latite - phonolite
-  Inaccessible workings

Note: Dikes and veins not to scale

Figure 13. Plan map of Ajax 3100 level. Note position of Carlton drainage tunnel. Long section and cross section lines are shown. Sample locations 31-BTS-(1,2), 31-NS-1, 31-NM-3 and 31-XT-1 are also shown.

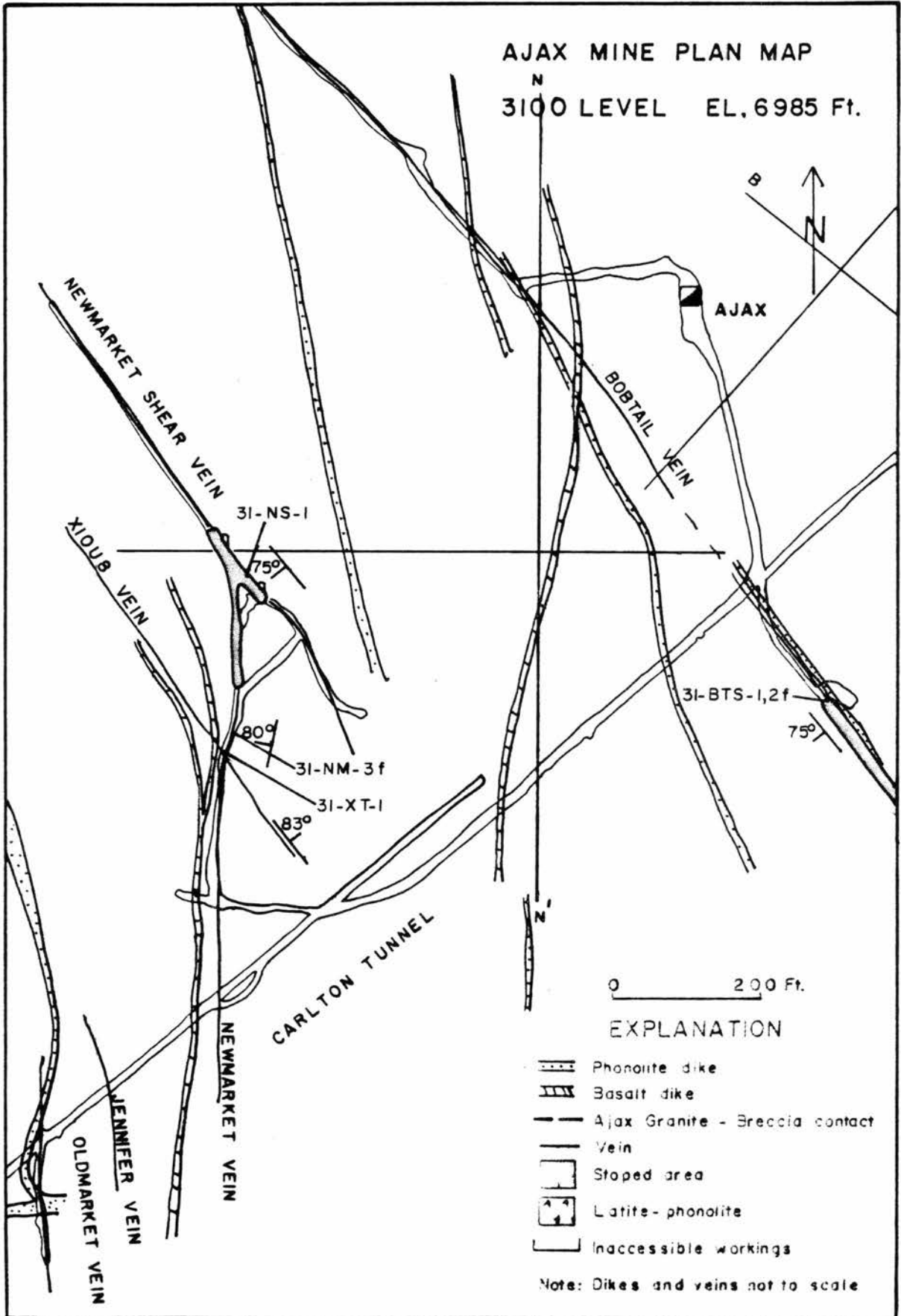
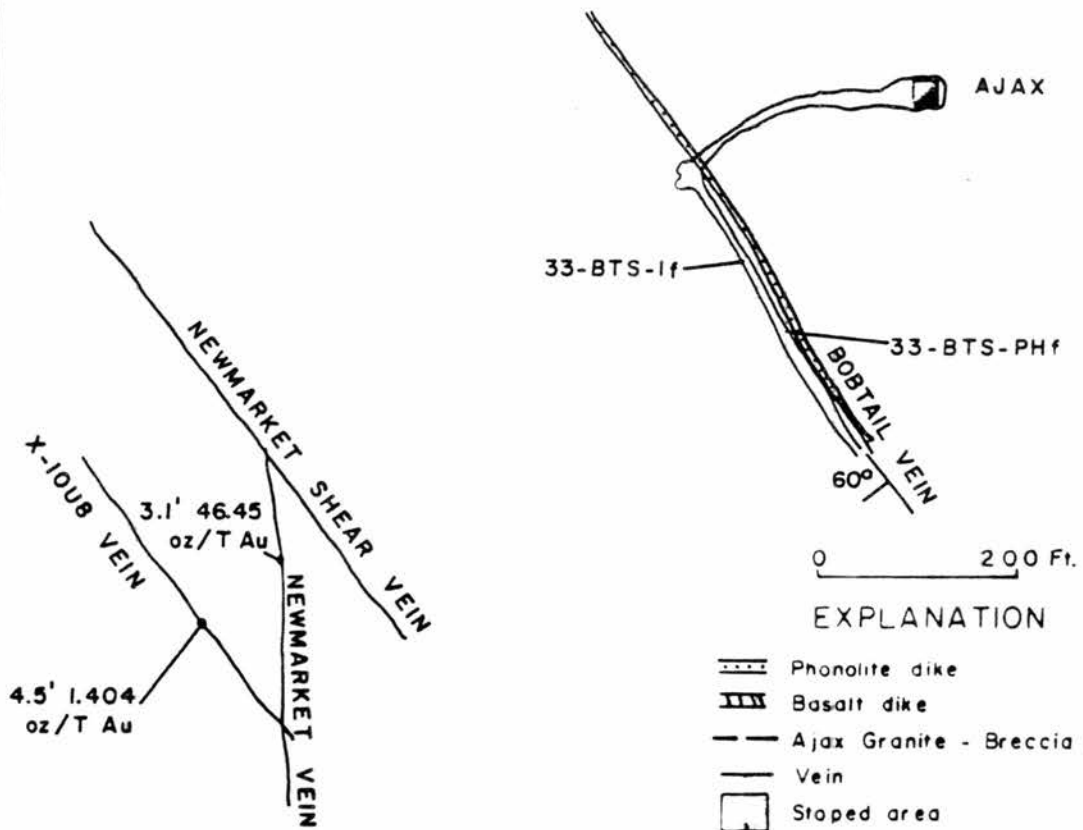


Figure 14. Plan map of Ajax 3350 level. Level is currently being developed. Sample locations 33-BTS-1, 33-BTS-PH are shown.

AJAX MINE PLAN MAP
3350 LEVEL EL. 6742 Ft.



0 200 Ft.

EXPLANATION

-  Phonolite dike
-  Basalt dike
-  Ajax Granite - Breccia contact
-  Vein
-  Stoped area
-  Latite-phonolite
-  Inaccessible workings

Note: Dikes and veins not to scale

system follow three distinct trends: north-south, north-northwest, and west-northwest. The three trends are members of a master shear zone developed due to compression from the south (Loughlin and Koschmann, 1935); they are locally controlled by the erratic contact between granite and breccia.

The relationship of the phonolite and basalt dikes with the mineralized veins has been a source of confusion in the past. Lindgren and Ransome (1906) believed that the dikes were intruded prior to mineralization and commonly acted as permeability barriers to the ore-bearing solutions. In a report dealing specifically with the Ajax, Colburn (1913a) stated the phonolite and basalt dikes formed subsequent to ore deposition as evidenced by their lack of control on mineralization. In a later report, Colburn (1913b) refutes his earlier suggestion by maintaining that the phonolite dikes act as dams to the ore-forming solutions and the basalt dikes, being more reactive to the hydrothermal solutions, have acted as ore fluid channelways. From personal observation, it is apparent that the dikes generally had only a minor influence on ore location although they were intruded prior to the ore-forming event. In summary, the relationship between dikes and veins of the Ajax is similar to that noted by Denholm (1967) at Vatukoula, Fiji. At Vatukoula, stresses creating major shear zones along which dikes were intruded were reutilized to form subsequently mineralized fissure systems. A similar situation exists at the Ajax mine where the vein-dike association is predominately coincidental in nature. Dikes shown on the plan maps (Figs. 4-14) are generally greater than 5 ft (1.5 m) wide; smaller dikes, although common, were not mapped; they trend both parallel to the vein structure and at random orientations.

Fracture systems of the Ajax consist of subsequent tension fractures along which structural displacement rarely occurred. Movement which has occurred generally consists of a subtle widening or contracting of the fissures with no lateral or vertical displacement. Although in cross section the veins appear to be one continuous fissure (Figs. 15, 16), in actuality they consist of a series of mineralized, en echelon fissures comprising an individual vein. In general, the veins are extremely variable in mineralogy and morphology. The variability is more vertical than lateral in nature. An extreme contrast in composition commonly is exhibited by the same vein within 300 to 500 ft (91-152 m) of vertical distance. A vein dominated by a particular stage of mineralization on one level may be dominated by an entirely different stage on other levels. This compositional variability is the result of minor structural activity which selectively sealed off and reopened structures at different times during mineralization. The Newmarket fault is the only fault along which significant post-mineral movement has been recognized (Fig. 16). The fault has 120 ft (37 m) of vertical displacement and negligible horizontal displacement (Loughlin and Koschmann, 1935).

2. North-south veins

The Newmarket vein was sampled on the 1000, 2000, 2600, 3000, and 3100 levels. It is the only member of the north-south set that was sampled. The Newmarket trends due north to $N.5^{\circ}W$ (Fig. 6-14) and dips 80° to 88° west (Fig. 16). It is characterized by narrow, branching veinlets (less than 1.5 in (3.8 cm)) with thin alteration selvages ranging from one to three times the vein width (Fig. 17). The vein is not associated with a dike on the upper levels, but on the lower levels

Figure 15. Cross section through Bobtail vein. Note vein-dike association. Also note discontinuity in granite-breccia contact occurring just below the 2000 level.

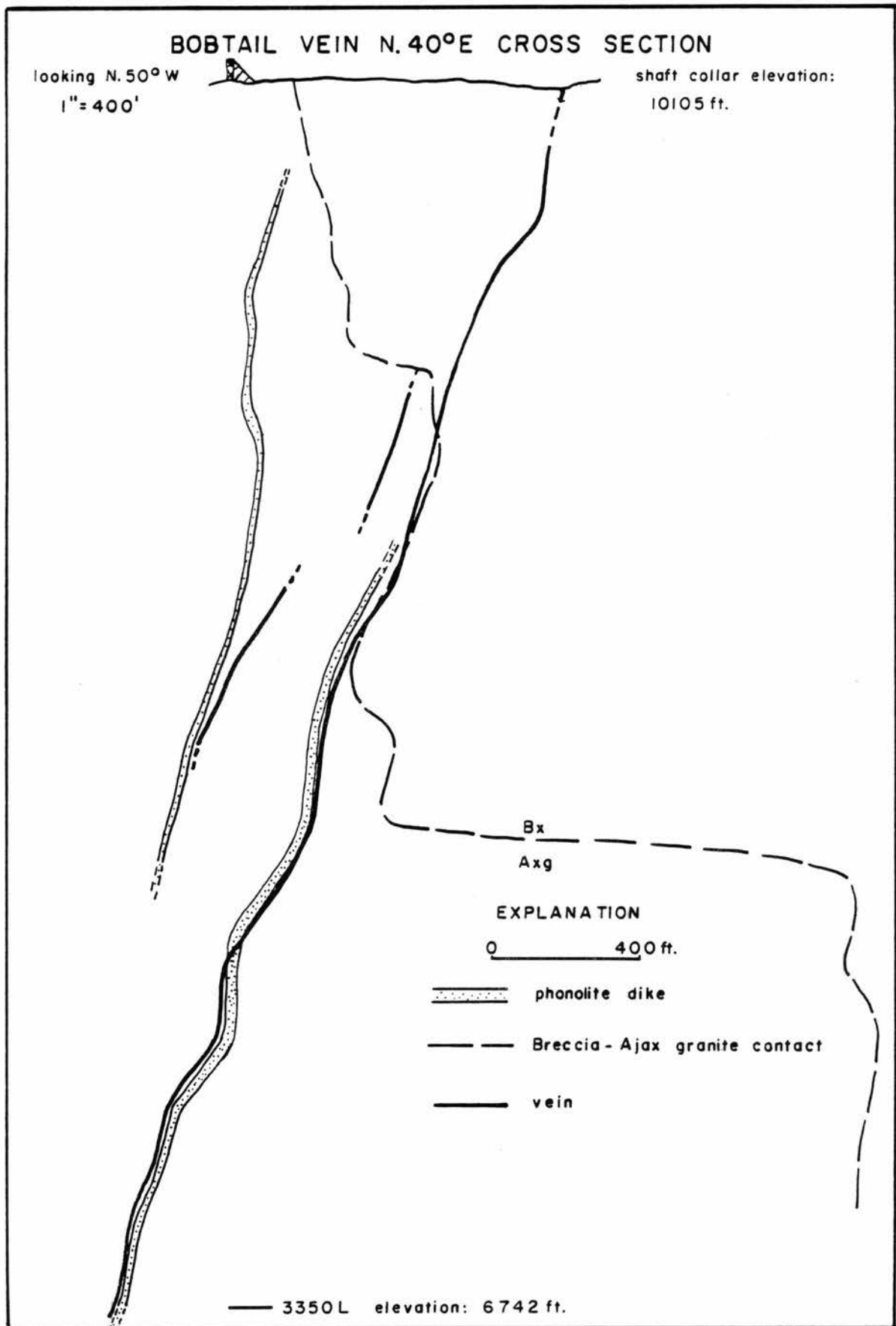


Figure 16. Cross section through Newmarket vein. Note Newmarket fault.

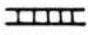
NEWMARKET VEIN N.90°E CROSS SECTION

looking due North

1" = 400'

0 400 ft.

EXPLANATION

 basalt dike

 vein

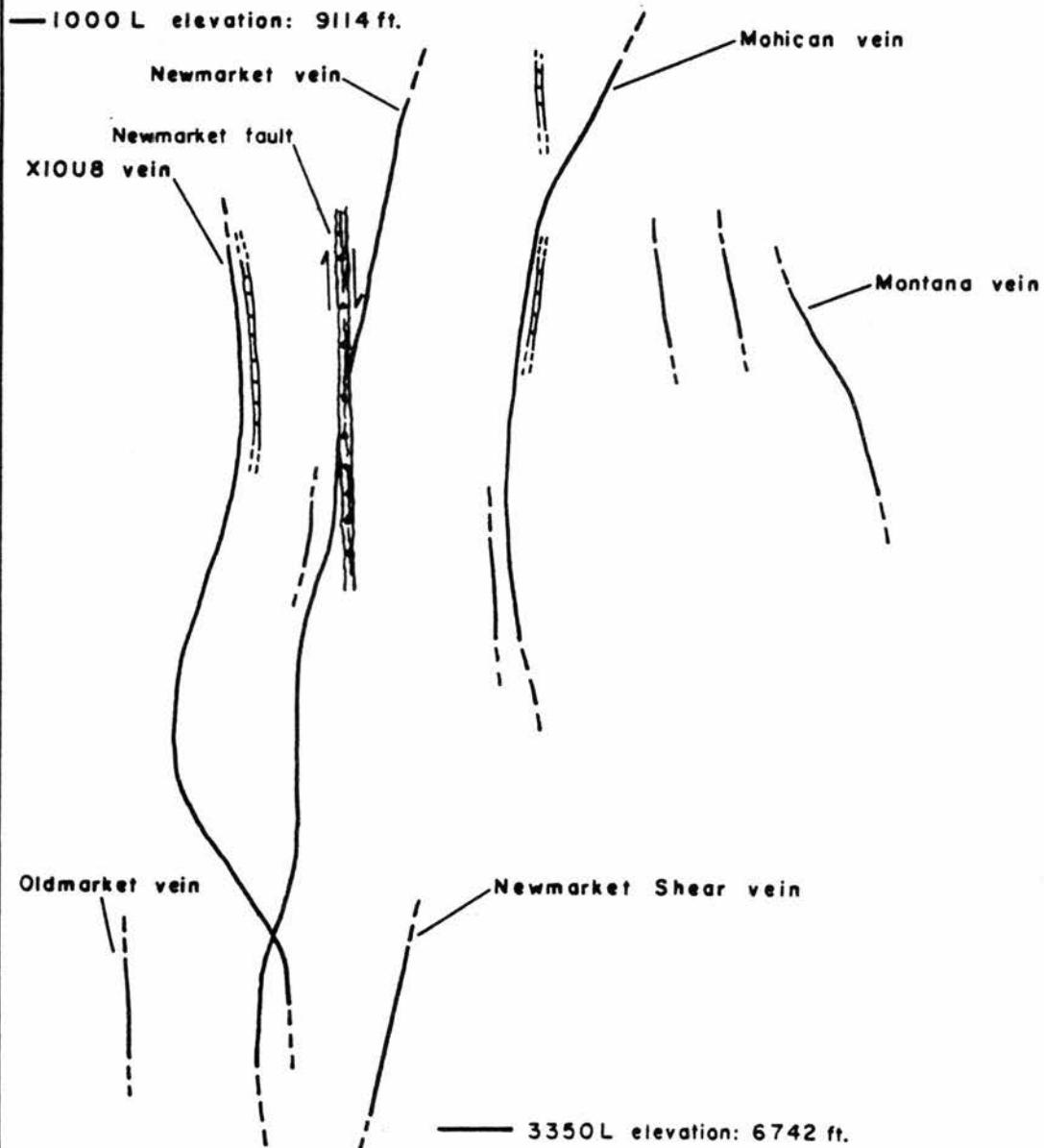
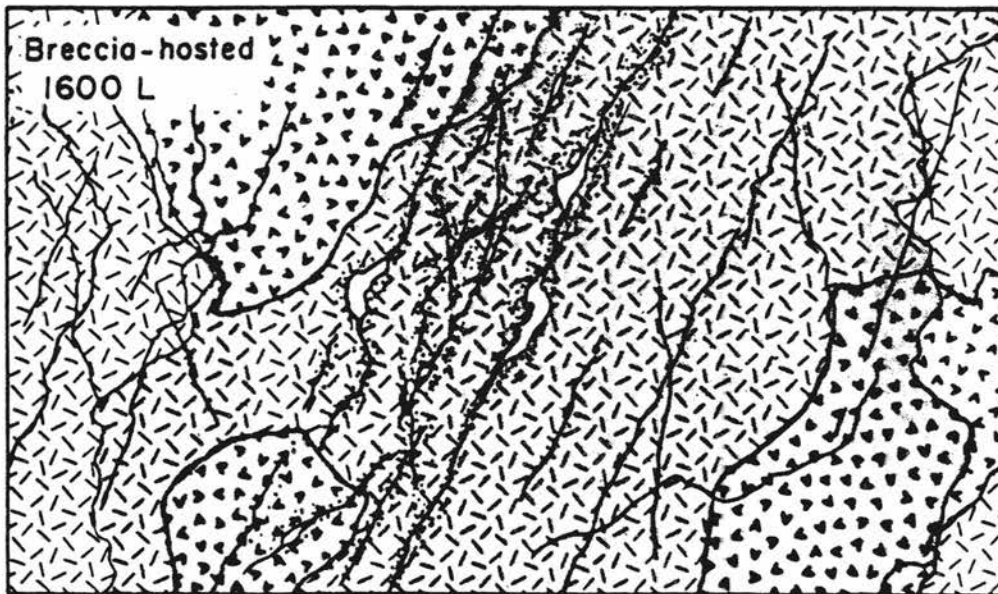
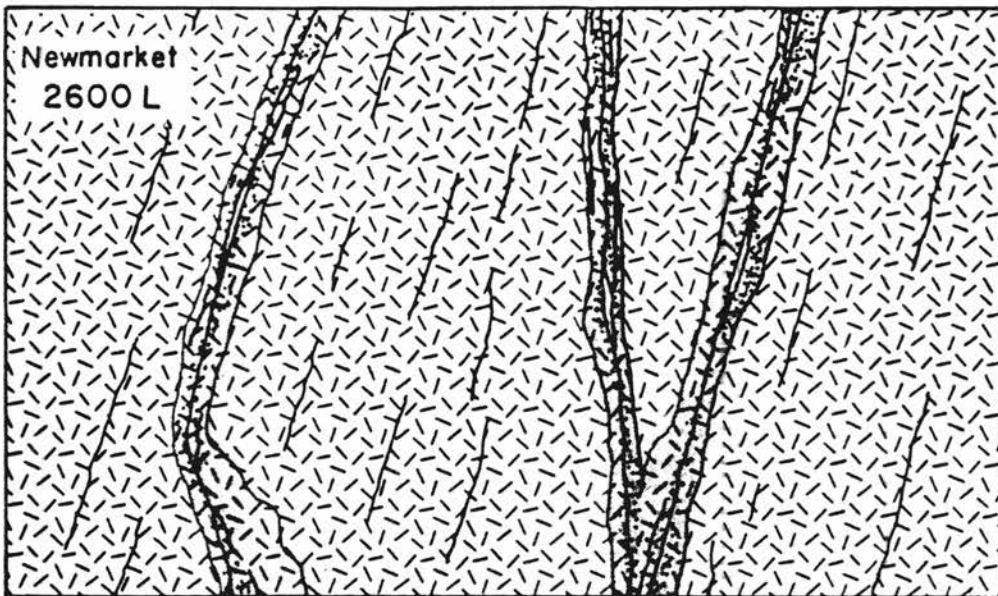


Figure 17. Schematic cross sectional diagram of Newmarket (2600 level) and breccia-hosted (1600 level) veins. Note characteristic branching and narrow alteration selvage of the Newmarket. Note the pervasive alteration and extensive sheeting of the breccia-hosted vein.


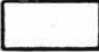

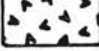
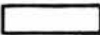
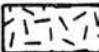
NEWMARKET AND BRECCIA-HOSTED VEIN CROSS SECTION

looking North
1" = 2'

0 2 ft.



EXPLANATION

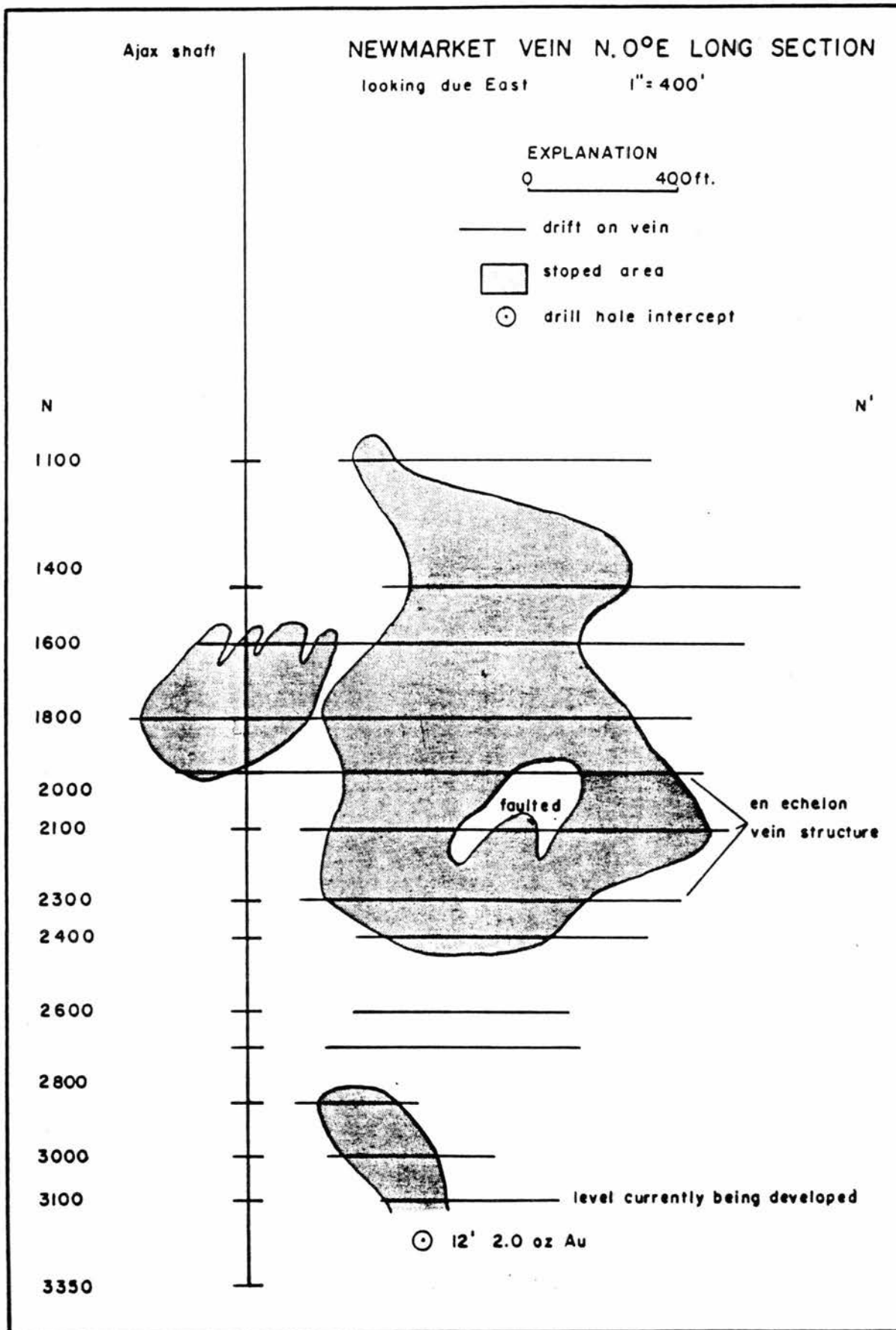
- | | |
|--|---|
|  barren fracture |  vein-related alteration |
|  mineralized fracture |  latite-phonolite |
|  open vug |  Ajax granite |

a basalt dike parallels the vein on the hanging wall side. Koschmann and Loughlin (1935) believe that the Newmarket fissure was not opened until after first stage mineralization ended and was the result of tension during a north-northeastward shearing movement. Recent work by the author has determined the presence of a minor but identifiable first stage component in the Newmarket system. As inferred by the lack of associated phonolite dikes and weak development of stage one mineralization, it is probable the Newmarket fissure was formed at a later time than the north-northwest and west-northwest fissures. The weak vein-related alteration is the result of low fracture density, narrow width, and near vertical dip of the structure. Although the Newmarket is rather unimpressive in appearance when compared to the typical vein of the Ajax system, it is one of the highest grade, most extensively stoped veins in the mine (Fig. 18). The ore shoot has a vertical rake. Although a lower grade interval exists between the 2400 and 2800 levels, the vertical continuity of the vein is extensive as evidenced by high grade drill hole intercepts on the 3350 level (Figs. 14, 18).

3. North-northwest veins

The Mohican, Newmarket Shear, and X-10-U-8 veins are members of the north-northwest set. The veins strike N.15°W to N.25°W and dip 75° to 85° west (Figs. 4-14). The Mohican was sampled on the 700, 1600, and 2300 levels. The Newmarket Shear vein was sampled on the 2600, 2800, and 3100 levels. The X-10-U-8 vein was sampled on the 3000 and 3100 levels. In general, the veins are variable in morphology and mineralogy from level to level and have a greater degree of alteration than is present in the Newmarket system. Vein width varies from less than 1 in

Figure 18. Long section of the Newmarket vein. Shaded area indicates stoped ground.



to 2.5 ft (2.5 cm-0.75 m) and the alteration selvage is from one to three times vein width dependent on the degree of fracturing. Dikes are not generally associated with veins of the north-northwest set. A 6 inch (15 cm) hanging wall phonolite dike parallels the Mohican vein on the 1600 level; other dikes too small to be mapped occur in association with some of the veins.

4. West-northwest veins

The Apex, Bobtail, and Christensen veins are members of the west-northwest set sampled. The Bobtail vein was sampled on the 2000, 2300, 2600, 3000, 3100, and 3350 levels. It is the most important member of the west-northwest set with a strike of N.40°W to N.60°W and a dip of 60° to 75° southwest. The Bobtail vein is the most vertically continuous vein in the Ajax system (Fig. 15). Above the 1600 level, it is either within the breccia or parallels the granite-breccia contact and is contained within the Portland mine workings. Below the 1600 level, it is associated with a phonolite dike crossing from the hanging wall side of the vein to the footwall side between the 2300 and 2600 levels. The Bobtail is characteristically a wide (2 ft (0.6 m)-4 ft (1.2 m)) sheeted structure having several stages of mineralization present and the most intense alteration halo of all the granite-hosted veins (Fig. 19). The vein commonly exhibits multiple stages of fracturing which occurred during the first and third stages of mineralization. In many places, granite clasts rimmed by first stage mineralization and clasts composed of first stage minerals are overgrown by minerals of the third and fourth stages. The phonolite dike had no apparent control on the mineralization. In zones where the vein cuts

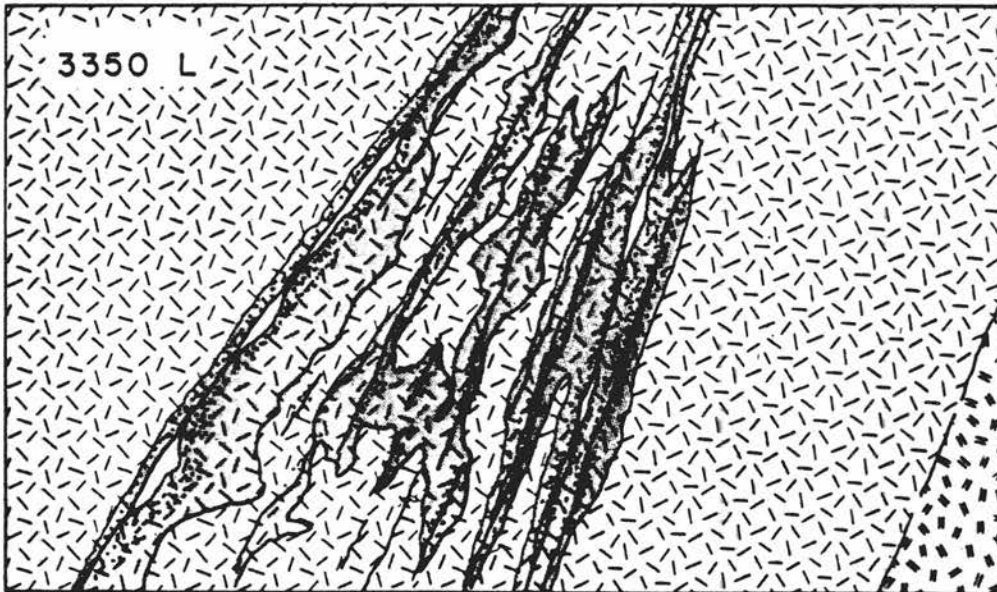
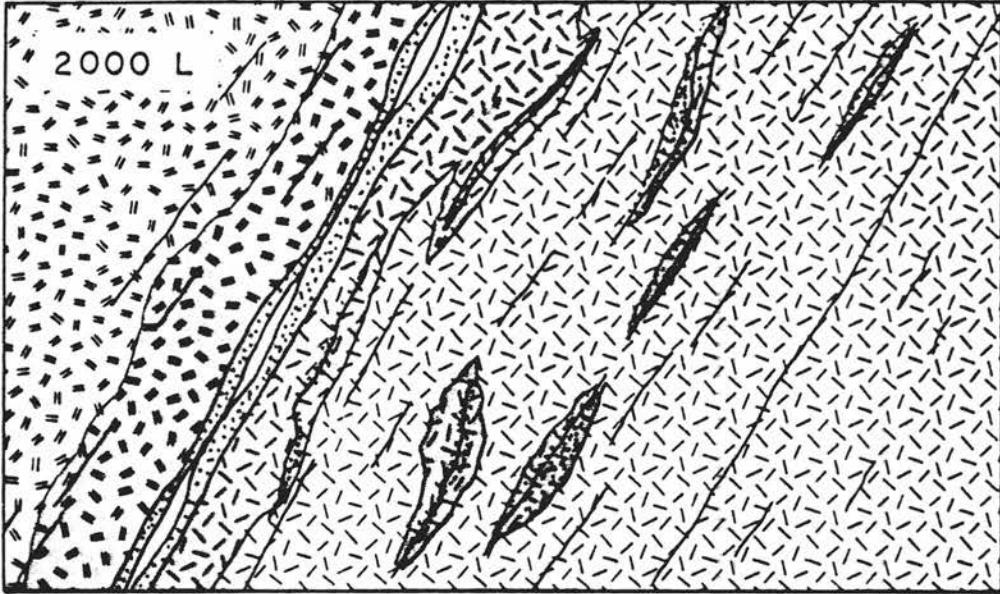
Figure 19. Schematic cross sectional diagram of Bobtail vein (2000 level and 3350 level). Note position of phonolite dike on both levels. Note fracture control of alteration and vuggy structure.

BOBTAIL VEIN CROSS SECTION

looking NW

1" = 2'

0 2 ft.



EXPLANATION

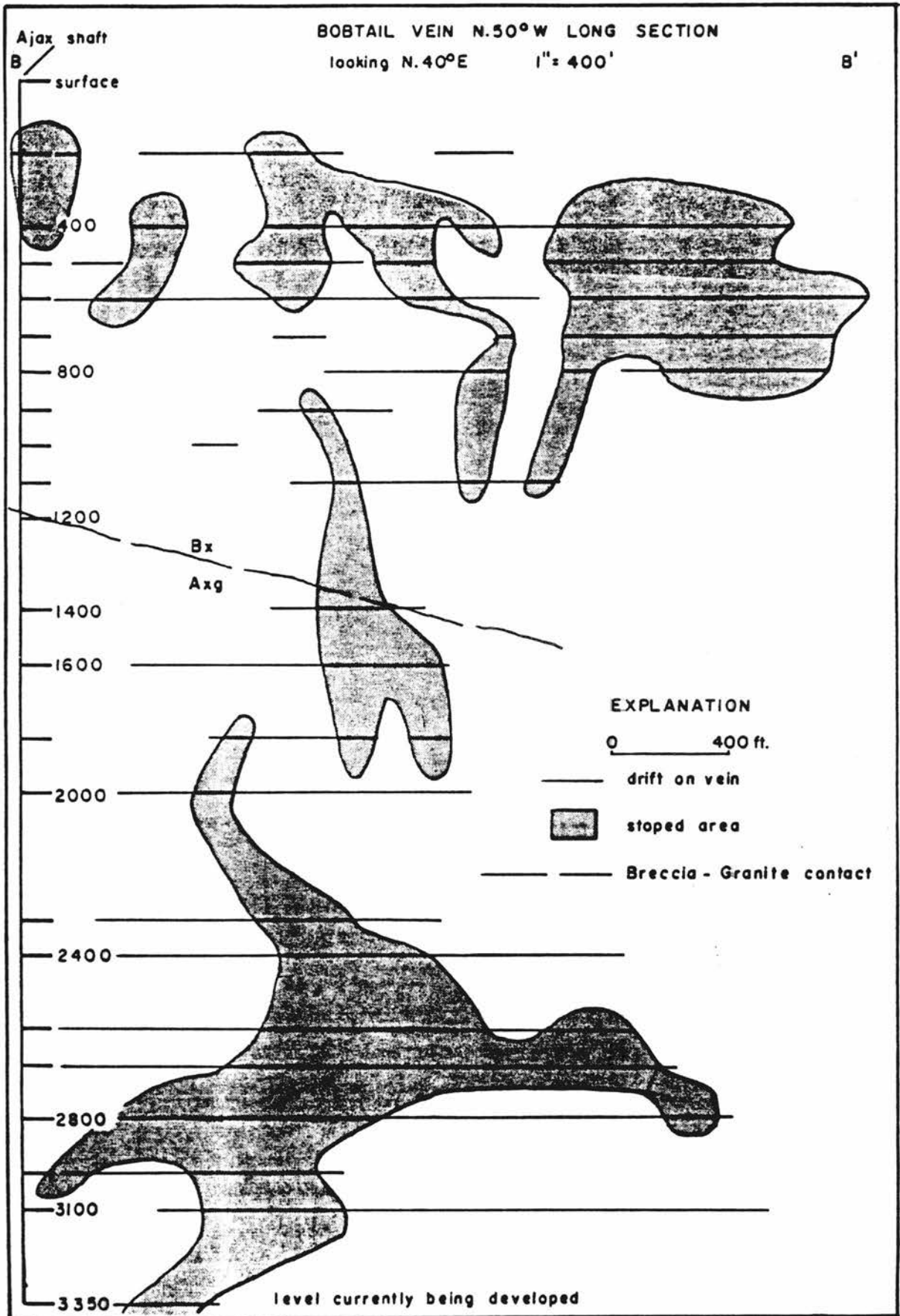
- | | |
|--|---|
|  barren fracture |  vein-related alteration |
|  mineralized fracture |  phonolite dike |
|  open vug |  Ajax granite |

the dike, the sheeted zone is wider and more intensely fractured due to the more brittle character of the phonolite as opposed to the granite (Fig. 30a). Greater development of mineralization and alteration in the Bobtail is attributed to the flatter dip and sheeted nature of the structure. The ore shoots of the Bobtail vein (Fig. 20) are irregularly shaped and do not follow any consistent trend. A possible breccia-hosted, northerly extension of the Bobtail was sampled on the 1600 level (sample 16-Z)(Fig. 32b). The mineralized zone on the 1600 level consists of numerous irregular stringer veinlets of first and third stage mineralization in a poorly defined vuggy sheeted zone 4 ft (1.2 m) to 6 ft (1.8 m) wide (Fig. 17, 32b). The breccia, consisting of altered fragments of granite and latite-phonolite, was well lithified prior to mineralization. Several fracture events have occurred during mineralization, and the alteration assemblage is well developed throughout the mineralized zone.

The Christensen vein was sampled on the 1400 and 1600 levels (Figs. 7, 8). It is similar to the Bobtail in attitude although the vertical extent of the vein, as currently defined, is considerably less.

The Apex vein or a parallel split from the Apex was sampled on the 400 level near the granite-breccia contact (Fig. 4). It consists of a 4 ft (1.2 m) wide sheeted fracture zone containing a 1 ft (0.3 m) wide band of first and third stage mineralization.

Figure 20. Long section of Bobtail vein. Shaded area indicates stoped ground. Note irregular attitude of ore shoots.



CHAPTER IV
VEIN MINERALOGY AND PARAGENESIS

A. General

In the first work on paragenesis and vein mineralogy of Cripple Creek ores, Lindgren and Ransome (1906) identified three stages of mineralization. Subsequent workers (Koschmann and Loughlin, 1953; Loughlin, Koschmann, Tunell, and Kasnda, 1940) briefly address the paragenetic sequence but have not added significantly to the early work of Lindgren and Ransome (1906).

In this study, both ore microscope and petrographic analyses were utilized to determine the vein mineralogy and paragenesis of the Ajax vein system. Polished sections were analyzed using reflected light and a Vickers hardness testing microscope. Unknown opaque minerals were identified by electron microprobe at the U.S. Geological Survey laboratory in Lakewood, Colorado. Gangue mineralogy was determined from thin section and X-ray diffraction analyses of the veins. Polished sections and thin sections were prepared from vein samples collected at the locations shown on Figures 4-14.

The paragenetic sequence determined for the Ajax vein system is a generalized compilation of information obtained from laboratory work and underground observations (Fig. 21). Five stages of mineralization have been identified in the veins of the Ajax system. No individual vein sample exhibits the complete five stage sequence of mineralization.

Figure 21. Paragenetic diagram of Ajax vein system mineralization. Thickness of bars indicates relative volume abundance of the minerals in each stage. Note variation in volume percent of each stage present between the Bobtail and Newmarket veins.

| MINERALS | | STAGES | | | | |
|----------------|--|--------|-------|-------|-------|-------|
| | | 1 | 2 | 3 | 4 | 5 |
| QUARTZ | | ————— | ----- | ————— | ————— | ----- |
| FLUORITE | | ————— | | ————— | | ----- |
| ADULARIA | | ————— | | | | |
| DOLOMITE | | ----- | | | | ----- |
| PYRITE | | ————— | ----- | ----- | ----- | |
| HEMATITE | | | | ----- | | |
| RUTILE | | | | ----- | ----- | |
| SPHALERITE | | | ----- | | | |
| GALENA | | | ----- | | | |
| MARCASITE | | ----- | ----- | | | |
| CHALCOPYRITE | | | ----- | | | |
| PYRRHOTITE | | | ----- | | | |
| CALAVERITE | | | | | ----- | |
| ACANTHITE | | | | | ----- | |
| VOLUME % | | | | | | |
| BOBTAIL VEIN | | 35 | 5-20 | 10-60 | 5 | 1 |
| NEWMARKET VEIN | | 5-35 | 0-5 | 10-35 | 20-50 | 0 |

Generally, the veins are composed of minerals belonging to either two or three of the five stages. The complete sequence was determined by sampling and observing the vein at different vertical and horizontal locations.

Open-space filling dominated the vein-forming process with very minor replacement along the vein-wallrock contact. Replacement is more common on upper levels of the mine where the veins are breccia-hosted and fracturing is more intense. Overall, replacement type mineralization is minor in terms of tons produced.

B. Paragenesis and Mineralogy

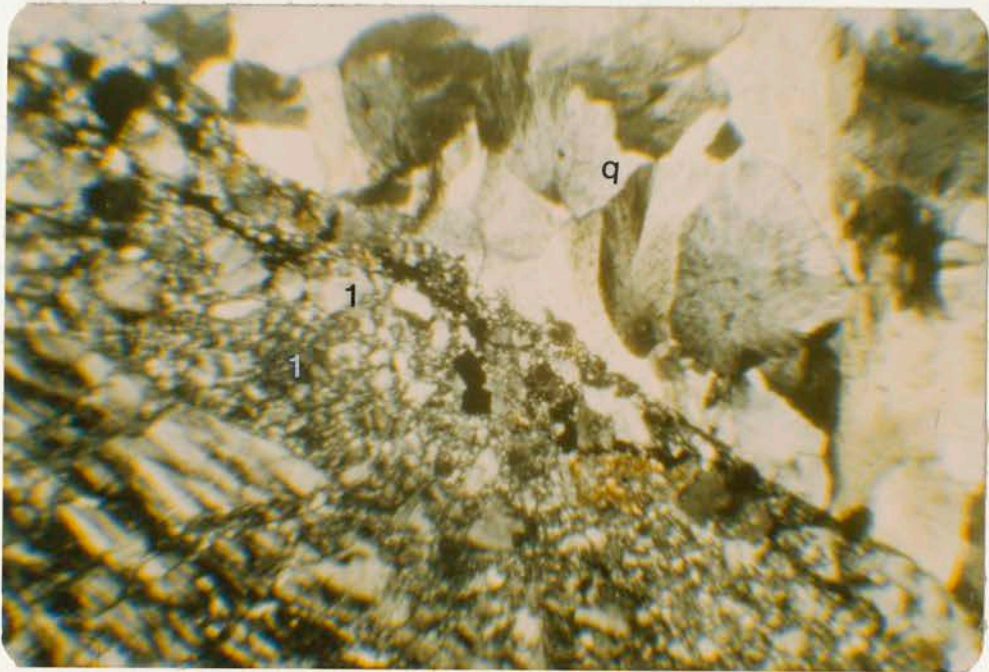
1. Stage 1

Minerals formed during the first stage of mineralization include quartz, fluorite, adularia, dolomite, and pyrite intergrown with variable amounts of marcasite. Megascopically the first stage assemblage is a dark, blueish-grey, jasper-like material that contains fragments of wall-rock derived microcline (Fig. 22a). In thin section the assemblage consists of a variable amount of microcline fragments (0.05-2.0 mm) which are rimmed and veined by adularia and surrounded by a matrix of granular quartz, euhedral fluorite, anhedral dolomitic carbonate, and subhedral to euhedral pyrite (0.01-1.5 mm) (Fig. 22b). The relatively high flow velocity of first stage ore fluid is illustrated by the presence of apparent unsupported microcline fragments occurring within the assemblage (Fig. 22b).

2. Stage 2

Stage 2 mineralization is restricted in its occurrence and is most prevalent in the Bobtail vein and in a mineralized fault zone on the

- Figure 22. A. Photograph of Bobtail vein (3100 level), hand specimen. Showing dark grey stage 1 mineralization, white-euhedral stage 4 quartz(q) with late calaverite(c). Note vuggy texture of vein and weak development of alteration. Fresh primary biotite is present within 5 cm of vein.
- B. Photomicrograph of thin-section from Bobtail vein, same sample as above (horizontal field of view = 3 mm). Showing contact between stage 1 and stage 4 mineralization. Note brecciated nature of stage 1(l), composed of microcline and quartz fragments in a matrix of smaller fragments, silica, fluorite, and pyrite. Note feathery texture of stage 4 euhedral quartz(q).



1000 level. The mineralization consists of minor pyrite containing rounded inclusions (15 to 60 μm) of chalcopyrite exsolving from pyrrhotite; sphalerite and galena are present containing rare chalcopyrite inclusions (Fig. 23). Pyrite is intergrown locally with arsenic-rich marcasite and commonly is replaced by both sphalerite and galena (Figs. 24a). Pyrite-marcasite locally have replaced alteration-related magnetite grains (Fig. 23b). Sphalerite is commonly replaced by galena (Fig. 24b). All minerals of the second stage are cut by veinlets of later stage quartz. Second stage mineralization is a volumetrically minor component in the veins and is distinguishable only in polished section or in thin section where it occurs as thin veins of opaque minerals paragenetically separable from minerals of the other stages (Fig. 25a).

3. Stage 3

Stage 3 mineralization is characteristically either the dominant component in the veins or totally absent from the vein assemblage. Where present it consists of a variable ratio of intergrown quartz and euhedral purple fluorite with minor pyrite occurring as minute (0.05-0.5 mm) subhedral grains and overgrowths (Figs. 25a, 25b, 28b, 30a, 30b, 32a). The light purple color of stage 3 fluorite distinguishes it from fluorite of the other paragenetic stages. Fluorite of stage 3 hosts abundant fluid inclusions (4-45 μm) suitable for heating and freezing stage analysis. When viewed in thin-section at high magnification (800X), third stage fluorite occurs as well developed, growth-zoned euhedral crystals (200-500 μm). Specular hematite and rutile are tenuously placed in the third stage. Specular hematite occurs as bladed (50 μm) inclusions in the pyrite of stage 3 (Fig. 26a). Rutile occurs

- Figure 23. A. Photomicrograph of polished-section from Bobtail vein, 2600 level (horizontal field of view = 0.265 mm). Showing pyrrhotite(p) and chalcopyrite(c) inclusion in pyrite(py).
- B. Photomicrograph of polished-section from Newmarket vein, 3100 level (horizontal field of view = 0.265 mm). Showing magnetite(m) partially replaced by quartz(q) with later replacement of both by pyrite-marcasite(p).

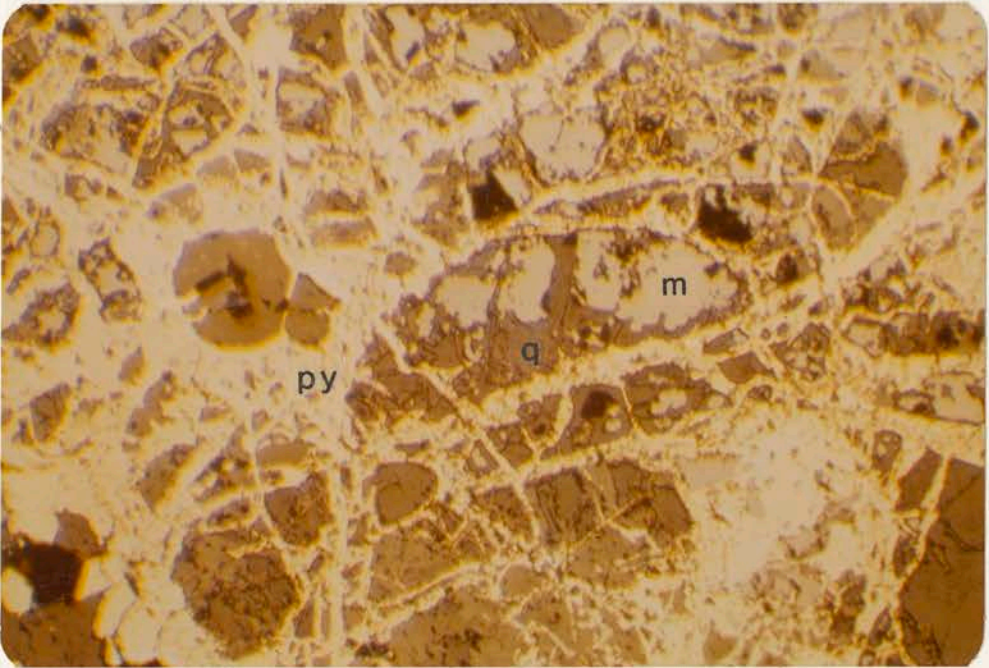
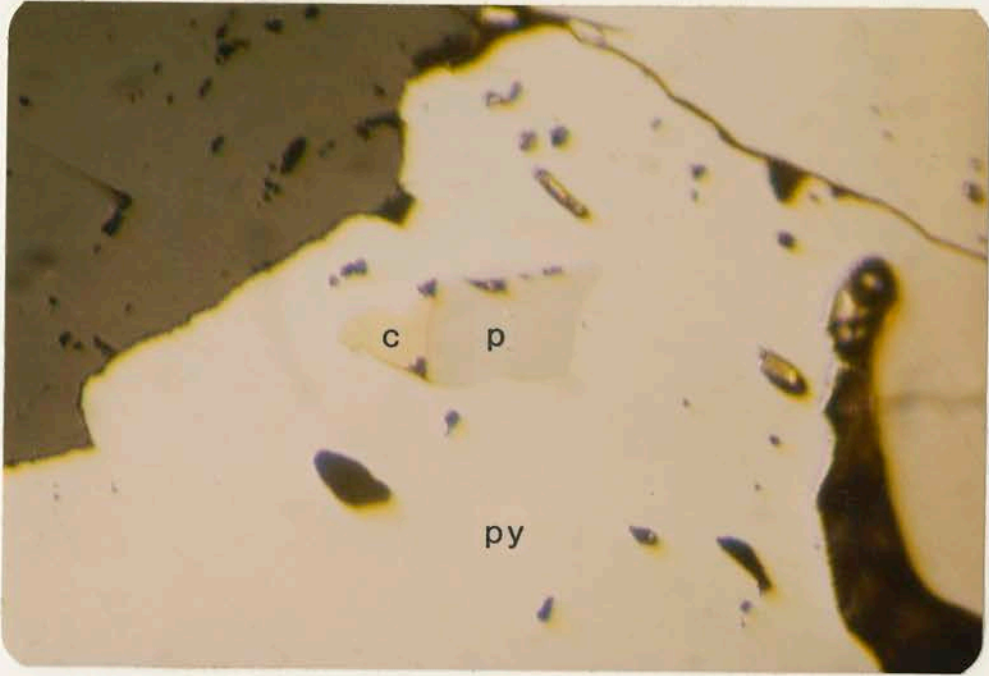
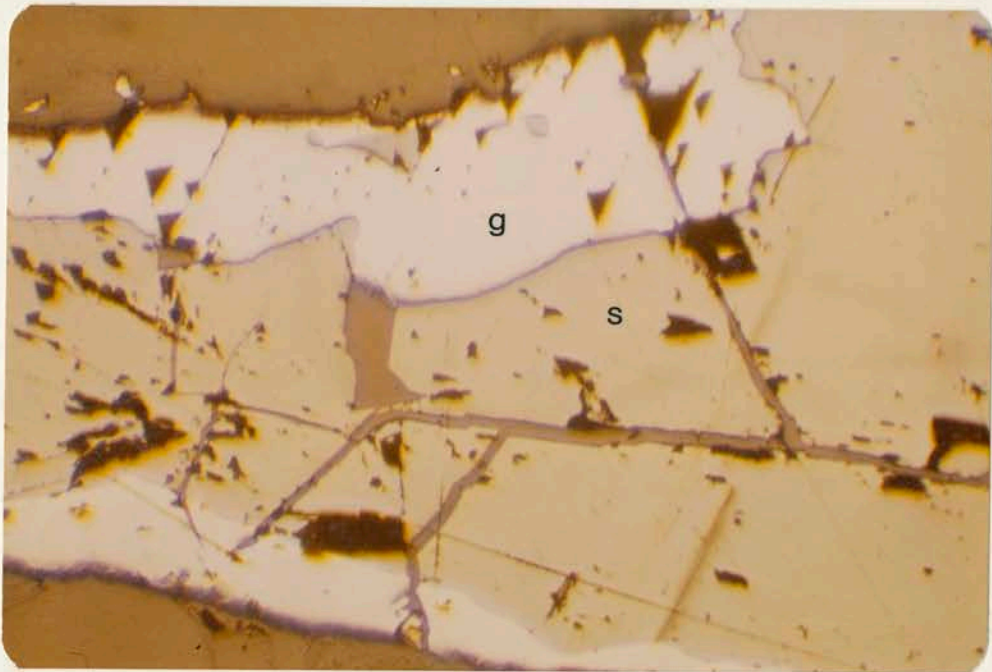
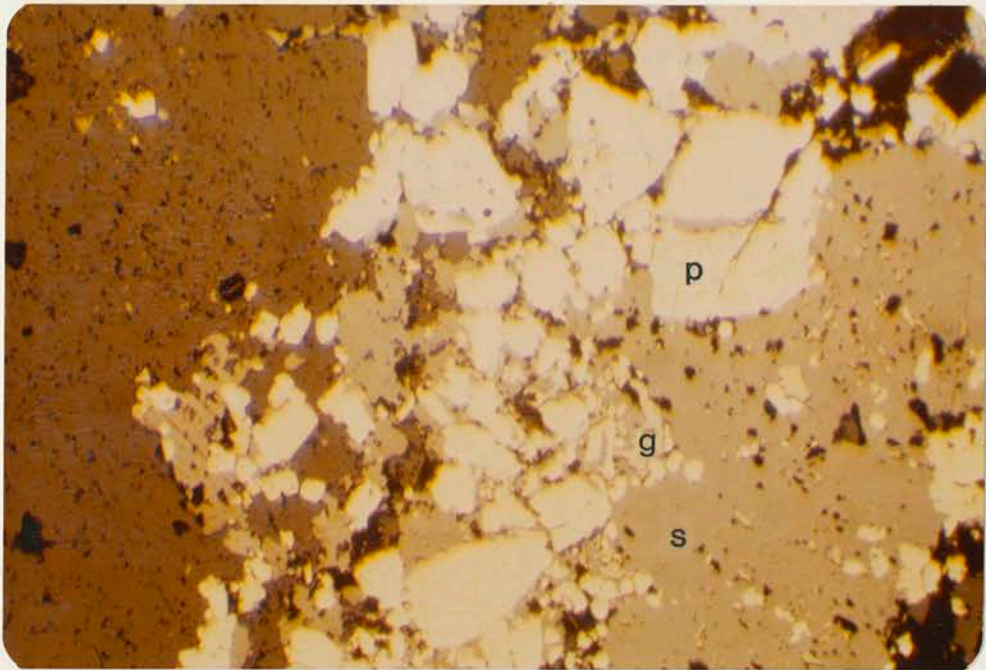
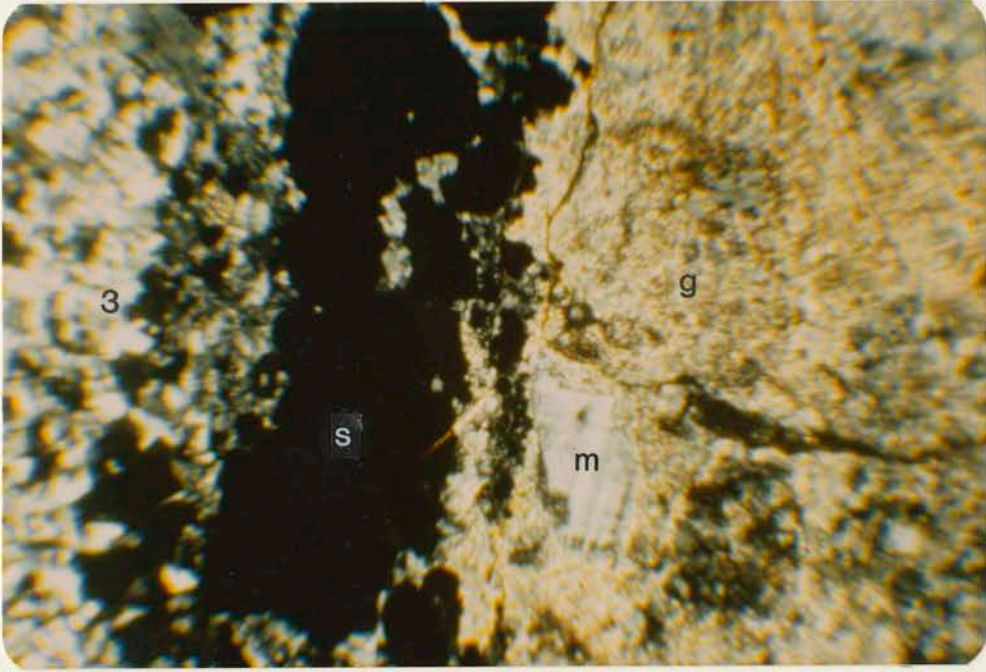


Figure 24. A. Photomicrograph of polished-section from Bobtail vein, 3350 level (horizontal field of view = 0.63 mm). Showing pyrite(p) replaced by sphalerite(s) and galena(g).

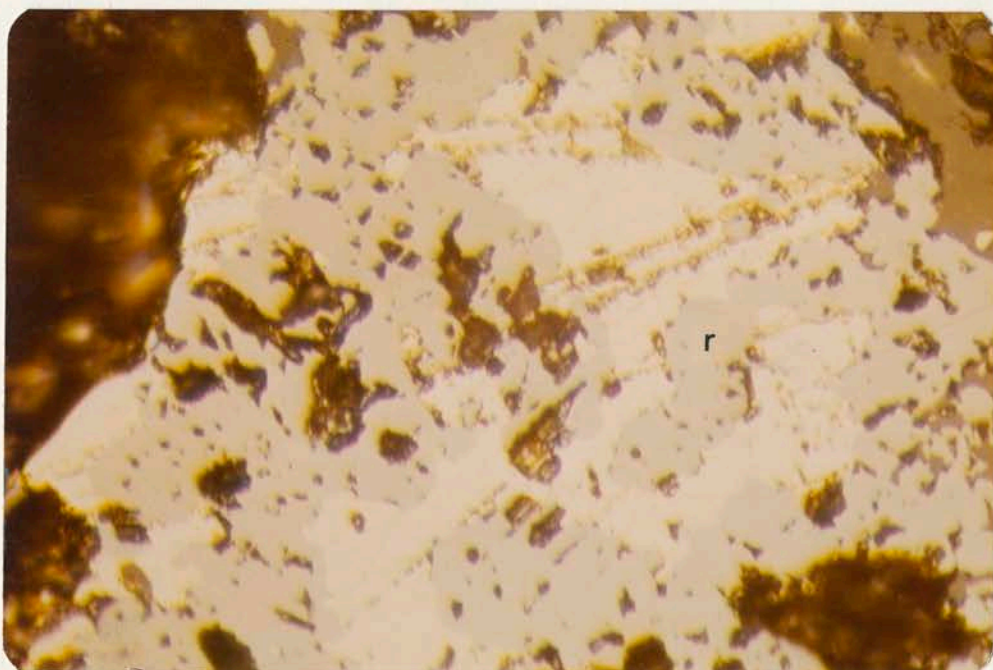
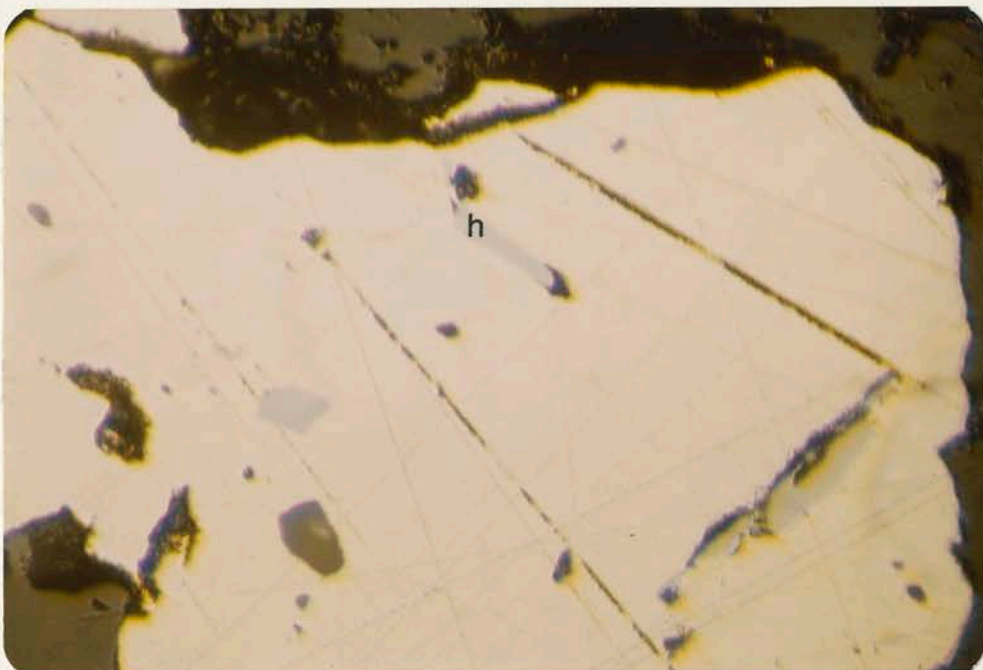
B. Photomicrograph of polished-section from unnamed vein, 1000 level (horizontal field of view = 0.63 mm). Showing galena(g) replacing sphalerite(s).



- Figure 25. A. Photomicrograph of thin-section from Bobtail vein, 2600 level (horizontal field of view = 3 mm). Showing altered granite wallrock(g) (note fresh microcline(m)) in contact with stage 2 opaque sulfides(s). Stage 2 is overgrown by stage 3 quartz and fluorite(3).
- B. Photograph of Bobtail vein (2600 level), hand specimen. Showing stage 3 quartz-fluorite intergrowth(3) and fracture control of alteration. Note more intense alteration on footwall side of vein associated with two parallel fractures.



- Figure 26. A. Photomicrograph of polished-section from Bobtail vein, 2600 level (horizontal field of view = 0.265 mm). Showing specular hematite inclusions(h) in pyrite.
- B. Photomicrograph of polished-section from Christensen vein, 1400 level (horizontal field of view = 0.63 mm). Showing rutile overgrowth(r) on pyrite.

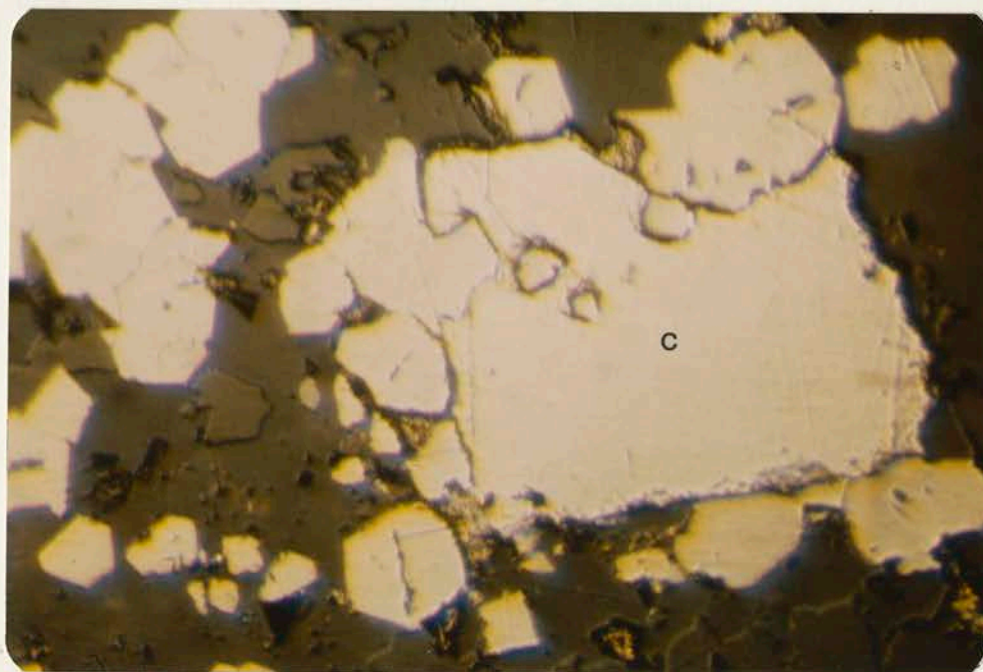
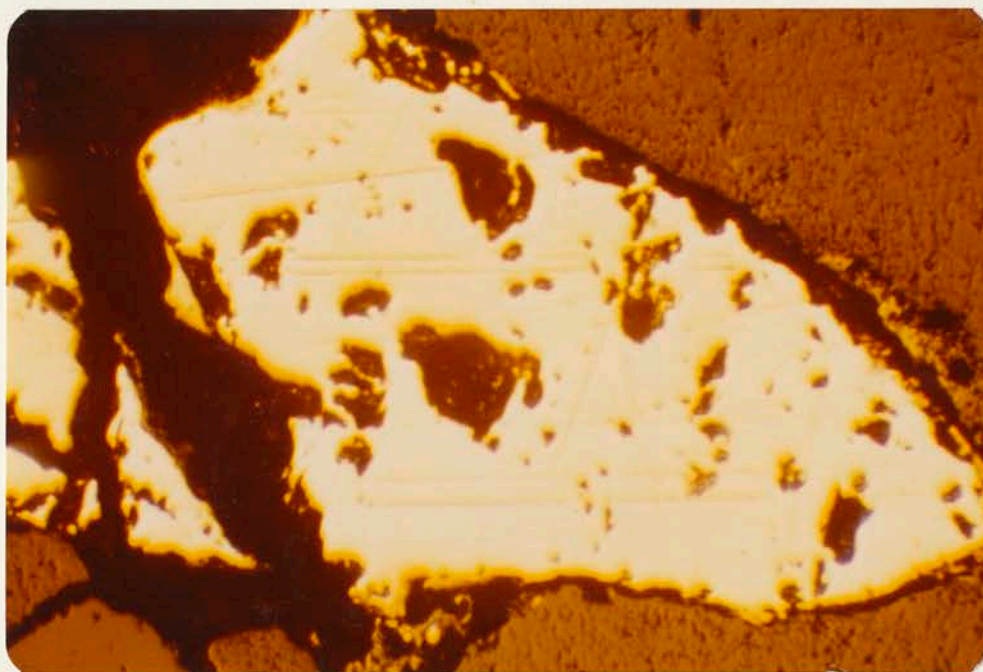


as anhedral overgrowths on the pyrite of stages 1, 2, 3, and 4 (Fig. 26b). Rutile also occurs as isolated globular aggregates. The presence of titanium and iron oxides in association with sulfide minerals has significant bearing on the physical chemistry of the ore system. The exact time of oxide introduction is difficult to ascertain, and it is possible that more than one period of oxide mineralization has occurred. In a brief reference to Cripple Creek, Ramdohr (1980) states that as the result of increasing sulfur ion concentration due to falling temperature and pressure, pyrite replaces specular hematite in the Cripple Creek ores. No textures indicating replacement of hematite by pyrite were observed in polished sections of the Ajax veins.

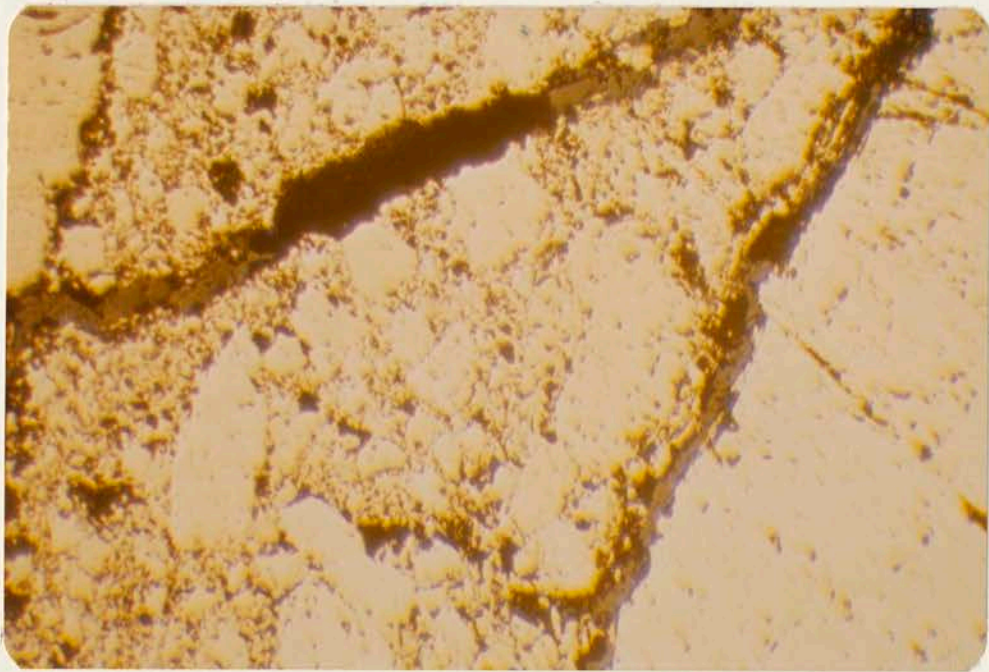
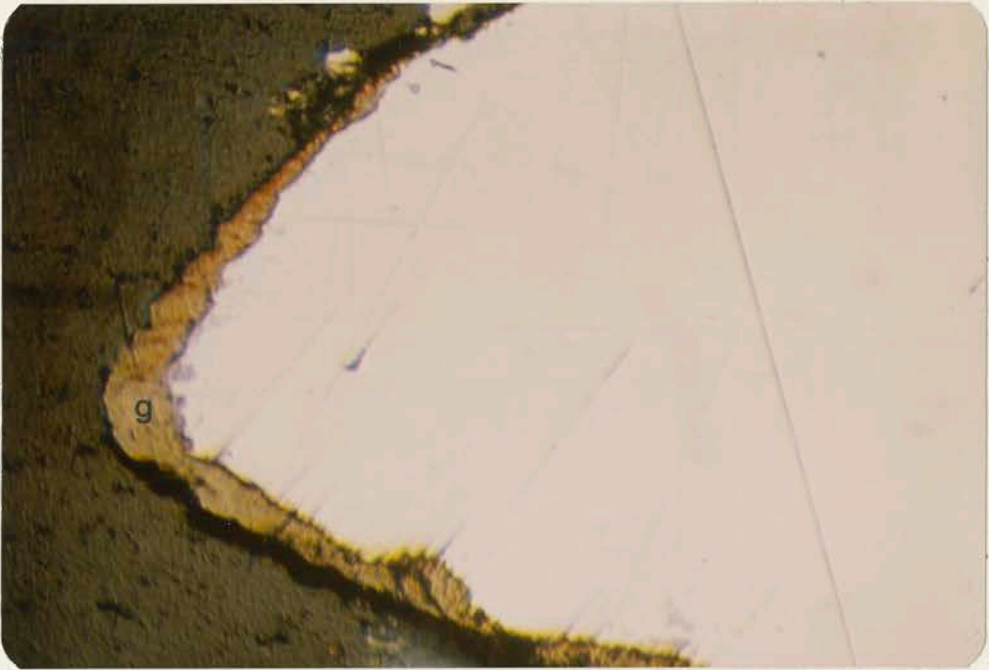
4. Stage 4

The fourth stage of vein mineralization is the most economically important stage. Where best developed it consists of milky white euhedral quartz that partially fills open vugs, fine subhedral (15-25 μm) pyrite, and bladed calaverite crystals (Figs. 22a, 27a, 29b, 31a, 31b). Rutile is present both as discrete anhedral grains and as overgrowths on pyrite. The vuggy nature of this stage is significant, since the highest gold values invariably occur where the vuggy texture is present. The absence of fourth stage quartz does not preclude gold-telluride mineralization. Calaverite was observed replacing the pyrite of earlier stages in several sections (Fig. 27b). Generally, the calaverite replaces the latest pyrite of the earlier stage and does not replace fourth stage pyrite. Electron microprobe analysis of the calaverite indicates that it is composed of 30% gold, 3.5% silver, and approximately 66% tellurium. Calaverite was the only telluride positively identified. Acanthite intergrown with calaverite was

- Figure 27. A. Photomicrograph of polished-section from Bobtail vein, 3100 level (horizontal field of view = 0.63 mm). Showing stage 4 calaverite in quartz.
- B. Photomicrograph of polished-section from Newmarket vein, 3100 level (horizontal field of view = 0.265 mm). Showing stage 4 calaverite(c) replacing pyrite of an earlier stage.



- Figure 28. A. Photomicrograph of polished-section from Bobtail vein, (same section as 27-A) (horizontal field of view = 0.265 mm). Showing free gold-tellurite rim (g) on calaverite.
- B. Photomicrograph of polished-section from Bobtail vein, 3350 level (horizontal field of view = 0.63 mm). Showing brecciated early pyrite with later pyrite overgrowth and matrix filling. Note late quartz veinlet cutting pyrite.



observed in one section and a brownish-gold rim composed of 75% gold, 10% silver, and 15% tellurium (normalized) occurs on the same grain (Figs. 27a, 28a). The composition and optical properties of the rimming mineral do not correspond to any of the known tellurides (Uytenbogaardt and Burke, 1971). It may represent a mixture of tellurite and native gold formed by the oxidation of calaverite. Lane (1976) reports a similar occurrence in ores of the El Paso mine.

5. Stage 5

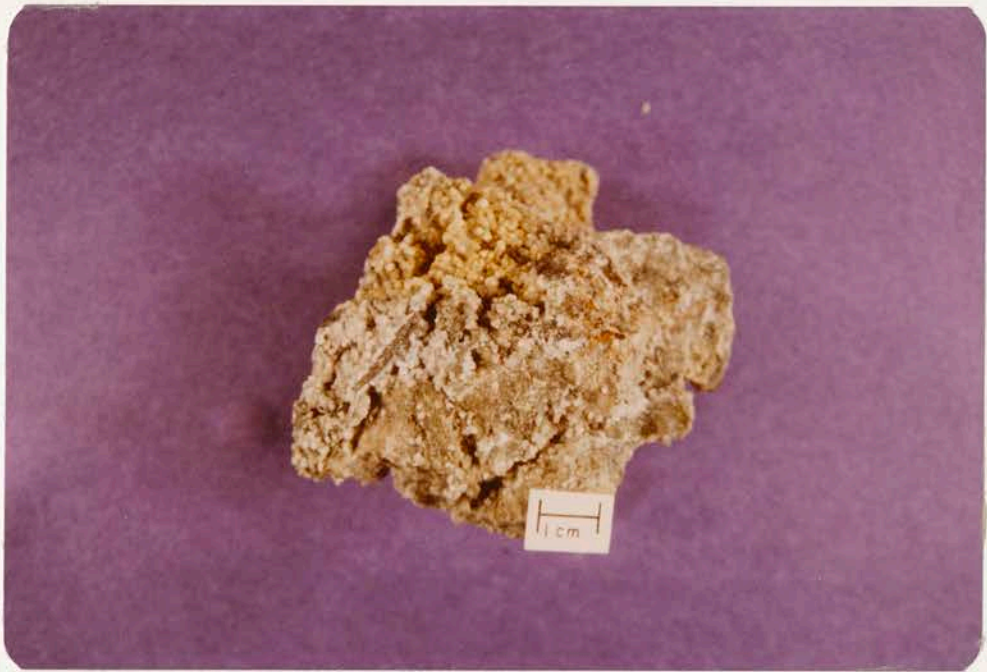
Stage five represents a relatively minor constituent of the vein assemblage. Fifth stage mineralization occurs only where open vugs were still present following fourth stage deposition. Stage five consists of fine euhedral fluorite, minute quartz euhedra, and euhedral dolomite, all of which occur as vug-filling minerals (Fig. 29a, 29b). A late stage drusy opaline quartz was observed in samples from the Newmarket and Newmarket Shear veins. The significance of fifth stage mineralization is that it commonly obscures minerals of the fourth stage. A valid assumption that can be made is that the presence of stage five generally implies the presence of stage four.

C. Vein Morphology

1. Bobtail vein

The Bobtail characteristically exhibits the most complete development of the paragenetic sequence. Although all five stages are not present in any one vein section, generally at least two, and more commonly, three or four stages are represented (Fig. 22a, 25b, 29a, 29b, 30a). The Bobtail also exhibits the most complex structural activity of the veins sampled. As many as four fracture events can be documented in

- Figure 29. A. Photograph of Bobtail vein, (3350 level), hand specimen. Showing vuggy, stage 5 euhedral dolomite coating fragments of altered granite.
- B. Photograph of Bobtail vein (cut slab of same sample as above). Showing roscoelite(r) altered granite fragments overgrown by dark grey stage 1(l), euhedral stage 4 quartz(q) and calaverite, and stage 5 dolomite(d).



- Figure 30. A. Photograph of Bobtail vein (3350 level), hand specimen. Showing stage 3 quartz-fluorite(3) in highly fractured phonolite.
- B. Photograph of Bobtail vein (2300 level), hand specimen. Showing multiple fracture events (1-4) and mineral repetition in stage 3. Note weak wallrock alteration.



Bobtail vein samples (Fig. 30b). The movement was limited to a subtle opening and occasional minor breccia formation with no recognizable lateral or vertical offset. The amount of opening that occurred is generally less than 1 cm but can be as much as 5 cm. This structural activity in the form of minor opening and breccia development is the principal reason for the diverse composition of the Bobtail. The fissures that host the veins were selectively opened and closed, causing fluctuations in both the ore locus and the physio-chemical conditions influencing vein mineral deposition. This caused the observed partial omissions of the paragenetic sequence.

2. Newmarket vein

The Newmarket vein composition sharply contrasts that of the Bobtail. The Newmarket is dominated by the milky white, euhedral quartz of stage four (Fig. 31a, 31b). Stages one and three may be present, but their development is minor. Stages two and five are rarely present with the exception of a minor stage two component observable in thin section and one sample containing stage 5 quartz and fluorite. The Newmarket generally does not exhibit evidence of multiple stages of fracturing, and the sheeted structure characterizing the Bobtail is absent (Fig. 17). Similar to the Bobtail, the Newmarket exhibits variable composition and partial omission of the paragenetic sequence indicating minor movement did occur during vein deposition. The lack of stage repetition and breccia development indicate the movement occurring along the Newmarket structure was less significant than the movement along the Bobtail.

- Figure 31. A. Photograph of Newmarket vein (2000 level), hand specimen. Showing exclusion of all stages except stage 4 quartz. Note extremely weak wallrock alteration.
- B. Photograph of Newmarket vein (3100 level), hand specimen. Showing "bughole granite" type mineralization. Formed by dissolution of biotite and plagioclase with subsequent infilling of vugs by late stage mineralization.



3. Other veins

The other veins sampled generally exhibit a composition corresponding to the particular fracture trend to which they belong. These veins were not sampled in enough detail to be specifically defined. The Christensen and Apex veins are similar to the Bobtail vein in morphology and composition. The X-10-U-8, Mohican, and Newmarket Shear veins are all members of the north-northwest set. Although sampling of these veins was sporadic, a few general characteristics of each can be noted.

The X-10-U-8 vein consists primarily of second and third stage mineralization with the second stage component occurring in minute vugs. The vein is unsheeted with no evidence of multiple shearing events and varies in width from 1-4 cm.

The Mohican is a narrow, unsheeted vein. Extremely variable in composition, it ranges from dominantly second and third stage minerals to dominantly first and fourth stage minerals. The vein exhibits no evidence of multiple fracturing and is 1-2 cm wide (Fig. 32a).

The Newmarket Shear has the most diverse morphology of the north-northwest set. Characteristically, it consists of multiple subparallel mineralized fractures. The fractured zone is 0.5 ft (15 cm) to 2 ft (0.6 m) wide. Fracturing occurred prior to mineralization, as evidenced by the lack of symmineral or postmineral fracturing.

D. Vertical Metal Zonation

The purpose of sampling the Ajax vein system was to examine the ore fluid metal chemistry as reflected in the composition of the veins and altered wallrock. As reported in Table I, vein samples are 4 to 6 in (10-15 cm) wide and are composed of vein mineralization only. Samples

Table I. Geochemical Analyses of vein and wallrock samples: Ajax Vein System, Cripple Creek, Colorado

| Sample no. and Location | Sample Type | Concentration, ppm | | | | | | | | | | | | |
|-------------------------|-------------|--------------------|-------|--------|--------|-----|-----|-----|------|-----|------|------|------|-------|
| | | Au:Ag | Au:Te | Au | Ag | Cd | Co | Cu | Mo | Ni | Pb | Te | V | Zn |
| 4-B | V | 0.81 | 1.08 | 0.063 | 0.078 | 15. | 9. | 7. | 35. | 6. | 160. | 2.0 | L15. | 2200. |
| 4-B | V | | | 0.005 | 0.106 | | | | | | | 0.4 | | |
| 4-B:FW | FG | | | L0.005 | L0.005 | | | | | | | 0.4 | | |
| 7-M-1 | V | | | 0.012 | 0.406 | 1.5 | 5. | 25. | 120. | 4. | 75. | 6.2 | 15. | 180. |
| 7-M-2 | V | 7.0 | 0.88 | 1.07 | 0.153 | 2.7 | 7. | 10. | 40. | 5. | 140. | 41.5 | 65. | 250. |
| 7-M-1:HW | AG | | | 0.012 | 0.108 | | | | | | | 1.4 | | |
| 7-M-1:HW | FG | | | L0.005 | L0.005 | | | | | | | 0.4 | | |
| 10-A-1 | V | | | 0.01 | 0.53 | 45. | 21. | 12. | 320. | 15. | 240. | 1.2 | L15. | 6500. |
| 10-NM-2 | V | 1.96 | 0.53 | 0.100 | 0.051 | 0.9 | 9. | 10. | 13. | 7. | 16. | 6.4 | 60. | 25. |
| 10-NM-2:HW | AG | | | L0.005 | L0.005 | | | | | | | 0.2 | | |
| 14-C-1 | V | 0.67 | 0.73 | 0.178 | 0.267 | 4.0 | 14. | 18. | 170. | 12. | 80. | 8.4 | 230. | 110. |
| 14-C-1 | AG | 1.61 | 1.2 | 0.063 | 0.039 | | | | | | | 1.8 | | |
| 14-C-1 | FG | | | L0.005 | L.005 | | | | | | | 0.4 | | |
| 14-M-1 | V | 0.20 | 0.44 | 0.118 | 0.58 | 1.6 | 17. | 8. | 45. | 9. | 17. | 9.2 | 120. | 25. |
| 14-M-2 | AG | | | L0.005 | L0.005 | | | | | | | 0.4 | | |
| 16-X | V | | | 0.032 | 0.050 | 3.0 | 10. | 6. | 90. | 8. | 250. | 0.8 | L15. | 130. |
| 16-X:PH | AP | | | L0.005 | L0.005 | | | | | | | 0.6 | | |
| 16-C | V | 0.93 | 0.62 | 0.190 | 0.204 | 1.3 | 6. | 16. | 360. | 5. | 160. | 10.4 | 80. | 80. |
| 16-Z | V | 1.0 | 1.05 | 0.123 | 0.126 | 2.0 | 7. | 11. | 430. | 6. | 190. | 4.0 | 130. | 140. |
| 16-M | V | 4.0 | 1.15 | 0.478 | 0.118 | 0.9 | 3. | 16. | 170. | 3. | 8. | 14.2 | 500. | 80. |
| 16-M:PH | AP | | | L0.005 | L0.005 | | | | | | | 1.0 | | |
| 20-BT | V | 15.0 | 0.74 | 1.71 | 0.114 | 4.2 | 15. | 12. | 25. | 18. | 55. | 79.0 | 240. | 100. |
| 20-BT:FW | AG | | | L0.005 | L0.005 | | | | | | | 0.4 | | |
| 20-BT:PH | AP | | | L0.005 | L0.005 | | | | | | | 0.8 | | |
| 20-BT | AG | | | L0.005 | L0.005 | | | | | | | 0.6 | | |
| 20-NM-1 | V | 1.1 | 0.99 | 0.130 | 0.12 | 0.2 | 4. | 12. | 5. | 4. | 9. | 4.5 | 25. | 20. |
| 20-NM-1:HW | AG | | | L0.005 | L0.005 | | | | | | | 0.2 | | |
| 20-NM-2 | V | 4.7 | 0.93 | 0.299 | 0.064 | 0.6 | 12. | 11. | 11. | 5. | 15. | 11.0 | 130. | 50. |
| 20-U | V | | | 0.019 | 0.034 | 3.4 | 13. | 18. | 40. | 12. | 40. | 1.2 | 85. | 140. |
| 23-BT | V | 1.4 | | 0.197 | 0.137 | 3.4 | 10. | 30. | 95. | 9. | 170. | 8.8 | 130. | 250. |

Table I. (continued) Geochemical Analyses: Ajax Vein System, Cripple Creek, Colorado

| Sample no. and Location | Sample Type | Concentration, ppm | | | | | | | | | | | | |
|-------------------------------|----------------|--------------------|-------|--------|--------|------|-----|-----|------|-----|------|-------|------|-------|
| | | Au:Ag | Au:Te | Au | Ag | Cd | Co | Cu | Mo | Ni | Pb | Te | V | Zn |
| 23-BT:HW | AG | | | 0.030 | 0.032 | | | | | | | 1.2 | | |
| 23-BT | FG | | | 10.005 | 10.005 | | | | | | | 0.4 | | |
| 23-M | V | 7.3 | 0.93 | 1.3 | 0.177 | 7.0 | 30. | 30. | 230. | 8. | 320. | 48.0 | 260. | 600. |
| 23-M:HW | FG | | | 10.005 | 10.005 | | | | | | | 0.2 | | |
| 26-BT | V | 0.83 | 0.97 | 0.079 | 0.095 | 26. | 12. | 30. | 200. | 11. | 350. | 2.8 | 100. | 4100. |
| 26-BT | V | 0.93 | 1.82 | 0.085 | 0.091 | | | | | | | 1.6 | | |
| 26-BT:FW | AG | 4.1 | | 0.114 | 0.028 | | | | | | | | | |
| 26-BT:PH | AP | | | 10.005 | 0.005 | 1.1 | 8. | 12. | 230. | 5. | 9. | 0.4 | 115. | 75. |
| 26-BT:HW | FG | | | 10.005 | 10.005 | | | | | | | 0.4 | | |
| 26-NM-1 | V | 4.9 | 0.68 | 0.441 | 0.089 | 0.8 | 10. | 8. | 9. | 6. | 20. | 22.0 | 55. | 45. |
| 26-NMS | V | 2.2 | 0.59 | 0.152 | 0.070 | 2.8 | 14. | 11. | 260. | 18. | 150. | 8.8 | 260. | 330. |
| 30-BT | V | 0.48 | 0.38 | 0.665 | 1.38 | 3.7 | 11. | 80. | 470. | 7. | 310. | 60.0 | 540. | 460. |
| 30-BT:HW | AG | | | 0.029 | 0.005 | | | | | | | 1.2 | | |
| 30-BT:FW | AG | | | 0.011 | 0.006 | | | | | | | 0.4 | | |
| 30-BT:PH | AP | | | 0.012 | 0.012 | | | | | | | 1.4 | | |
| 31-BT | V | 23.0 | 1.25 | 20.8 | 0.904 | | | | | | | 570.0 | | |
| 31-BT-2 | V | 8.3 | 0.77 | 5.24 | 0.629 | 4.2 | 11. | 40. | 160. | 10. | 550. | 233.0 | 210. | 570. |
| 31-BT:HW | AG | 4.0 | 1.02 | 2.88 | 0.72 | | | | | | | 97.0 | | |
| 31-BT:HW | AG | | | 0.011 | 0.010 | | | | | | | 3.0 | | |
| 31-NM-3 | V | 4.6 | 0.77 | 0.779 | 0.170 | 0.8 | 9. | 17. | 18. | 6. | 35. | 34.4 | 190. | 30. |
| 31-NM:BH | V | 3.6 | 0.49 | 0.417 | 0.117 | | | | | | | 29.0 | | |
| 31-N-1 | V | 4.5 | 0.54 | 1.90 | 0.423 | 1.5 | 11. | 30. | 40. | 8. | 80. | 120.0 | 410. | 35. |
| 31-NS-1 | V | 11.2 | 1.09 | 3.82 | 0.340 | 1.0 | 8. | 25. | 11. | 6. | 19. | 296.0 | 180. | 30. |
| 31-XT-1 | V | 2.7 | 0.78 | 0.153 | 0.056 | 3.5 | 9. | 12. | 160. | 8. | 30. | 6.7 | 260. | 280. |
| 33-BT-4 | V | 1.7 | 0.74 | 0.511 | 0.305 | 10.6 | 8. | 90. | 200. | 7. | 480. | 23.5 | 950. | 2300. |
| 33-BT-2 | V | 1.7 | 0.76 | 0.239 | 0.140 | 12.6 | 10. | 35. | 240. | 9. | 250. | 10.8 | 200. | 2200. |

Table I. (continued) Geochemical Analyses: Ajax Vein System, Cripple Creek, Colorado

| Sample no. and Location | Sample Type | Au:Ag | Au:Te | Au | Ag | Cd | Co | Cu | Concentration, ppm | | | | | |
|-------------------------------|----------------|-------|-------|--------|--------|-----|-----|-----|--------------------|-----|------|------|------|-------|
| | | | | | | | | | Mo | Ni | Pb | Te | V | Zn |
| 33-BT:PH | V | 0.27 | 0.51 | 0.183 | 0.685 | 23. | 15. | 30. | 200. | 15. | 690. | 12.2 | 760. | 3100. |
| 33-BT:HW | AG | | | 0.024 | 10.005 | | | | | | | 2.2 | | |
| 33-BT:FW | AG | | | 10.005 | 10.005 | | | | | | | 1.2 | | |

4 = 400 level, 7 = 700 level, 10 = 1000 level, 14 = 1400 level, 16 = 1600 level, 20 = 2000 level, 23 = 2300 level, 26 = 2600 level, 30 = 3000 level, 31 = 3100 level, 33 = 3350 level

B = B vn, M = Mohican vn, A = unnamed vn, NM and N = Newmarket vn, C = Christensen vn, X and Z = breccia-hosted vns, BT = Bobtail vn, U = unnamed vn, NMS and NS = Newmarket Shear vn, V = vein

FG = fresh granite, AG = altered granite, AP = altered phonolite, FW = footwall, HW = hanging wall, PH = phonolite dike, BH = bughole granite

Au and Ag reported in oz/ton, lower detection limit = 0.005 oz/ton

Base metals reported in PPM, L150 indicates less than 150 ppm

Note: see sample locations on plan maps (Figs. 4-14)

- Figure 32. A. Photograph of Mohican vein (2300 level), hand specimen. Showing stage 3 quartz-fluorite vein. Note weak wallrock alteration.
- B. Photograph of breccia-hosted vein (1600 level), hand specimen. Showing pervasive alteration of breccia and irregular fracturing. Note stage 3 fluorite(f) in vugs.



of granite and phonolite are hand specimens approximately 3 to 6 in (7.5-15 cm) wide.

No consistent vertical variation in Au/Ag ratio has been recognized (Table I). Au/Ag ratios vary from 23:1 to 0.20:1. Magnitude of the ratio is controlled by gold content; higher ratios correlate with increased gold tenor.

Au/Te ratios were calculated in an attempt to determine whether gold content in the tellurides (calaverite) varies with depth. As shown in Table I, the Au/Te ratio varies from 0.38 to 1.82 in mineralized samples (Au 0.06 oz/T), and exhibits no consistent vertical variation.

Lack of precious metal zoning in the Ajax system contrasts with the gold-telluride bearing vein systems of Vatukoula, Fiji (Denholm, 1967). At Vatukoula, gold-tellurides are replaced by more argentiferous tellurides and sulfides with increasing depth. Zoning at Vatukoula can be recognized within a vertical distance of 900 feet (274 m).

A subtle increase in base metal values occurs in samples from the lower mine levels of the Ajax (Table I). This may reflect initial development of a subtle zoning pattern similar to that observed at Vatukoula. Sample data from the Ajax vein system are far from conclusive.

As shown in Table I, the Newmarket vein has significantly lower base metal enrichment than the Bobtail. This is further evidence in support of the suggestion that the Newmarket fissure opened at a later time than the Bobtail.

An additional inference present in the geochemical data regards silver content of the veins. Although not independent of gold content, silver content can be relatively high without correspondingly high gold

values. This indicates that significant silver is present in association with stage 2 sulfides. No silver minerals were identified in stage 2. Lack of correlation between silver and other base metals indicates that silver is present as a discrete mineral phase, erratically distributed in stage 2 mineralization.

The lack of or weak development of metal zonation in the Ajax veins may indicate that the mineralization was formed by a hydrothermal system of relatively great dimension.

CHAPTER V
VEIN-RELATED ALTERATION

A. Introduction

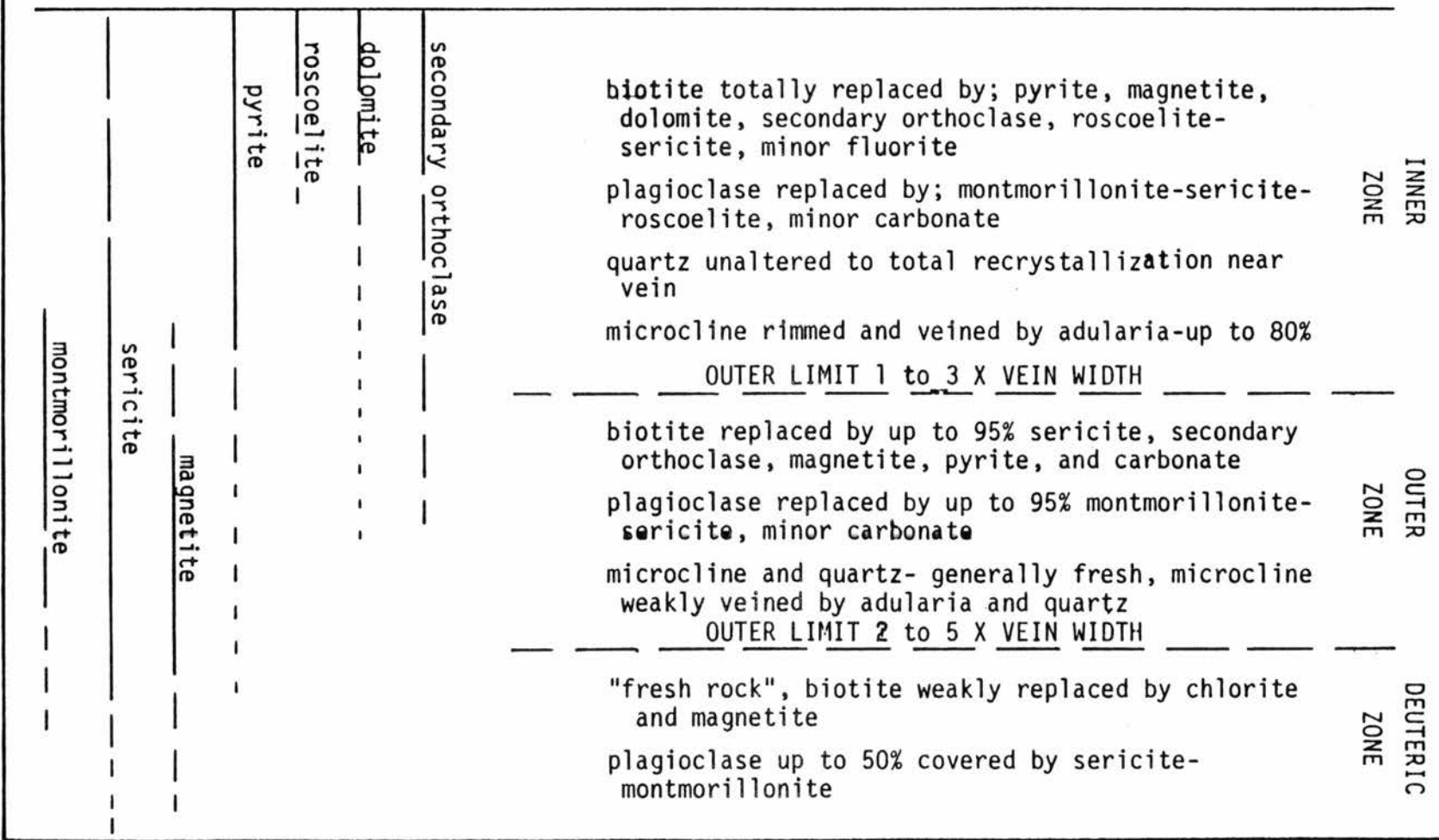
Wall-rock alteration associated with the Ajax vein system was studied using thin section and X-ray diffraction analyses. Sequential thin sections of cross sections through the different veins were prepared to determine mineral composition, intensity, and extent of the alteration assemblage. In addition to petrographic analysis, X-ray diffraction was used to identify the more obscure minerals. By these methods, two distinct zones of vein-related alteration have been identified (Fig. 33).

The only previous work on vein-related alteration in the district was performed by Lindgren and Ransome (1906), although pertinent observations specifically dealing with alteration of the granite were made by Rickard (1902).

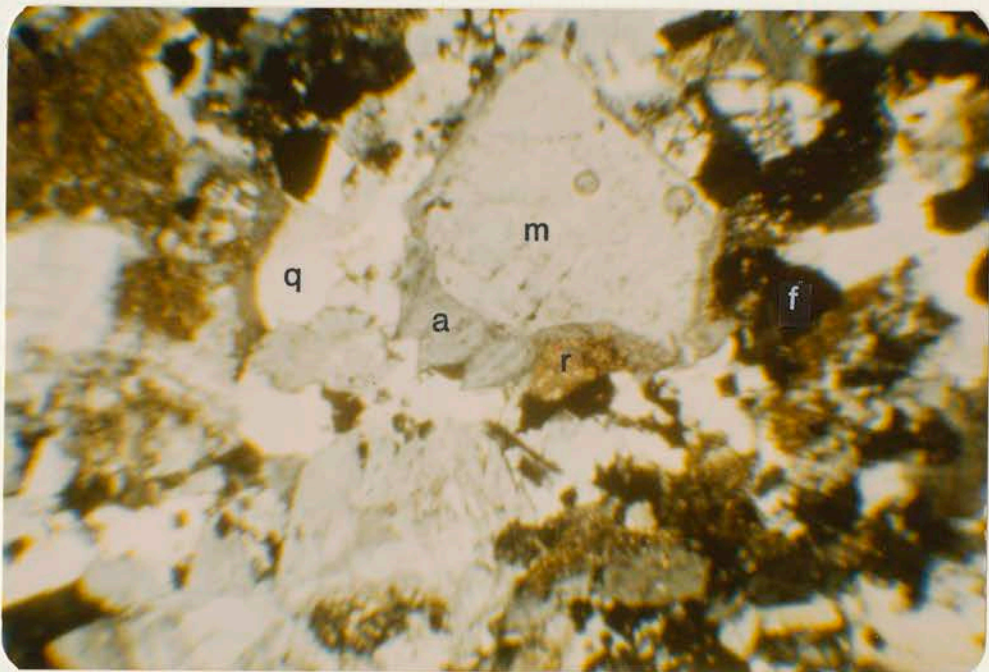
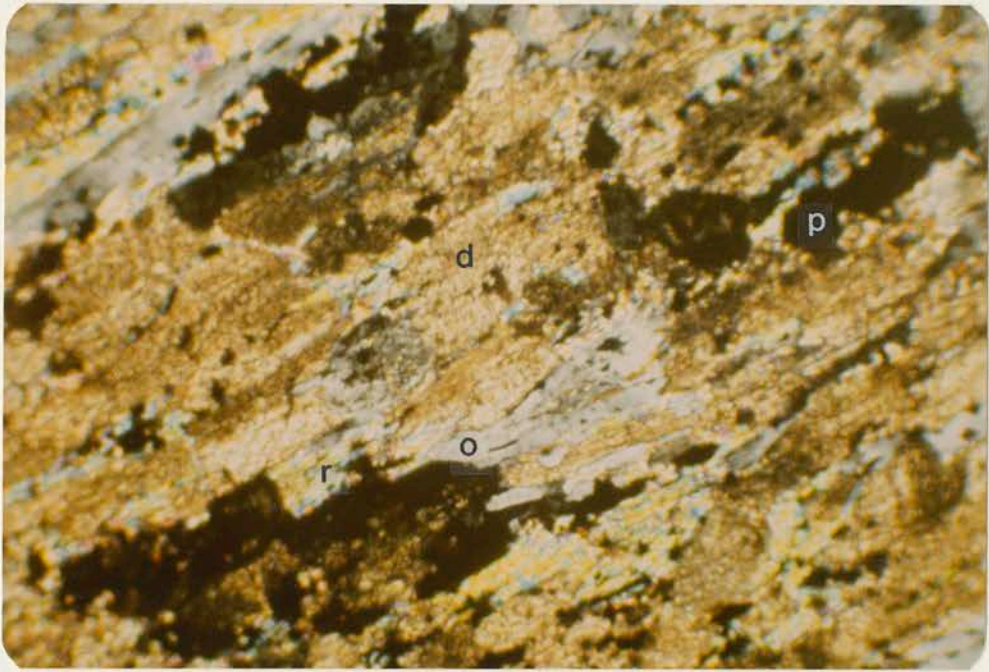
An attempt to determine the age of alteration by K/Ar methods was unsuccessful. Roscoelite, a vanadium-bearing sericite, was the mineral on which the age determination was attempted. Roscoelite intergrown with sericite replaces primary Precambrian biotite and plagioclase in the Ajax system. The result of the age determination, 153 ± 5 MYBP, is significantly older than determinations made on alkaline intrusive-volcanic rocks in the district (Chap. II, A). From observed field relations, it is known that vein mineralization post-dates the most

Figure 33. Diagram showing vein-related alteration in the Ajax vein system.

V E I N



- Figure 34. A. Photomicrograph of thin-section from Bobtail vein, 2600 level (horizontal field of view = 1 mm). Showing pseudomorphic replacement of biotite by dolomite(d), secondary orthoclase(o), roscoelite-sericite(r), and pyrite(p).
- B. Photomicrograph of thin-section from Bobtail vein, 3350 level (horizontal field of view = 3 mm). Showing inner zone alteration; adularia(a) rimming microcline(m), roscoelite(r), recrystallized quartz(q), and fluorite(f).



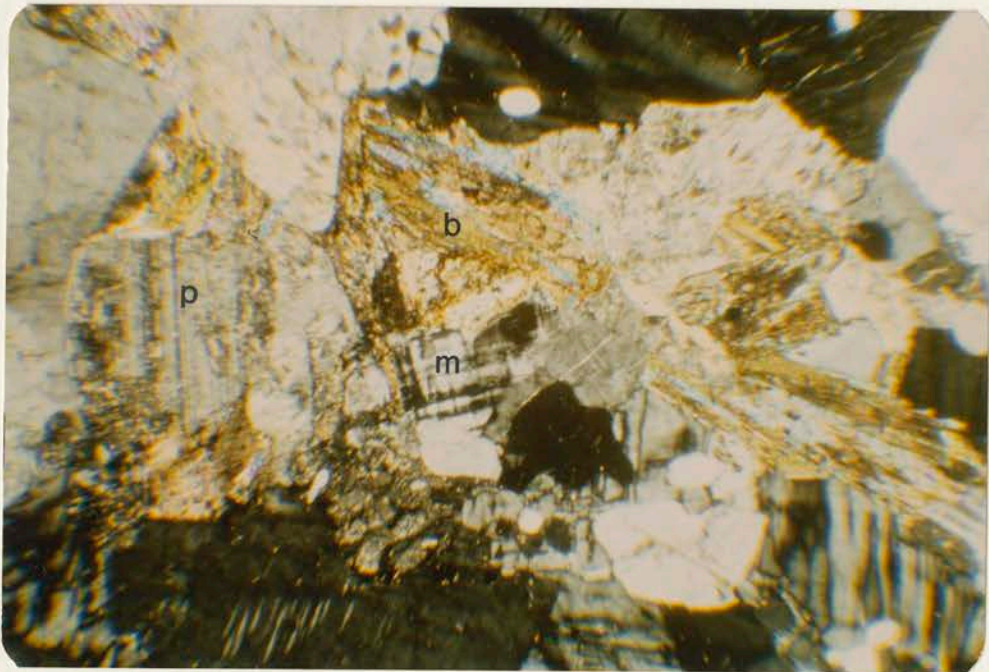
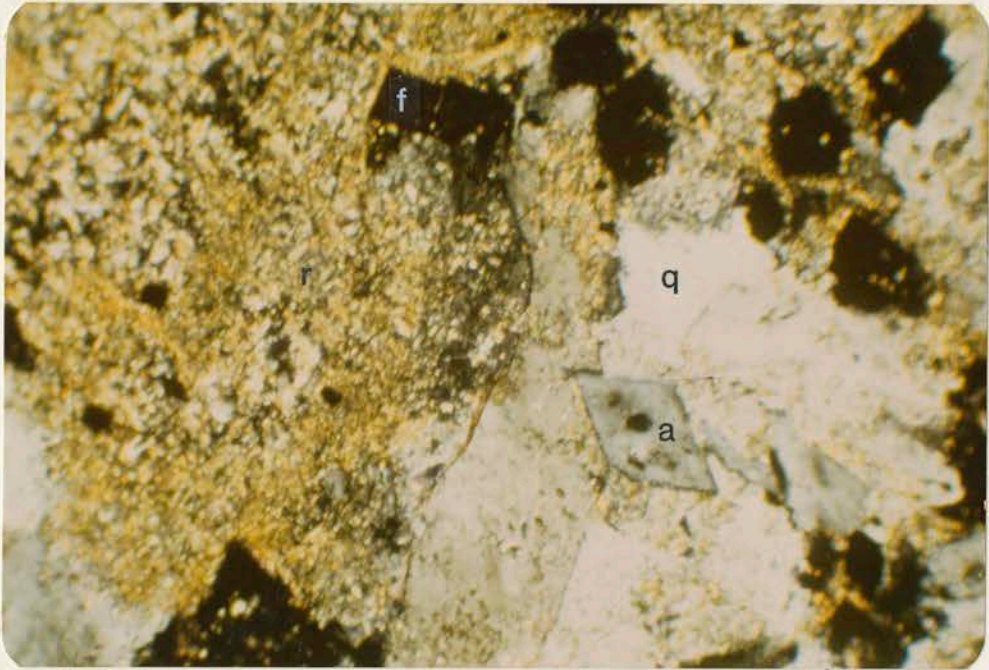
recent intrusive activity. Therefore it is implausible that the roscoelite-determined date is accurate. A likely explanation is that the alteration did not completely replace the primary Precambrian biotite and/or the sericite may be deuteritic. Although adularia is present in the Ajax veins, and is amenable to K/Ar dating, it is not coarse enough to allow collection of a separate of sufficient volume.

B. Lateral Zonation

1. Inner zone

The inner zone of vein-related alteration is easiest to recognize megascopically. Varying in width from less than one to three times the width of the vein, it is characterized by total replacement of biotite by variable amounts of pyrite, magnetite, dolomite, secondary orthoclase, roscoelite-sericite, and minor fluorite (Fig. 34a). Rickard (1902) was the first to study the alteration of granite hosting the veins and recognize the inner zone of biotite destruction. Honeycombing (dissolution vugs) of the granite and the presence of valencianite (adularia) also were documented by Rickard (1902). Microcline of the inner zone is rimmed and veined by adularia (20%-80%) and weakly dusted by sericite (Fig. 34b). Minor secondary quartz occurs locally with the adularia replacement of microcline. The plagioclase (oligoclase) of the inner zone is totally replaced by variable amounts of veinlet-controlled montmorillonite, sericite, roscoelite, and minor carbonate (Fig. 35a). Inner zone quartz has undergone a slight recrystallization and, in the more intensely altered areas, a complete dissolution and reprecipitation has occurred. Secondary quartz is easily distinguished by its characteristic feathery habit seen in thin section. Apatite and zircon are unaltered even in the areas of most intense alteration. They

- Figure 35. A. Photomicrograph of thin-section from Bobtail vein, 3350 level (horizontal field of view = 1 mm). Showing inner zone alteration; euhedral adularia(a), roscoelite(r), recrystallized quartz(q), and scattered fluorite(f).
- B. Photomicrograph of thin-section from X-10-U-8 vein, 3100 level (horizontal field of view = 3 mm). Showing outer zone alteration; sericite-dolomite-adularia after biotite(b), montmorillonite-sericite on plagioclase(p), adularia rimming microcline(m), and slightly recrystallized quartz.



commonly have been deposited as xenocrysts within the veins.

This inner alteration zone associated with the Ajax veins is similar in nature to alteration associated with the pyritic-gold-telluride veins of Jamestown, Colorado. As described by Bonorino (1959), alteration around the veins is characterized by the stability of quartz and microcline and the introduction of sericite, secondary orthoclase, and minor secondary quartz.

Lindgren and Ransome (1906) first identified roscoelite as an alteration product associated with the telluride veins of Cripple Creek. In this study, identification of roscoelite was performed both by petrographic and X-ray analysis. Significant discrepancies exist in the X-ray data reported for roscoelite. Heinrich and Levinson (1955) report results from a study dealing specifically with the X-ray characteristics of roscoelite. X-ray results for Ajax "roscoelite" correlate well with the data of Heinrich and Levinson (1955). A poorer correlation exists between data reported for roscoelite in the J.C.P.D.S. powder diffraction file (Berry, 1974) and the data obtained in this study, although the pattern for roscoelite is still the best fit. The optical properties of Ajax "roscoelite" as seen in thin section are similar to muscovite. However, a yellow-green tint of variable intensity is present when viewed in unpolarized light, apparently caused by the presence of vanadium. This distinguishing characteristic agrees with previously reported information regarding roscoelite (Lindgren and Ransome, 1906). Whether the material identified as roscoelite in this study is a true roscoelite or a vanadiferous muscovite is still open to question. Most likely, a solid-solution exists between the two mica species and the composition and structure of the Ajax material lies

somewhere between the two end members. As documented by Kelly and Goddard (1969), roscoelite occurs in the gold-telluride veins of Boulder County, Colorado. Although the roscoelite recognized at Boulder County occurs as a vein constituent, it probably is present as an alteration product as well.

2. Outer zone

The inner boundary of the outer zone of vein-related alteration is defined by the presence of relict biotite cores (Fig. 35b). Extent of the outer zone of alteration varies from two to five times the width of the vein. Biotite is up to 95% replaced by sericite, secondary orthoclase, magnetite, pyrite, and carbonate. Plagioclase of the outer zone is characterized by a slightly less intense alteration in which twin planes can be distinguished. Plagioclase is replaced by up to 95% montmorillonite-sericite and minor carbonate. Quartz and microcline are generally fresh in the outer zone, although the microcline is occasionally veined by adularia and quartz.

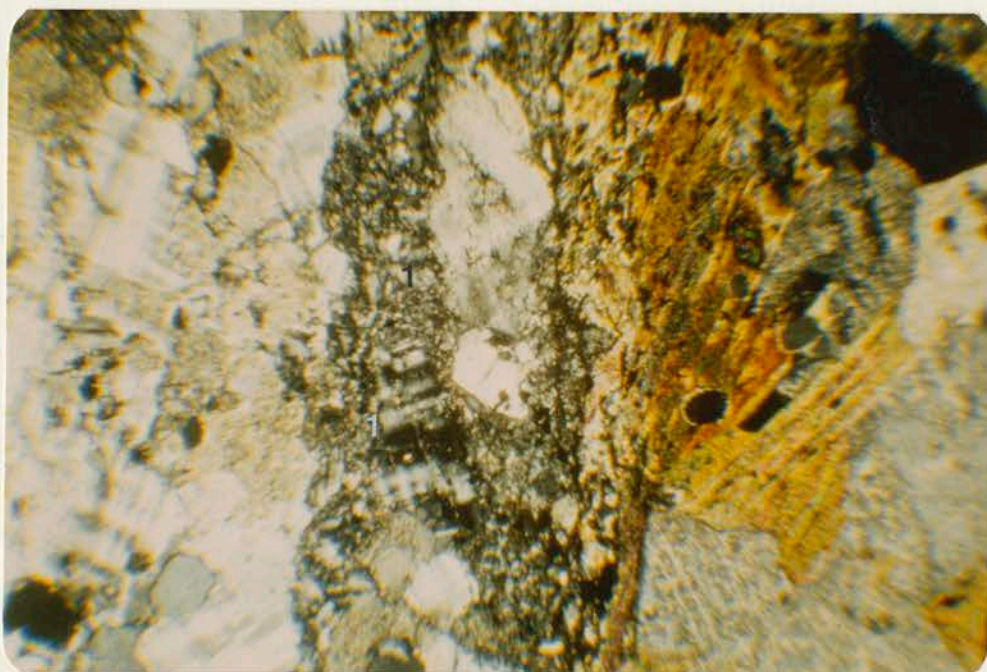
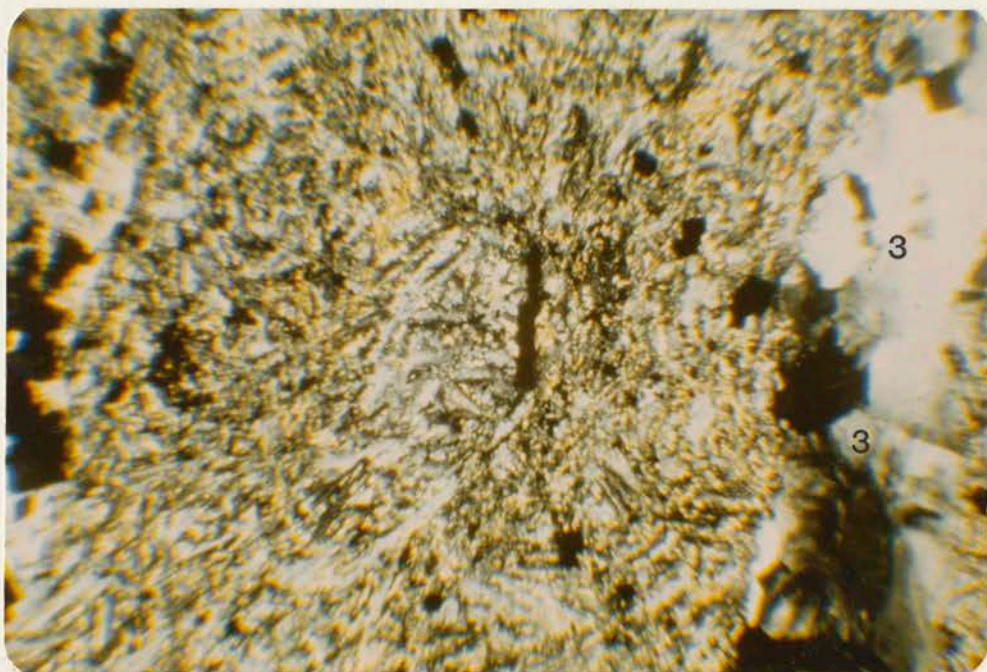
3. Deuteric zone

Deuteric alteration is characterized by predominately fresh biotite which may be weakly altered to chlorite and magnetite. Plagioclase is covered by up to 50% veinlet-controlled sericite. All other constituents of the granite are fresh in the deuteric zone.

C. Alteration of Phonolite and Basalt Dikes

The intensity of dike alteration is dependent on proximity to a mineralized structure. Alteration of the phonolite consists of bleaching, devitrification and silicification of the groundmass with introduction of pyrite, sericite-montmorillonite, minor roscoelite, and

- Figure 36. A. Photomicrograph of thin-section from phonolite-hosted Bobtail vein, 3350 level (horizontal field of view = 3 mm). Showing alteration of vein-associated phonolite; stage 3 quartz-fluorite veins(3) in roscoelite dusted groundmass of alkali feldspar.
- B. Photomicrograph of thin-section from Newmarket vein, 3100 level (horizontal field of view = 3mm). Showing veinlet of stage 1 mineralization(1) and weak wallrock alteration. Note sericite-montmorillonite on plagioclase, partial replacement of biotite by sericite, and fresh microcline.



fluorite (Fig. 36a). The feldspathoid phenocrysts and microcline xenocrysts are core-replaced by quartz and fluorite.

Alteration of the basalt dikes is similar to that observed in the phonolites. Basalt dikes are commonly altered by supergene processes that mask hypogene alteration. The dikes are extensively bleached and the groundmass is replaced by sericite, roscoelite, and pyrite. Silicification and devitrification of the groundmass is common but to a lesser degree than is present in the phonolites. The feldspathoids are partially replaced by quartz.

In both types of dikes, a vuggy texture commonly is developed from the dissolution and only partial replacement of the feldspathoid minerals.

D. Chemical Changes

Chemical changes caused by hydrothermal alteration in the district have been addressed briefly by Gott et al. (1969). Potassium enrichment at the expense of sodium occurs throughout the district, and areas of greatest enrichment correlate well with the highest gold and silver concentrations (Gott, et al. 1969). A chemical comparison between unaltered and altered granite of the Ajax mine reported by Lindgren and Ransome (1906) serves to corroborate the mineralogical changes previously mentioned (Table II).

E. Alteration Controls

The principal controls on alteration in the Ajax vein system are: vein width, fracture intensity, host-rock lithology, dip of the mineralized structures, and the relative time at which the ore-hosting structure became receptive to mineralizing fluids. Since a combination

Table II. Comparative analysis of fresh (A) and altered (B) granite wallrock (from Lindgren and Ransome, 1906).

| | A. | B. | | A. | B. |
|--------------------------------|-------|-------|-------------------------------|--------|-------------------|
| SiO ₂ | 66.20 | 59.58 | SO ₃ | None. | None. |
| Al ₂ O ₃ | 14.33 | 16.00 | Cl | Trace. | (?) |
| Fe ₂ O ₃ | 2.09 | 0.30 | F | (?) | ^a 0.69 |
| FeO | 1.93 | 0.65 | FeS ₂ | 0.12 | ^b 4.78 |
| MgO | 0.89 | 0.03 | MnO | 0.13 | Trace. |
| CaO | 1.39 | 2.03 | BaO | 0.18 | 0.11 |
| Na ₂ O | 2.58 | 0.98 | SrO | Trace. | 0.01 |
| K ₂ O | 7.31 | 11.93 | Li ₂ O | Trace. | Trace. |
| H ₂ O- | 0.48 | 0.32 | V ₂ O ₃ | | 0.39 |
| H ₂ O+ | 0.83 | 0.81 | MoO ₃ | | 0.01 |
| TiO ₂ | 0.65 | 0.75 | | 99.74 | 99.95 |
| ZrO | 0.02 | (?) | | | |
| CO ₂ | 0.36 | 0.26 | Less 0 | | 0.29 |
| P ₂ O ₆ | 0.25 | 0.32 | | | 99.66 |

^a1.42 CaF.

^b2.55 S.

A. Ajax mine, level 6.

B. Ajax mine, level 6, 1 foot from 345.

of alteration parameters generally are present, the relative individual importance of the controls is difficult to ascertain. Vein width and fracture intensity are the dominant alteration controls. This is markedly similar to controls on alteration noted in the Sunnyside vein system by Casadevall and Ohmoto (1977). No vertical zonation of the alteration assemblage was recognized in the Ajax system. Host rock lithology is of minor importance as the bulk of mineralization in the Ajax system is granite hosted. Vein associated basalt and phonolite dikes undergo a more pervasive alteration than does the granite due to a more brittle fracture response and subsequent greater permeability. Alteration in the granite is characterized by irregular boundaries often with no recognizable control. At least some local control appears to be related to biotite. Alteration of plagioclase in particular is generally much more intense near altered biotite phenocrysts. Other controls on alteration are best exemplified by studying the associated alteration selvages of characteristic veins. Alteration associated with all veins sampled in the Ajax system may be defined by the controls operative on the Bobtail and Newmarket veins.

1. Bobtail vein

The Bobtail vein is commonly a sheeted, relatively flat-lying structure locally exhibiting good development of all stages of mineralization. The Bobtail exhibits the most intense alteration of all the veins in the Ajax system. As evidenced by the presence of well developed first stage mineralization, the structure was generally receptive to early stage, highly reactive fluids. The highly fractured and sheeted nature of the structure is the primary control on alteration intensity, similar to what has been reported at other precious metal

vein deposits (Buchanan, 1980). This control is exemplified by fracture localization of the alteration (Fig. 25b). The combination of sheeted fracturing, as opposed to single fissure development, with flat dip tends to impede fluid flow and allow more intense alteration to develop (Fig. 34b, 35a). The flat dip of the structure is of lesser importance due to the impermeable nature of the hosting granite. No general increase in alteration intensity on the hanging wall of the mineralized structures was observed. This is contrary to what would be expected if the dip of the structure had significantly influenced alteration development (Buchanan, 1980, 1981).

2. Newmarket vein

The Newmarket vein is markedly dissimilar to the Bobtail in terms of fracture development and associated alteration. It is a steeply dipping (70° - 80°), poorly fractured structure that generally has only minor development of the first three stages of mineralization. The Newmarket exhibits the weakest alteration of any vein within the Ajax system (Fig. 31a, 31b, 36b). Variation in vein-related alteration along different mineralized structures has been reported in other districts (Sawkins, O'Neil, and Thompson, 1979). Alteration intensity is controlled by the relative time at which the structure became receptive to altering fluid. The Newmarket fissure is believed to have opened at a later time than the Bobtail (Loughlin and Koschmann, 1935). The Newmarket does not appear to have been accessible to ore-forming fluids until after the first stage of mineralization. As previously mentioned, recent work by the author has revealed the presence of a minor first stage component in the Newmarket vein. The principal control on alteration associated with the Newmarket is the fracture intensity. Of

lesser importance is the steep dip of the structure, which allowed relatively unrestricted fluid flow and subsequent weak alteration development. Fracture dilation is minor; alteration-mineralization along some of the tighter fractures consists of fracture localized dissolution vugs partially filled with fourth and fifth stage minerals (Fig. 31b). This type of mineralization is equivalent to the "bughole" mineralization noted by Loughlin and Koschmann (1935).

3. Breccia

Breccia-hosted veins were sampled in two locations. Conclusions drawn regarding alteration in the breccia must be regarded as tenuous. Alteration of the breccia is much more pervasive than that in the granite due to greater permeability in combination with the irregular sheeted nature of the breccia-hosted veins. In the areas sampled, inner zone alteration was pervasive and no outer zone was present (Fig. 32b). The pervasive nature of the alteration is the result of an increase in overall width of the sheeted fracture zone that was developed.

CHAPTER VI
FLUID INCLUSION ANALYSIS

A. Introduction and Methods

The only previous fluid inclusion study in the Cripple Creek district that has been published is by Lane (1976). In a thesis on the El Paso mine, Lane reports homogenization temperatures for 17 barite-hosted inclusions and 12 fluorite-hosted inclusions. Homogenization temperatures ranged from 162 to 266°C in barite and from 168 to 190°C in fluorite. Although no detailed paragenetic study was performed on the vein mineralization, fluorite was deposited later than the barite (Lane, 1976). These results from the El Paso correlate well with the stage three homogenization temperature results from the Ajax system (VI.B.3).

Primary fluid inclusions from 12 different elevations (Figs. 39, 41) in the Ajax mine were analyzed in an attempt to gain some insight into the character of the mineralizing fluid. Thirty-four doubly polished plates were prepared from the vein samples. Minerals containing the most suitable inclusions for analyses were quartz and fluorite. One vein sample contained coarse sphalerite that was suitable for heating stage analysis. An unsuccessful attempt was made to determine filling temperatures of dolomite-hosted fluid inclusions from the Bobtail vein. The incompetent nature of the dolomite caused decrepitation prior to homogenization.

The analyses were performed on a Roman-Science heating-freezing stage mounted on a Lietz Ortholux II Pol-Bk microscope. Only inclusions with distinctively primary characteristics (Roedder, 1979) were used in this study. Initially, fluid inclusions were measured, sketched, and classified based on their physical appearance.

Suitable inclusions were then analyzed for homogenization temperature, freezing temperature, temperature of NaCl dissolution, and clathrate melting temperature. Homogenization temperatures were determined for 120 inclusions. Maximum uncertainty of homogenization temperatures as indicated by three replicate measurements is $\pm 3.0^{\circ}\text{C}$. Freezing temperatures were measured on 60 inclusions and maximum uncertainty is $\pm 1.4^{\circ}\text{C}$, based on two replicate measurements. NaCl dissolution temperatures were determined for 30 fluid inclusions. Due to the inconsistency of halite recrystallization, replicate measurements for NaCl dissolution were performed on only five inclusions. Maximum uncertainty is $\pm 3.7^{\circ}\text{C}$ for NaCl dissolution. Clathrate (CO_2 -hydrate) melting points were determined for five inclusions. Maximum uncertainty for clathrate melting temperatures is $\pm 0.2^{\circ}\text{C}$, based on two replicate measurements per inclusion.

B. General Characteristics

Fluid inclusions were analyzed from stages 1, 2, 3, and 4, with the greatest emphasis on stages 1 and 3. A double meniscus of varying width was observed in some of the inclusions from stages 1, 3, and 4 indicating presence of CO_2 in the ore fluids (Roedder, 1972). Results of the fluid inclusion analyses are shown in Tables III and IV.

Quartz contains the only useable inclusions in the first stage of mineralization. The inclusions are a combination of types III and IV

TABLE III. Fluid Inclusion Data: Ajax Vein System, Cripple Creek, Colorado

| Sample number | Mineral | Location | Stage | Filling Temperatures ($^{\circ}\text{C}$) | | | Salinity (eq. wt. % NaCl) | | |
|---------------|---------|-----------|-------|---|------------------------------------|------------------|---------------------------|----------------|---------------|
| | | | | No. inclusions | Temp. range | Mean temp. | No. inclusions | Salinity range | Mean Salinity |
| 4-B-1 | QTZ | 400L-A | 1 | 11 | 302 ⁰ -510 ⁰ | 400 ⁰ | 8 | 32-47 | 37 |
| 4-B-1 | QTZ | 400L-A | 3 | 5 | 183 ⁰ -216 ⁰ | 194 ⁰ | 4 | 0-5.9 | 3.0 |
| 7-M-1 | QTZ | 700L-M | 1 | 10 | 259 ⁰ -371 ⁰ | 303 ⁰ | 6 | 36-47 | 42 |
| 7-M-1 | QTZ | 700L-M | 3 | 3 | 200 ⁰ -205 ⁰ | 203 ⁰ | 3 | 6.6-6.7 | 6.6 |
| 10-A-1 | SL | 1000L-U | 2 | 4 | 271 ⁰ -289 ⁰ | 282 ⁰ | 1 | 0.3 | 0.3 |
| 10-NM-1 | QTZ | 1000L-NM | 3 | 1 | 178 ⁰ | 178 ⁰ | 1 | 3.1 | 3.1 |
| 14-C | QTZ | 1400L-C | 1 | 8 | 288 ⁰ -362 ⁰ | 325 ⁰ | 8 | 40-47 | 43 |
| 14-C | FLR | 1400L-C | 3 | 7 | 181 ⁰ -279 ⁰ | 231 ⁰ | 1 | 0 | 0 |
| 16-C | QTZ | 1600L-C | 1 | 3 | 258 ⁰ -389 ⁰ | 334 ⁰ | --- | --- | --- |
| 16-Z | FLR | 1600L-BX | 3 | 5 | 225 ⁰ -261 ⁰ | 244 ⁰ | 3 | 4.0-7.3 | 4.6 |
| 16-X | QTZ | 1600L-BX | 1 | 5 | 278 ⁰ -361 ⁰ | 317 ⁰ | 2 | 37-39 | 38 |
| 16-X | FLR | 1600L-BX | 3 | 6 | 148 ⁰ -286 ⁰ | 218 ⁰ | 5 | 0-1.8 | 0 |
| 20-BTS | FLR | 2000L-BT | 3 | 4 | 209 ⁰ -243 ⁰ | 222 ⁰ | 3 | 1.0-6.0 | 1.3 |
| 20-NM-2 | QTZ | 2000L-NM | 3 | 4 | 270 ⁰ -285 ⁰ | 280 ⁰ | 2 | 1.0-6.8 | 1.9 |
| 20-NM-2 | FLR | 2000L-NM | 3 | 6 | 189 ⁰ -279 ⁰ | 240 ⁰ | 1 | 1.7 | 1.7 |
| 23-BTS | FLR | 2300L-BT | 3 | 3 | 175 ⁰ -187 ⁰ | 183 ⁰ | 1 | 2.3 | 2.3 |
| 23-M | QTZ | 2300L-M | 1 | 2 | 289 ⁰ -297 ⁰ | 293 ⁰ | 1 | 36 | 36 |
| 23-M | FLR | 2300L-M | 3 | 3 | 248 ⁰ -261 ⁰ | 254 ⁰ | --- | --- | --- |
| 26-BTS | QTZ | 2600L-BT | 1 | 6 | 206 ⁰ -275 ⁰ | 236 ⁰ | 1 | 37 | 37 |
| 26-BTS | FLR | 2600L-BT | 3 | 8 | 123 ⁰ -252 ⁰ | 183 ⁰ | 2 | 0 | 0 |
| 26-NM-1 | QTZ | 2600L-NM | 1 | 3 | 259 ⁰ -320 ⁰ | 284 ⁰ | 1 | 30 | 30 |
| 28-NMS | QTZ | 2800L-NMS | 1 | 3 | 238 ⁰ -278 ⁰ | 254 ⁰ | --- | --- | --- |
| 30-J | QTZ | 3000L-J | 1 | 3 | 305 ⁰ -309 ⁰ | 307 ⁰ | --- | --- | --- |
| 30-BTS | FLR | 3000L-BT | 3 | 3 | 236 ⁰ -276 ⁰ | 251 ⁰ | 3 | 0-2.3 | 0.2 |
| 31-NM-3 | FLR | 3100L-NM | 3 | 7 | 185 ⁰ -350 ⁰ | 271 ⁰ | 1 | 0 | 0 |
| 31-NM-3 | QTZ | 3100L-NM | 4 | 5 | 144 ⁰ -159 ⁰ | 151 ⁰ | --- | --- | --- |
| 31-BTS-2 | QTZ | 3100L-BT | 4 | 8 | 105 ⁰ -143 ⁰ | 129 ⁰ | 7 | 1.4-3.5 | 2.3 |
| 33-BTS-1 | QTZ | 3350L-BT | 1 | 4 | 328 ⁰ -332 ⁰ | 330 ⁰ | 3 | 32-33 | 33 |
| 33-BTS-PH | FLR | 3350L-BT | 3 | 3 | 269 ⁰ -286 ⁰ | 278 ⁰ | 2 | 2.8-8.3 | 4.8 |

QTZ=quartz, SL=sphalerite, FLR=fluorite; L=level; A=Apex vein, M=Mohican vn, U=Unnamed vn, NM=Newmarket vn, C=Christensen vn, BX=breccia-hosted vn, BT=Bobtail vn, NMS=Newmarket Shear vn, J=Jennifer vn.

Table IV. Fluid Inclusion Data: Ajax Vein System, Cripple Creek, Colorado

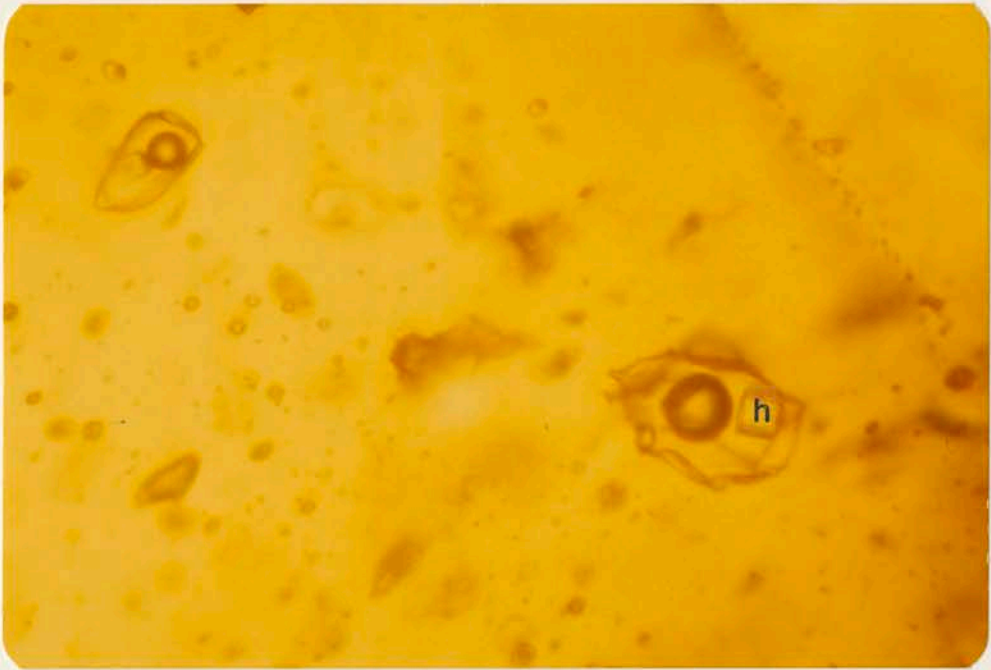
| Stage | Homogenization Temperatures (°C) | | Salinity (eq. wt% NaCl) | | Density g/cc | Trapping Pressure (bars) | Internal CO ₂ Pressure (bars) | CO ₂ content (mole %) | Maximum depth to boiling (meters) |
|----------|----------------------------------|------|-------------------------|------|--------------|--------------------------|--|----------------------------------|-----------------------------------|
| | Range | Mean | Range | Mean | | | | | |
| <u>1</u> | 206-510 | 308 | 30-47 | 37 | | | | | |
| 3350L | | | | | 1.163 | | | | Haas(1971): 120-990 |
| 700L | | | | | 1.254 | | | | |
| 328°C | | | | | | 215 | 27 | 2.8 | 1771 700L 1909 3350L |
| 206°C | | | | | | 155 | 27 | 2.0 | 1277 1376 |
| <u>3</u> | 123-350 | 228 | 0-8.3 | 2.1 | | | | | |
| FLR | 123-350 | 231 | | | | | | | |
| QTZ | 178-285 | 212 | | | | | | | |
| 3350L | | | | | 0.97 | | | | Haas(1971): 3-600 |
| 3100L | | | | | 0.94 | | | | |
| 700L | | | | | 1.00 | | | | |
| 400L | | | | | 0.96 | | | | |
| 269°C | | | | | | 260 | 44 | 4.0 | 2686 700L 2857 3100L |
| 123°C | | | | | | 370 | 44 | 2.6 | 3615 3846 |
| <u>4</u> | 105-159 | 140 | 1.4-3.5 | 2.3 | | | | | |
| 3100L | | | | | 0.97 | | | | Haas(1971): 3-45 |
| 144°C | | | | | | 360 | 44 | 2.8 | 3834 3100L |
| 105°C | | | | | | 400 | 44 | 2.2 | 4260 |

(Nash, 1976) and range in size from 10 μm to 45 μm in diameter. They commonly contain halite daughter minerals and hematite and sylvite daughters are present in some samples (Fig. 37). Neither hematite nor sylvite were observed as the sole solid phase; both occurred only in inclusions containing a halite daughter. CO_2 is a constituent of the ore fluids as indicated by the presence of a narrow double meniscus (Figs. 38a, 40a) and the formation upon freezing of a CO_2 -hydrate crystal that does not melt until temperatures reach $+8-9^\circ\text{C}$ (Roedder, 1963). The double meniscus is more common and better developed in stage 1 inclusions than in inclusions of later stages due to higher salinity causing greater immiscibility of CO_2 (Bodnar and Kuehn, unpub.). Vapor to liquid ratios of stage 1 primary inclusions are relatively constant, with vapor content ranging from 5 to 10%. A small percentage of primary inclusions in stage 1 are vapor rich, ranging from 20 to 50 volume % vapor (Fig. 40).

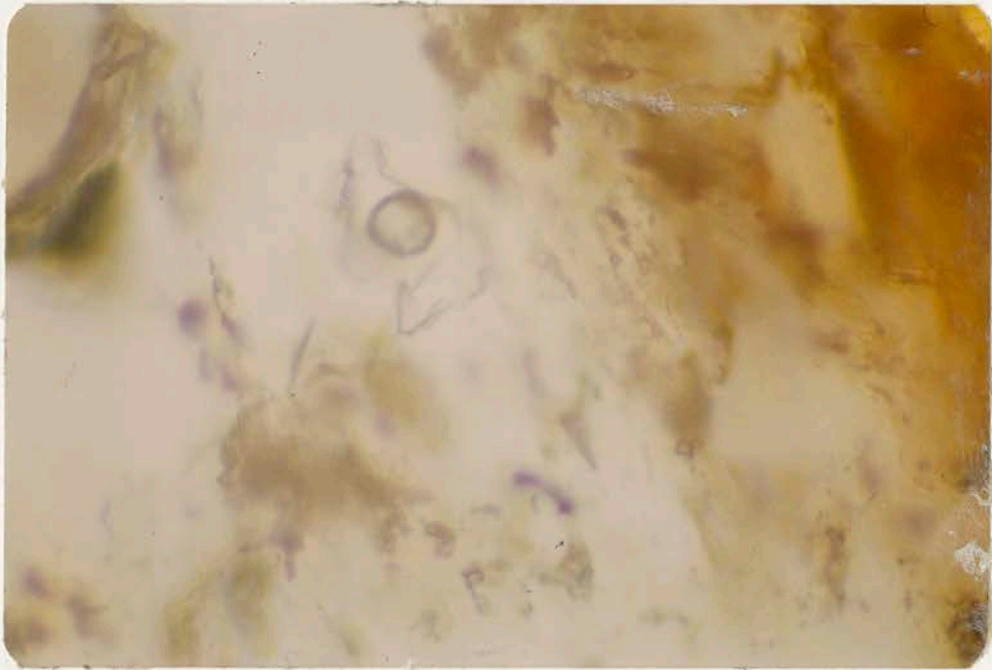
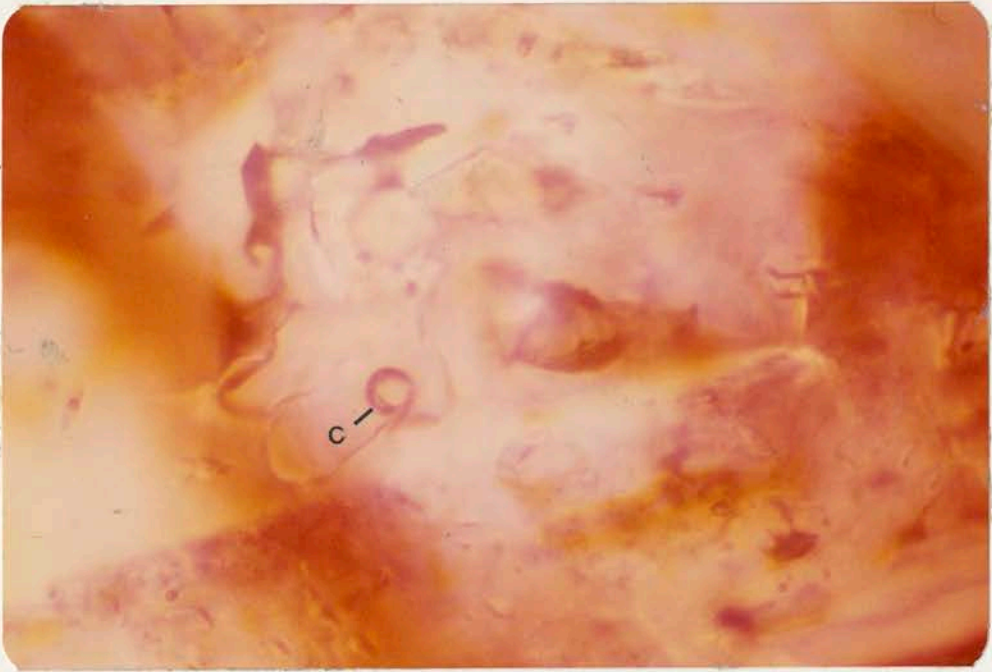
Only one sample of sphalerite from stage 2 contained suitable inclusions for analysis. The generally poor development and fine grained nature of stage 2 minerals hindered fluid inclusion analysis of this stage. Stage 2 inclusions are two phase, liquid-dominated inclusions containing 5-10% vapor and have a constant liquid to vapor ratio.

Stage 3 quartz and fluorite both contain abundant primary inclusions suitable for analysis. Inclusions in both minerals can be either two or three phase and are liquid-dominated with the exception of a few primary vapor-rich inclusions present in each section. Inclusions in quartz commonly contain 5-10% vapor and range in size from less than 10 μm to 30 μm in diameter. Fluorite inclusions have a slightly more

- Figure 37. A. Photomicrograph of doubly polished plate from Bobtail vein, 3350 level (horizontal field of view = 0.3 mm). Showing stage 1 quartz-hosted fluid inclusions with halite daughter minerals(h).
- B. Photomicrograph of doubly polished plate from Mohican vein, 700 level (horizontal field of view = 0.3 mm). Showing stage 1 quartz-hosted fluid inclusions with halite(h), hematite(he), and sylvite(s)(?) daughter minerals. Note thickened vapor-liquid contact indicating presence of CO₂.



- Figure 38. A. Photomicrograph of doubly polished plate from Bobtail vein, 2600 level (horizontal field of view = 0.3 mm). Showing stage 3 fluorite-hosted fluid inclusion with double meniscus(c) indicating presence of CO₂.
- B. Photomicrograph of doubly polished plate from Bobtail vein, 3100 level (horizontal field of view = 0.3 mm). Showing stage 4 quartz-hosted two phase fluid inclusion.



variable average vapor content of 5-15% and range in size from less than 10 μm to 40 μm in diameter (Fig. 38a). The presence of CO_2 was indicated by a thin double meniscus in approximately 20% of stage 3 inclusions. CO_2 does not show any preference for either fluorite or quartz, occurring in the inclusions of both minerals with equal frequency.

Difficulties in obtaining stage 4 material are inherently obvious. Since stage 4 quartz hosts high-grade gold-telluride mineralization, it was only rarely overlooked. The milky white quartz of stage 4 is somewhat irregular in fluid inclusion content. Of the several sections of stage 4 quartz that were prepared, only two contained useable fluid inclusions. Where present, stage 4 inclusions range from 10 to 60 μm in diameter. Stage 4 inclusions are two or three phase, liquid-dominated, with a generally constant liquid to vapor ratio (Fig. 38b). Vapor content of most stage 4 inclusions ranges from 5 to 15%. A small percentage of stage 4 inclusions are vapor-rich, ranging from 20 to 40 volume % vapor.

C. Fluid Temperature

1. Stage 1

A total of 58 stage 1 fluid inclusions were replicate measured and had an average homogenization temperature of 308°C. Temperatures of stage 1 inclusions exhibit a wide variation, ranging from a minimum of 206°C ((2600 level)(7537 ft)) to a maximum of 510°C ((400 level)(9688 ft)) (Table IV). Temperature variation in a single stage 1 sample increases from 4°C on the 3350 level (6742 ft) to 208°C on the 400 level (9688 ft). A noticeable increase in homogenization temperature variation occurs on the 1600 level (8485 ft) and persists to the 400

level (9688 ft) (Fig. 39). Examination of the data (Table III) indicates that the increase may be the result of an increased number of measurements; however, such is not the case. Fewer inclusions were measured on the deeper levels but for every measured inclusion several other inclusions in the same field of view homogenized within a few degrees of the inclusion being measured. In samples from the upper levels (1600 level - 400 level), inclusions separated by less than 100 μm often exhibited repeatable filling temperature differences of more than 100°C .

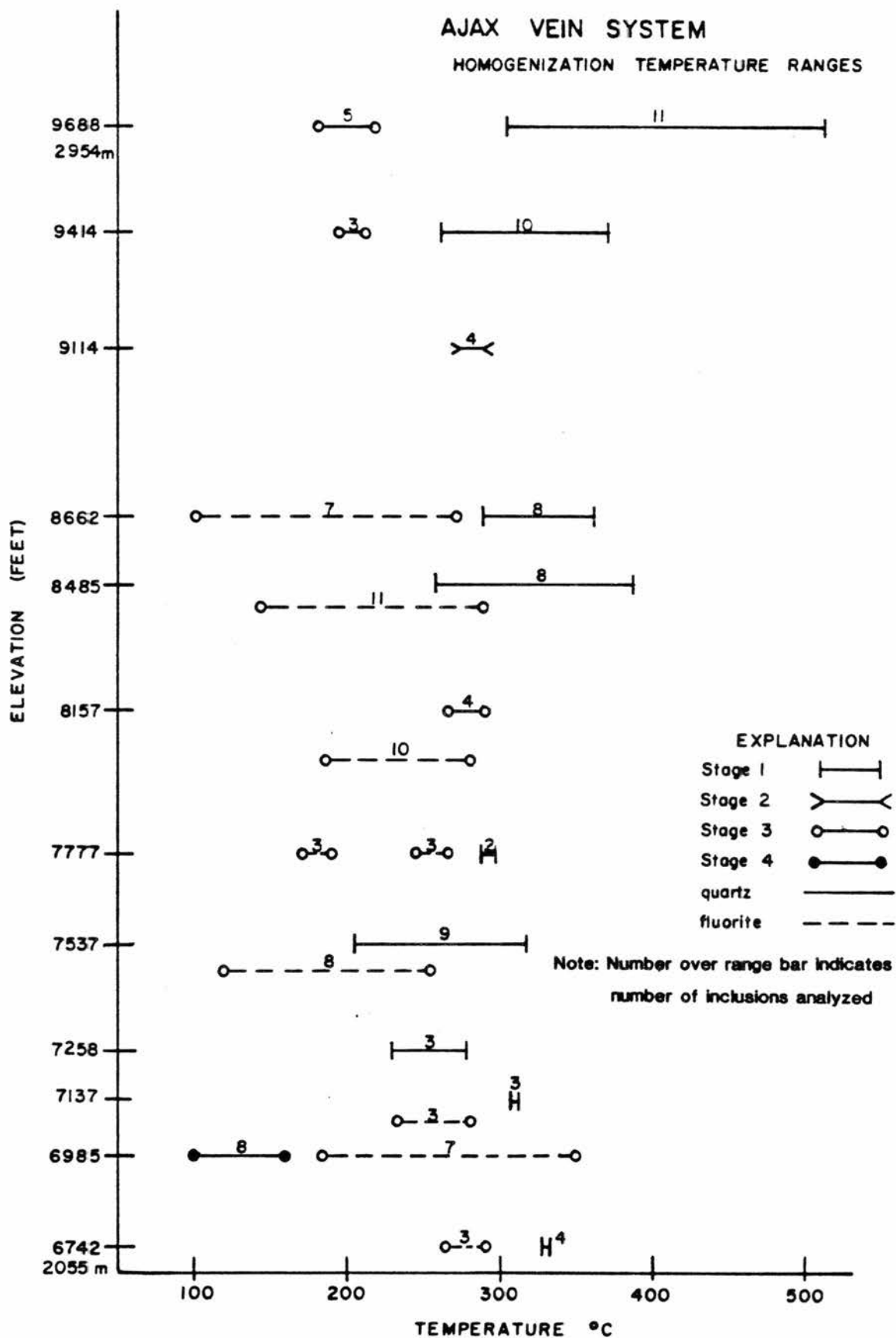
2. Stage 2

Homogenization temperatures of four inclusions from stage 2 sphalerite were measured in a sample from the 1000 level (9114 ft). Temperatures ranged from 271 to 289°C with an average of 282°C .

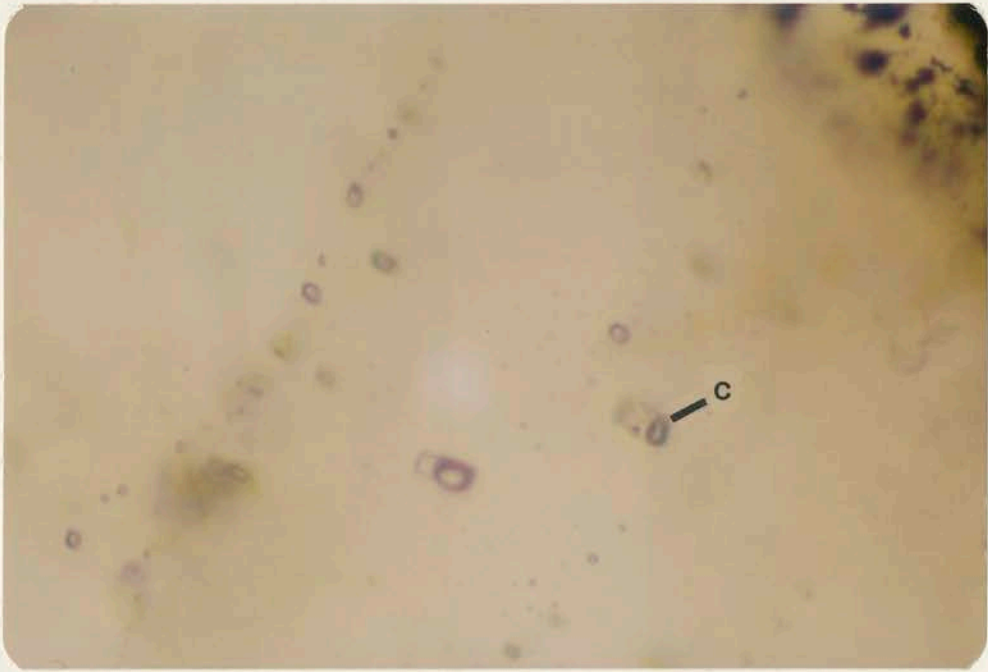
3. Stage 3

A total of 63 homogenization temperatures were determined on inclusions in stage 3 quartz and fluorite. Temperatures ranged from 123 to 350°C with an average of 228°C . Temperature variation in 13 quartz-hosted inclusions ranged from 178 to 285°C with an average of 212°C . Variation in the 55 fluorite-hosted inclusions analyzed was much greater than in quartz, ranging from 123 to 350°C with an average of 231°C . Greater homogenization temperature variation in fluorite-hosted inclusions is due to the high abundance of inclusions present throughout the growth zoned fluorite crystals. Fluorite is an excellent inclusion host in the Ajax system and temperatures were obtained from the inner and outer zones of many crystals. The homogenization temperature range

Figure 39. Diagram showing homogenization temperature ranges for the different stages and elevations.



- Figure 40. A. Photomicrograph of doubly polished plate from Mohican vein, 700 level (horizontal field of view = 0.3 mm). Showing stage 1 quartz-hosted fluid inclusions. Note double meniscus(c) indicating presence of CO₂ and variable liquid to vapor ratios indicating boiling.
- B. Photomicrograph of doubly polished plate from Christensen vein, 1400 level (horizontal field of view = 0.3 mm). Showing stage 1 quartz-hosted fluid inclusions with variable liquid to vapor ratios. Note vapor dominated inclusion(v) adjacent to liquid dominated(l) inclusion.



of fluorite closely represents the entire variation in fluid temperature occurring during deposition of stage 3 minerals.

4. Stage 4

Homogenization temperatures of stage 4 quartz were measured in samples from the Newmarket and Bobtail veins on the 3100 level (6985 ft). Temperatures ranged from 105 to 159°C with an average of 140°C. Five inclusions from the Newmarket were analyzed and temperatures obtained ranged from 144 to 159°C with an average of 151°C. Eight inclusions from the Bobtail vein were analyzed and temperature variation was from 105 to 143°C with an average of 129°C. Stage 4 fluid temperatures agree well with the estimated temperature of telluride mineralization in the veins of Boulder County, Colorado (Kelly and Goddard, 1969). From a summary of geothermometers, Kelly and Goddard (1969) predict that the bulk of telluride mineralization in Boulder County occurred within a temperature range of 100 to 160°C.

D. Fluid Salinity

Fluid salinity estimates of stages 1, 2, 3 and 4 are presented in Tables III and IV. Only one inclusion was analyzed from stage 2 and the value obtained appears to be erroneously low. As the stage 2 value was determined on dark colored sphalerite, transmission of light was poor and the determination should be disregarded. Estimates on stages 1, 3 and 4 are regarded as accurate and will be utilized to propose a model for fluid evolution.

1. CO₂ effect

The presence of a CO₂ liquid phase in fluid inclusions has been recognized by earlier workers (Roedder, 1963, 1972, and Nash, 1976).

Roedder (1963) was the first to note formation of a CO_2 hydrate (clathrate) in fluid inclusions during freezing studies (Roedder, 1963). Only recently has the effect of clathrate formation on freezing point depression salinity estimates been quantitatively examined (Collins, 1979). During the freezing of CO_2 -bearing H_2O -NaCl inclusions, CO_2 forms a hydrate (clathrate) effectively removing H_2O molecules from solution and causing a salinity increase in the residual solution. The freezing temperature measured is lowered and subsequently the salinity estimate is too high. Collins (1979) proposed a method using the clathrate melting temperature to estimate salinity. An inherent problem with this method is the difficulty in recognizing clathrate formation in an inclusion. The clathrate is isotropic and has refractive indices similar to the aqueous solution, making it extremely difficult to identify (Roedder, 1963). In this study, clathrate formation was recognized in fluid inclusions from stages 1, 3 and 4. As documented by Collins (1979), the CO_2 effect on salinity becomes more pronounced as CO_2 and NaCl content of the original fluid increases. Presence of halite daughter minerals in stage 1 inclusions rendered the clathrate melting point method unamenable as published data are available only for NaCl unsaturated solutions (Collins, 1979). The method did prove useful for salinity determination of stage 3 and 4 fluids. However, freezing temperatures of stage 3 and 4 fluids proved to be relatively unaffected by CO_2 due to their low relative salinities. Additional effects of CO_2 with regard to boiling will be examined in a later section.

2. Stage 1

Initially the freezing point depression method was employed to determine salinity of stage 1 inclusions. After obtaining salinity

estimates that were unreasonably high, it was recognized that CO_2 was adversely affecting the method. Due to lack of published data on clathrate formation in NaCl super-saturated solutions, efforts to obtain the salinity of stage 1 inclusions by freezing were discontinued.

Presence of halite-bearing stage 1 inclusions in sections from most of the levels sampled allowed application of a method proposed by Erwood, Keslar, and Cloke (1979). Their method involves measuring temperatures of halite dissolution to obtain an accurate estimate of fluid inclusion salinity. In samples from lower mine levels (3350-2300 level), with the exception of one inclusion, halite dissolution temperature was less than vapor homogenization temperature. However, on upper levels (1600-400 level) approximately 50% of the inclusions homogenized by halite dissolution, i.e., the vapor phase homogenized prior to halite dissolution. Roedder and Bodnar (1980) believe that homogenization by halite dissolution in the H_2O -NaCl system indicates the inclusions were trapped at higher pressures than inclusions homogenizing by vapor disappearance. The effect of CO_2 in association with high salinity fluids significantly influences the trapping pressure. Lack of published information on the system H_2O -NaCl- CO_2 and the complex nature of stage 1 fluids necessitates a simplification of the analysis. The view expressed by Erwood et al. (1979) that higher halite homogenization temperatures relate primarily to higher NaCl concentrations rather than to higher pressures is adopted in this study.

Based on the above, salinity of stage 1 fluid inclusions varied from less than 26 wt% eNaCl in a few rare inclusions containing no NaCl daughter minerals (Rose and Burt, 1979), to as much as 47 wt% eNaCl. Results of 30 determinations using the halite dissolution temperature

method range from 30 to 47 wt% eNaCl, with an average of 37 wt% eNaCl. Salinity estimates increase slightly with higher elevation as shown in Table III.

3. Stages 3 and 4

Due to the presence of CO_2 in stage 3 and 4 fluids, clathrate melting points were measured in order to minimize the error present in salinity estimates. Published data of Collins (1979) were ideally suited to the NaCl-undersaturated fluids of stage 3 and 4. However, difficulty in clathrate recognition rendered this method unfeasible for widespread application to stage 3 inclusions. Several large inclusions were selected from stage 3 minerals in order to obtain clathrate melting temperatures. The freezing temperature of the liquid was also measured on the same inclusions (Roedder, 1962). This was an attempt to generate a correction factor that could be applied to stage 3 freezing point depression data.

Two clathrate melting temperatures were measured in stage 3 inclusions and a range of 1.6 to 4.0 wt% eNaCl (average 2.8) was determined. Freezing point determinations on the same inclusions yielded salinity estimates that were within 1 wt% eNaCl of the clathrate estimated value. As determined from the above, a combination of low salinity and CO_2 content in stage 3 inclusions allows salinity estimates to be made without correction. This is in agreement with Collins (1979) data showing the CO_2 effect at low NaCl and CO_2 contents to be minor. Freezing temperatures were measured on 32 stage 3 inclusions and yielded an estimated salinity range of 0-8.3 wt% eNaCl with an average of 2.1. The average obtained by this method was lower than that obtained by the clathrate method.

Only one sample of stage 4 quartz was suitable for analysis with the freezing stage. Three clathrate melting points were measured and yielded an estimated salinity range of 1.4-3.5 wt% eNaCl with an average of 2.0. Freezing temperatures were measured on seven stage 4 inclusions and a salinity range of 2.4 to 3.5 wt% eNaCl was estimated with an average of 2.3%. Similar to stage 3, the effect of CO₂ on stage 4 salinity estimation is insignificant.

E. Additional Fluid Parameters

1. Fluid density

Density estimates of stage 1, 3 and 4 fluids were made utilizing relative volumes of each phase present. The inclusions were measured using a calibrated microscope ocular and the relative percentage of each phase present was estimated (Roedder, 1979, unpub.). Density values of the contained phases were taken from the CRC handbook (1981-1982). The gas phase was assumed to be pure CO₂ vapor with a density of 0.1956 g/cc, corresponding to the density of CO₂ gas in contact with CO₂ liquid at room temperature. Density of the unsaturated aqueous solution varied from a minimum of 1.0 g/cc (0 wt% eNaCl) to a maximum of 1.1972 g/cc (26.0 wt% eNaCl). Results are shown in Table IV.

Stage 1 fluids have the highest densities, ranging from 1.163 to 1.254 g/cc. Fluids of stages 3 and 4 have lower density values, ranging from 0.94 to 1.00 g/cc. Density is dependent on relative salinity and vapor content of the fluids. The effect of temperature on fluid density is significant. With increasing temperature, fluid density is lowered, and density differences provide a mechanism for convective fluid movement. Increasing salinity results in higher fluid density and tends

to counter the temperature effect on density (Fisher, 1976). In the Ajax system, high-temperature fluids have correspondingly high salinities, and low-temperature fluids have lower salinities (Table III). Based on the above, net temperature effect on density of the Ajax ore fluid was minor and is not considered in this study.

2. Trapping pressure

Trapping pressure is the pressure at which a fluid inclusion is trapped. Trapping pressure is influenced by lithostatic load, hydrostatic head, CO_2 content, and NaCl content. As the Ajax system is believed to have been boiling (section VI.E.4.a.), no lithostatic pressure is in effect (Roedder and Bodnar, 1980).

By determining internal CO_2 pressure of the inclusions and knowing the homogenization temperature, trapping pressure can be estimated (Bodnar and Kuehn, unpub.). Stage 1 fluids are NaCl-saturated under freezing conditions; therefore, internal CO_2 pressure within the inclusions is estimated at 27 bars (Collins, 1979). Average salinity of stage 3 and 4 fluids is less than 5 wt% eNaCl, based on clathrate melting point and freezing point depression methods. Internal CO_2 pressure in fluid inclusions of stage 3 and 4 is estimated at 44 bars (Collins, 1979). Lower internal CO_2 pressure in stage 1 inclusions is caused by increased CO_2 immiscibility in the presence of higher salinity solutions (Bodnar and Kuehn, unpub.).

Trapping pressures have been determined for the lowest minimum and highest minimum homogenization temperature values for stages 1, 3 and 4 (Table IV). Use of the minimum temperature range in each stage is an attempt to minimize the effect of boiling. In a boiling system the lowest homogenization temperature is closest to the true fluid

temperature and contains the least amount of primary gas (Roedder, 1967). As shown in Table IV, trapping pressures for stage 1 are lower than values calculated for stages 3 and 4. Lower trapping pressure is the result of lower internal CO_2 pressure. Low salinity of inclusions in stages 3 and 4 and subsequent high internal CO_2 pressure yields an increase in the calculated trapping pressure. Stage 4 inclusions have the highest trapping pressures resulting from high internal CO_2 pressure and low trapping temperature. However, this is somewhat contradictory in that a decrease in temperature causes an increase in CO_2 immiscibility; subsequently less CO_2 should be trapped in inclusions with lower homogenization temperatures. Stage 4 inclusions should have a slightly lower trapping pressure than higher temperature stage 3 inclusions, based on the behavior of CO_2 (Bodnar and Kuehn, unpub.). High trapping pressures of stage 4 inclusions are the result of fluctuations in the plotted data of Bodnar and Kuehn (unpub.) and may be caused by variations in CO_2 immiscibility at low temperatures. Lack of information on the subject precluded further investigation.

3. CO_2 content

Using the calculated trapping pressures in combination with trapping temperature (homogenization temperature), CO_2 content of the inclusions can be estimated (Bodnar and Kuehn, unpub.). The lowest minimum and highest minimum homogenization temperatures are again used to negate the effect of boiling.

CO_2 content of fluid inclusions in the Ajax system ranges from 2.0 mole % CO_2 to 4.0 mole % CO_2 (Table IV). Based on CO_2 content, trapping pressure, and trapping temperature, fluids in the Ajax system were composed of one phase when formation of the fluid inclusions occurred

(Bodnar and Kuehn, unpub.). Their position in the one phase field however, is essentially on the two phase boundary or "boiling point".

4. Boiling level

In a boiling system, the vapor pressure equals or exceeds hydrostatic pressure. If the vapor pressure is known, i.e. trapping pressure, then the maximum depth at which boiling can occur is calculated from the relationship: Pressure=density of fluid X depth, or, Depth=trapping pressure/fluid density. If the system is known to have been boiling during ore deposition then depth of formation can be estimated.

a. Evidence for boiling

Evidence indicative of violent boiling (Roedder, 1967) in the Ajax system is lacking. Vapor to liquid ratios of the inclusions generally show only minor variation. A small percentage (5-20%) of primary inclusions of stages 1, 3 and 4 exhibit higher vapor contents, ranging from 15 to 50 volume % vapor. The great vertical distribution of gold-telluride ores, with only minor variation in grade, and the absence of hydrothermal brecciation in the veins, are evidence against violent boiling.

As discussed in the previous section, Ajax fluids were trapped as one phase liquid inclusions close to the two phase boundary (boiling point). It is proposed that vein mineralization of the Ajax system occurred in weakly effervescing fluid conduits (fissures). The "boiling" was characterized by an escape of CO₂ gas caused by immiscibility. Evidence for CO₂ effervescence in the Ajax system is:

1. presence of a small percentage of primary, vapor-rich inclusions,
2. fluid inclusions of stages 1, 3 and 4 trapped near the two phase boundary (boiling point),
3. subtle increase in salinity with higher elevation in stage 1 and 3 inclusions, indicating more intense boiling,
4. slight increase in homogenization temperature range with elevation, most noticeable in stage 1 (Kamilli and Ohmoto, 1979), and
5. present mine water is effervescing CO_2 .

The open, vuggy nature, and vertical continuity of the veins is further evidence that pressure of deposition in the Ajax vein system was dominated by hydrostatic conditions.

b. Boiling depth

Importance of the CO_2 effect on determining chemical and physical parameters of the ore-forming fluid has been previously demonstrated. However, nowhere does the influence of CO_2 play a more important role than in the estimation of boiling depth.

The work of Haas (1971) on estimating maximum depth at which boiling can occur has been used extensively to predict depths of mineralization. Haas (1971) cautions that his method is accurate for the $\text{H}_2\text{O}-\text{NaCl}$ system only and the presence of dissolved gases will cause the depth estimate to be too low. Recent work has shown that most ore fluids are not simple $\text{H}_2\text{O}-\text{NaCl}$ solutions, but commonly contain one or more dissolved gas species, of which CO_2 is the most common (Roedder and Bodnar, 1980; Bodnar and Kuehn, unpub.).

Using the method proposed by Haas (1971) for the system $H_2O-NaCl$, maximum depths at which boiling can occur were predicted for fluids of stages 1, 3, and 4 (Table IV). Lowest minimum and highest minimum homogenization temperatures from each stage were used in order to minimize the boiling effect. Results of the estimations range from a minimum of 3 meters (stage 4) to a maximum of 990 meters (stage 1).

Due to the presence of CO_2 , maximum depth estimates by the Haas (1971) method are known to be too low. Depths were then calculated by the trapping pressure method outlined earlier. Again, trapping pressures corresponding to the lowest minimum and highest minimum trapping temperatures were used. Results are shown in Table IV. A comparison of stage 1 estimates shows only a minor difference between the two methods. High salinity of stage 1 fluids causes increased CO_2 immiscibility. Subsequently, stage 1 fluid contains less dissolved CO_2 and has a lower trapping pressure, resulting in a shallower depth at which boiling can occur. Stages 3 and 4 show a marked increase of great magnitude over the estimate based on the method of Haas (1971). The increase in maximum depth at which boiling can occur in stages 3 and 4 illustrates the importance of CO_2 recognition in fluid inclusions. The large discrepancy occurring in stage 4 between results of the trapping pressure method and the Haas (1971) method exemplifies the inverse temperature dependence of CO_2 effervescence versus conventional boiling. Depth estimates are critically important when determining depth of ore formation or attempting to derive a model of ore deposition.

F. Ajax Fluid Evolution

From results of the fluid inclusion analyses a hypothesis for fluid evolution in the Ajax mine can be derived.

Stage 1 fluids are magmatic in origin, indicated by their high salinity (Erwood, et al., 1979) and temperature. Halite-bearing fluid inclusions are rare in ore-forming fluids of epithermal gold deposits (Roedder, unpub.) yet are common in fluids derived from intrusive sources (Nash, 1976). The close proximity of alkaline intrusive-volcanic rocks (Fig. 2) to the Ajax system is further evidence in support of a magmatic origin for Stage 1 fluid.

Stage 1 fluid underwent a mixing with meteoric water prior to or during deposition of stage 2 sulfides. This mixing caused the pronounced salinity decrease exhibited by stage 3. Salinity data are lacking for stage 2 but evidence conclusively indicates mixing occurred prior to deposition of stage 3 minerals. In addition to the salinity decrease, a lowering of temperature also occurred as the result of magmatic-meteoric water mixing. Mixing was most likely caused by a decrease in magmatic fluid output allowing an influx of meteoric water to dominate the system. Following the mixing, a prolonged cooling occurred continuing through stages 4 and 5. During and subsequent to stage 4 deposition, the system has been quiescent, evidenced by the undisturbed nature of the veins.

CO₂ content of the fluid remained relatively constant during mineralization. Amount of CO₂ vapor in the ore fluid was controlled by salinity, depth, and temperature. A subtle CO₂ effervescence occurred in all stages of deposition at depths below the current deepest mine level. This subtle "boiling" may be a partial explanation for the lack of metal zoning in the system.

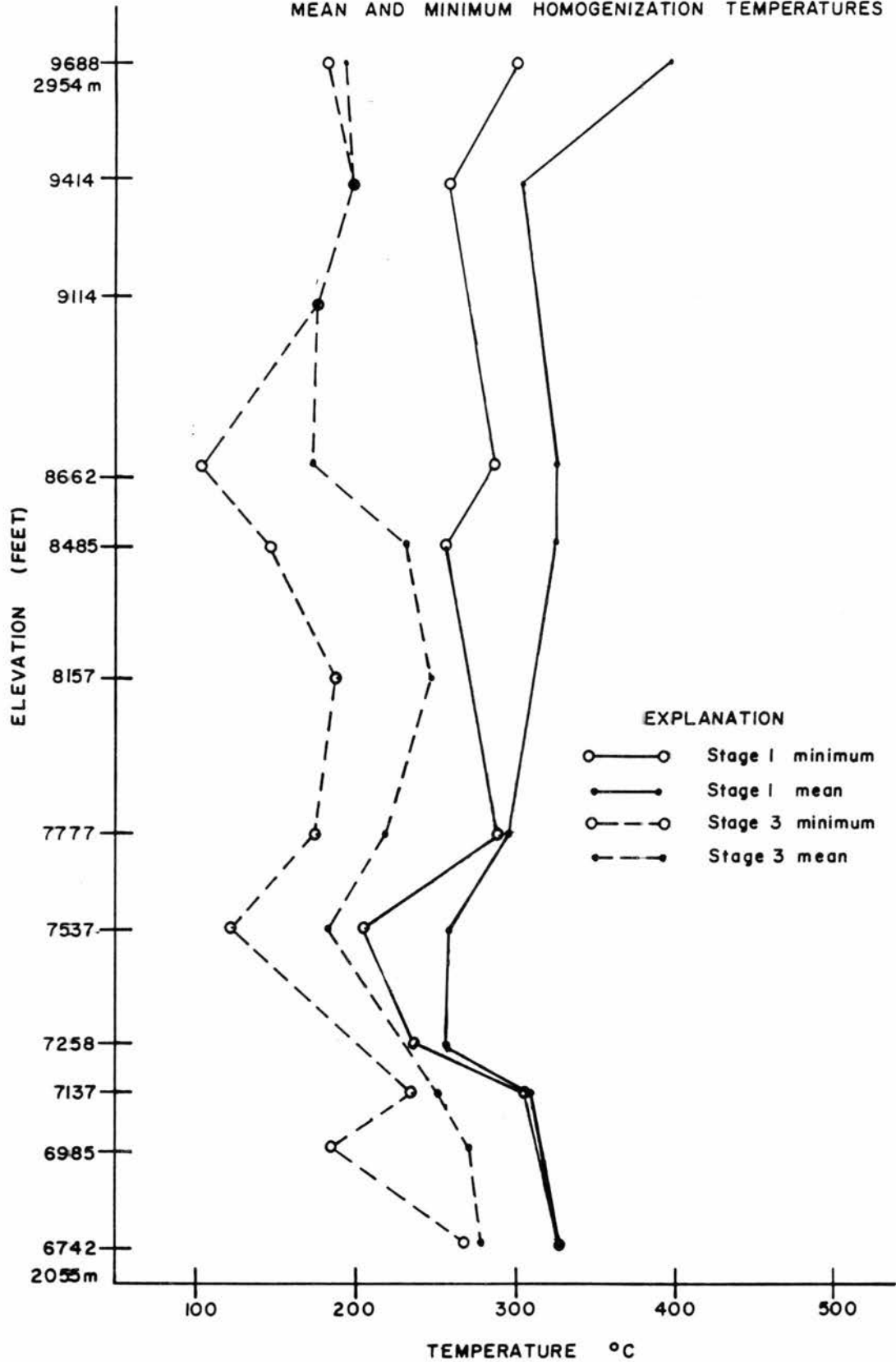
A plot of mean and minimum homogenization temperatures for stages 1 and 3 exhibits a distinct trend(s) in the vertical thermal gradient

(Fig. 41). A rough parallelism is observed between the plots of both stages and between plots of mean and minimum values for each individual stage. This implies that the measured values are a good representation of the true fluid temperature gradient. From the 3350 level (6742 ft) to the 2600 level (7537 ft), a gradual cooling occurs possibly caused by increased distance from a heat source. Above the 2600 level, trends reverse and fluid temperature increases until the 2000 level (8157 ft). With increasing elevation from the 2000 level, stage 3 temperatures again decrease and stage 1 temperatures remain relatively constant. Increase in temperature of both stages between the 2600 level and 2000 level possibly indicates the presence of an additional intrusive heat source(s) within the breccia. A discontinuity in the granite-breccia contact (Fig. 15) occurs just below the 2000 level and possibly influences the thermal gradient. Above the 2000 level, the vein system gradually becomes closer to the granite-breccia contact. On the 700 level (9414 ft), the contact lies just north of the Ajax shaft. Most of the sampled vein structures extend into the breccia. Fluid flow most likely had more of a horizontal component where the vein system is in close proximity to the breccia.

An alternative explanation for the observed vertical temperature reversals is that increased permeability in the Cripple Creek Breccia, relative to the granite, results in a higher fluid flow rate. Higher flow rate in the breccia could generate a "mushroom" isotherm configuration and may explain the temperature reversals. Of principal importance to this hypothesis is the relative permeability of the breccia. Mineralization in the breccia is more irregular and less confined to a single fissure than in the granite. However, this is more

Figure 41. Plot of mean and minimum homogenization temperatures for stages 1 and 3 at different elevations. Note variability of trends and parallelism between both trends of both stages.

AJAX VEIN SYSTEM
MEAN AND MINIMUM HOMOGENIZATION TEMPERATURES



a result of breccia fracture response then increased permeability. The lack of disseminated mineralization, except where secondary brecciation has occurred (Globe Hill), supports the idea that the Cripple Creek Breccia was well lithified prior to precious-metal mineralization. Based on observed and reported field evidence, the fluid flow patterns of the Ajax system were most likely controlled by well developed, subsequently-mineralized fractures rather than permeability differences.

Effect of thermal gradient variation on ore grade has not been investigated. Lack of zoning in both base metals and precious metals implies that if the gradient did influence ore grade, it did so in a very subtle way. The complexity of possibilities and lack of substantiating data inhibit further speculation. It is apparent that the hydrothermal fluid system responsible for Ajax vein mineralization was not a simple upward flow of heated fluid.

CHAPTER VII
CONTROLS ON ORE DEPOSITION

A. Introduction

As illustrated in previous chapters, the Ajax vein system exhibits many characteristics commonly present in "typical" epithermal systems. However, it is the presence of many atypical characteristics that set the Ajax apart from other vein systems. An attempt will be made to elucidate the atypical features and their effect on ore deposition.

B. Structural Control

Excellent discussions of the structural control of mineralization in the Cripple Creek district have been published, often with specific regard to mineralization in the Ajax mine (Lindgren and Ransome, 1906; Loughlin and Koschmann, 1935; Lovering and Goddard, 1950). This discussion will be limited to specific features observed during recent underground sampling and mapping.

Structure is the primary control of ore mineralization in the Ajax system. All known precious metal mineralization is hosted in or near fissures. The fissures acted both as fluid conduits and as ore receptors. On lower levels of the mine, mineralization is restricted to fissures corresponding to shear zones active during formation of the complex. With increasing elevation, main fissures tend to branch into many sub-parallel structures. Tonnage produced from upper mine levels

was greater, as a result of the increased number of mineralized structures.

As noted above (III.C.1), influence of phonolite and basalt dikes on mineralization is minor. Importance of dike-vein intersections depends on the angle at which intersection occurs. The brittle-fracture response of the dikes creates a broad sheeted zone with very minor dilation. If the angle of intersection is large, fluid ponding can occur and create a large volume of mineralized rock. Although enrichment may occur on both sides of a dike, the downflow side is more intensely mineralized. An example of this phenomenon is present on the 500 level of the Ajax (as reported by Lovering and Goddard, 1950). On the 3350 level, recent mining has exposed a low angle dike-vein intersection of the Bobtail vein with a phonolite dike. Although the sheeted zone is wider in the dike, ore grade and volume are not significantly increased.

No large-scale comprehensive cross section of the Ajax system has yet been attempted. It is likely that changes in dip of the imbricated fracture system, as well as irregularities in dip and strike of a single fissure, influence localization of the ore (Lovering and Goddard, 1950). Data sufficient to construct a detailed, large-scale cross section are not readily available. However, analysis of this type with the goal of recognizing a vertical and lateral structural pattern in the ore shoots may be a useful guide for future exploration and mining.

Aside from presence of an open fissure, the time at which the structure was receptive to ore-forming fluids is of principal importance. As described above (IV.B.1), weak expansion and contraction of the fissures selectively opened and closed different areas along the

veins. This weak movement occurred throughout the depositional history of the veins. As many as four fracturing events are documented in stage 3 mineralization on the 2300 level of the Bobtail vein. With the exception of one post-mineral fault displacing the Newmarket vein, no evidence was observed that indicated structural movement after initiation of stage 4 mineralization. If a fissure was not open prior to stage 4, then it will not host high-grade gold-telluride mineralization. Gold-telluride mineralization present in fissures without the common association of stage 4 quartz, occurs as calaverite replacing earlier stage pyrite (IV.A.4). The low viscosity of stage 4 fluid allows it to flow along previously mineralized and weakly developed structures. Contrast between the Bobtail and Newmarket veins exemplifies the importance of the relative time of fracture dilation. The Newmarket is the most unimpressive and narrow vein in the Ajax system and yet is one of the highest grade, most extensively stoped structures in the mine.

C. Gold Transport

The subject of gold transport is a continuing source of debate. Transport of gold by sulfide complexes and thiocomplexes provides a reasonable answer to the question of gold migration in some low-temperature, neutral-pH environments (Weissburg, 1970; Seward, 1973). At higher temperatures, increased oxygen fugacity may oxidize available sulfur into sulfate form, less suitable for gold complexing (Henley, 1973). Chloride complexing appears to be the most important mechanism of gold transport at high temperatures (300-500°C) (Krauskopf, 1951; Helgeson and Garrels, 1968; Henley, 1973). At temperatures lower than 300°C, gold transport by chloride complexing becomes strongly dependent

on pH of the solution (Helgeson and Garrels, 1968). Low pH requirements of gold-chloride complexing at low temperatures are difficult to justify, as most hydrothermal fluids tend to be neutral in pH (Boyle, 1969). The presence of tellurium in the ore solution and its possible effect on gold solubility have not been specifically addressed. Seward (1973) acknowledges that telluro complexes may significantly influence the transport of gold in deposits where gold-telluride mineralization is present. Clearly, the veins of the Ajax system require a unique evaluation in regard to the mobility of gold. The transporting scheme that will be proposed is based on field and laboratory evidence in conjunction with scarce published information on telluride-bearing systems. In order to better evaluate the relative amenability of various gold transporting agents, the chemical and physical parameters of the Ajax ore fluid are discussed below.

1. pH

Ajax ore fluid pH can be estimated from the stability fields of vein-related alteration minerals. The pH remained relatively unchanged throughout vein deposition. Oxygen fugacity-pH diagrams of Romberger (unpub.), showing stability fields of adularia, sericite, kaolinite, and alunite, illustrate that stability is controlled primarily by pH and temperature. Effect of the K^+/H^+ ratio is also illustrated and can be significant.

Presence of adularia in the inner zone of Ajax vein-related alteration implies a pH of greater than 6.25 at 300°C (0.1 m NaCl, 0.01 m S, 100 ppm K, 10 ppm Fe). The occurrence of fresh primary microcline and adularia in the inner zone imply a high K^+/H^+ ratio (Hemley and Jones, 1964). As illustrated by Romberger (unpub.), an increased K^+

content (1000 ppm K) causes the lower boundary of the adularia stability field to shift toward lower pH. Under the same conditions stated above, with the exception of increased K^+ content (1000 ppm), the inner pH boundary of adularia stability is approximately 5.25. A lowering of temperature to 200°C causes the inner boundary of adularia stability to increase by 0.5 pH units. This corresponds to the temperature dependence of pH. At higher temperatures, the neutral pH value is lowered.

Presence of fresh microcline adjacent to veins hosting only stage 4 mineralization implies that the K^+/H^+ ratio did not change significantly with time. Weak development of vein-related alteration in the Ajax indicates that the ore fluid was in chemical equilibrium with the wallrock. Therefore, minimum pH of Ajax ore fluid is estimated to be 5.5 (300°C). Neutral pH at 300°C is 5.56 (Casadevall and Ohmoto, 1977). Judging from the alkaline nature of alteration and gangue mineralogy, pH might be expected to be higher. As stated above, 5.5 is a minimum value, and actual pH may be higher, depending on the magnitude of the K^+/H^+ ratio. Ore-fluid pH increased slightly with time due to temperature decrease and subtle boiling. Boiling causes a pH increase in the residual fluid and can be responsible for adularia deposition (Romberger, unpub.). Influx of meteoric water (VI.F) following deposition of stage 1 does not appear to have influenced pH of the fluid. Meteoric water had a slightly lower pH initially but had time to equilibrate by wallrock interaction prior to becoming incorporated into the ore fluid.

2. Temperature and pressure

Temperature decrease during mineralization is explained in Chapter VI (VI.C). The ore fluid underwent cooling throughout mineralization. It is not known whether variation in the vertical thermal gradient present during deposition of stages 1 and 3 persisted in stage 4 (VI.F). The bulk of base-metal sulfide deposition occurred within a temperature range of 350 to 250°C. Absence of gold in association with sulfides indicates that gold may have migrated in a different manner than did the base metals. Gold-telluride mineralization occurred in a temperature range of 160 to 105°C.

Pressure conditions during mineralization were essentially hydrostatic. Pressure was sufficiently low to allow CO₂ effervescence to occur throughout the system. Pressure variation was not a significant influence in either base-metal or precious-metal deposition.

3. Salinity

High salinity of stage 1 fluids undoubtedly played an important role during initial scavenging of metals from the melt. The pronounced salinity decrease caused by mixing with meteoric water occurred prior to stage 3 and may have been the principal mechanism of base-metal deposition. Activity of chlorine ion decreases with salinity decrease, causing solubility of metals carried by chloride complex to decrease. Gold-telluride deposition was not influenced by variation in salinity. Following initial decrease prior to deposition of stage 3, salinity of the ore fluids remained constant, averaging slightly over 2.0 wt % eNaCl (VI.D.3).

4. Oxygen fugacity

The oxidation state of sulfur is dependent on oxygen fugacity. Whether sulfur is present as sulfide or sulfate determines its effectiveness as a gold-complexing agent.

Using the oxygen fugacity-pH diagrams (300°C) of Romberger (unpub.) and sulfur fugacity-oxygen fugacity diagrams (300°C) of Casadevall and Ohmoto (1977), estimates of oxygen fugacity can be made using mineral relationships present in the Ajax system. Coexistence of pyrite and pyrrhotite in early stage mineralization places a lower limit on oxygen fugacity of $\log f_{O_2} = -34.0$ to -36.0 . In stage 3, coexistence of pyrite and hematite places the upper limit of oxygen fugacity at -28.4 to -30.0 . Although data are not available for rutile (TiO_2), replacement of pyrite by rutile in stages 3 and 4 indicates increasing oxygen fugacity.

As indicated by the mineral relationships present, the ore fluid became more oxidized in the later stages of mineralization. This is probably due to mixing of magmatic water with oxidized meteoric water in conjunction with the subtle boiling effect. Although sulfides were deposited during stage 4 deposition, sulfate was the dominant form of sulfur and the ore fluid had an oxygen fugacity too high for gold transport as a bisulfide complex (Casadevall and Ohmoto, 1977).

5. Mechanism of gold transport

Lack of experimental data renders any gold-transport mechanism subject to question. Published work regarding gold solubility generally examines gold as a single metal phase. In hydrothermal solution, gold is associated with alkali and base metals, all of which must compete for available transporting complexes. The effect of tellurium, particularly

on solubility of gold-thiocomplexes, may be very important in deposits known to have high tellurium contents, such as the Ajax veins. Previous workers made passing references to the possibility of telluro-gold complexes, but no substantiating experimental work has been reported (Seward, 1973). The work of Marakushev (1977) specifically addressed the importance of tellurium in gold-bearing hydrothermal solutions. According to his study (1977) the presence of tellurium is one of the principal reasons that gold is deposited late in paragenetic sequences.

Metals present in early-stage fluids of the Ajax system were transported initially as chloride complexes. High salinity of stage 1 fluids and the relatively low sulfide content of the Ajax system make chloride complexing the most feasible method of gold and base-metal transport. The temperature, pH, salinity, and oxygen fugacity values of stage 1 fluid are well suited for metal transport as chloride complexes (Henley, 1973; Casadevall and Ohmoto, 1977).

An abrupt decrease in salinity occurred prior to deposition of stage 3 minerals (VI.F). Deposition of base-metal sulfides was caused by decreasing chlorine-ion activity in conjunction with dropping temperature. An increase in pH also may have aided in base-metal precipitation. Transport of base metals and gold by sulfide complexes can not be completely disregarded. However, the changes in salinity and other parameters mentioned above, occurring prior to base-metal deposition, are further evidence in support of base metal transport by chloride complex. The lack of gold in association with base metals implies that gold solubility was not significantly decreased prior to stage 3. It is here that the importance of tellurium in the hydrothermal solution becomes apparent.

The following interpretation is based on the work of Marakushev (1977). Gold has the highest relative affinity for tellurium of any metal. If present in sufficient quantity, tellurium separates gold and silver from the base metals by forming complex migration compounds. Deposition of base metal sulfides causes the $H_2Te: H_2S$ ratio, and consequently, stability of gold-telluride complexes, to increase. This explains the restriction of gold-telluride mineralization to late stages of epithermal parageneses.

In the Ajax, gold-telluride mineralization is restricted to the fourth stage of vein paragenesis. The high solubility of gold-telluride migration complexes allowed gold to remain in solution until decreasing temperature caused deposition of gold-telluride minerals. Association of gold-tellurides with quartz is further evidence that temperature is the principal control on deposition. Quartz solubility is dependent on temperature, and the principal cause of quartz precipitation is decreasing temperature (Romberger, unpub.).

As discussed by Marakushev (1977), the effect of tellurium in ore-forming solutions explains separation of gold-tellurides from base-metal sulfides. The lack of gold in association with stage 2 sulfides illustrates the effectiveness of tellurium complexing in a high-tellurium system such as the Ajax.

CHAPTER VIII

SUMMARY AND CONCLUSIONS

The purpose of this project was to examine in detail the physical and chemical nature of the Ajax vein system. Results and conclusions of this study should serve to elucidate the enigmatic nature of Cripple Creek vein mineralization.

A. General Summary

Mineralization in the Ajax vein system consists of open-space filling in narrow fractures, hosted by Precambrian granite and Tertiary breccia. Although breccia-hosted mineralization is important on the upper mine levels, inaccessibility limited sampling of breccia-hosted veins. No significant structural displacement, either pre- or post-mineral has occurred along the vein-hosting structures. The mineralized zones are quite variable in morphology. Some of the mineralization occurs in relatively wide, sheeted fracture zones, whereas other equally mineralized structures consist of a few narrow, branching fractures. Although five stages of vein mineralization have been recognized, no vein sampled contained all five stages. Content of the veins is dependent on the relative time at which the structure was receptive to ore-forming solutions. Stage 4 mineralization is economically the most important. The presence of well developed euhedral stage 4 quartz, commonly in association with calaverite, implies high grade gold

mineralization. Stage 4 calaverite commonly is present without euhedral quartz and occurs as a replacement of earlier pyrite.

The association of veins with phonolite and less frequently, basalt dikes, is coincidental in nature. However, where high-angle vein-dike intersections occur, downflow ponding of the ore-forming solution may create a volumetrically large mineralized area.

Vertical zoning of precious and base metal assemblages is not apparent. The Au/Ag ratio varies from greater than 20:1 to less than 1:1. Variability in the ratio is dependent on grade with higher Au/Ag ratios corresponding to higher gold values (Table I). No consistent vertical trend in Au/Ag has been recognized. A general increase in base metal values occurs with increasing depth, however, the trend is erratic and difficult to evaluate. A fluid temperature increase initiating at the 2600 level, persists at the 3350 level (Fig. 41) and quite probably continues at depth. Vertical metal zonation as the result of increasing temperature with depth should become apparent if mine development continues. An increase in base metal content and a decrease in Au/Ag ratio are expected with increasing depth. Lack of metal zonation on the upper mine levels may be due to a variation in vertical temperature change that does not allow a consistent metal zonation to develop.

Vein-related alteration in the Ajax system is unusually weak when compared to a "typical" epithermal vein deposit. Principal controls on alteration are, degree of fracturing and relative time at which the hosting structure was opened. The bulk of alteration occurred prior to, and during, first stage mineralization. No correlation exists between degree of alteration and gold tenor. Some of the highest grade veins in the mine exhibit only minor wallrock alteration. The generally weak

development of alteration, even where structures were open prior to Stage 1, implies chemical equilibrium between the altering fluid and wallrock. Vertical alteration zonation is not present in the Ajax system. Lack of zonation is caused by the hypogene nature and constant chemical composition of the early stage altering fluid.

Fluid inclusion analysis of the vein system reveals a complex fluid evolution. High salinity (30-47 wt % eNaCl) stage 1 fluids may have been magmatic in origin. Mixing with meteoric water occurred prior to stage 3 causing a dramatic salinity decrease (0-8.3 wt % eNaCl). Salinity then remained constant through stage 4 deposition. Fluid temperature gradually decreased with time. Cooling of stage 1 fluid was the result of mixing with meteoric water in conjunction with decreasing temperature of the magmatic heat source(s). Fluid temperature decrease from stage 3 (123-350°C) to stage 4 (105-159°C) was again caused by magmatic cooling. In addition to temperature decrease with time, a vertical thermal gradient is present in the vein system (Fig. 41). Temperature variation in stage 3 roughly parallels variation in stage 1. This is an indication that factors influencing the vertical thermal gradient remained unchanged during deposition of stages 1 through 3. From the 3350 level to the 2600 level, homogenization temperatures of stages 1 and 3 decrease, indicating increasing distance from a heat source. Above the 2600 level, temperatures increase and decrease erratically due to increasing proximity of the vein system to the breccia. Intrusive heat sources within the breccia in conjunction with lateral fluid flow, may be causes of the erratic vertical thermal gradient.

CO₂ was present in the fluids of stages 1, 3 and 4. A subtle boiling occurred in fluids of all stages due to the concentration levels of CO₂. Boiling (CO₂ effervescence) was weak and consistent throughout the vein system and did not significantly influence ore deposition. The effect of CO₂ greatly increases the maximum depth at which boiling can occur. Maximum depth at which boiling can occur in stage 4 fluids is 4000 meters (average). The current maximum depth of mining is 1025 meters. Sufficient evidence for geologic reconstruction of the Cripple Creek area has not been recognized. Therefore, the amount of erosion that has occurred since mineralization is unknown. Assuming 500 meters of erosion, current depth of mining is 2500 meters above the base of the estimated boiling level. This is not meant to imply that the Ajax vein system is continuous for 2500 meters below the deepest current level of development. However, the great depth at which boiling may occur implies an unusually large vertical dimension for the Ajax vein system.

Major controls on vein mineral precipitation in the Ajax system were decreases in salinity and temperature. Based on alteration mineral assemblages, pH was estimated to be a minimum of 5.5 in stage 1 fluid, increasing slightly in later stages. The high K⁺/H⁺ ratio present in the Ajax ore fluid influences the stability fields of alteration minerals and makes estimation of pH tenuous. Oxygen fugacity was estimated using mineral relationships of pyrite, pyrrhotite, and hematite. Estimated values for oxygen fugacity ranged from a minimum of log f_{O₂} = -36.0 in stage 1 to a maximum of log f_{O₂} = -28.4 in stage 3. Using the estimated pH and oxygen fugacity in conjunction with salinity, temperature, and pressure data obtained from fluid inclusion analyses, a gold transporting mechanism can be proposed.

In stage 1 fluids, metals were transported as chloride complexes. Upon mixing with meteoric water, chlorine ion activity decreased along with temperature, causing deposition of base metal sulfides. As base metal and gold chloride complexes decomposed, gold remained in solution by forming complexes with tellurium. Sulfide deposition raised the $H_2Te : H_2S$ ratio and subsequently, stability of the gold-tellurium complex increased. Gold remained in solution until decreasing temperature in stage 4 deposited both calaverite and quartz.

B. Metal Source

The hypothesis for a source of metals in the Ajax system is based on geological evidence. No isotopic data regarding source of metals currently exists for the Cripple Creek district.

Lack of sedimentary rocks in the area and the unaltered nature of granite surrounding the complex serve to severely restrict the possibility that rock leaching has supplied metals.

Enrichment of CO_2 in the ore fluids corresponds to the hypothesis of Gittins (1979) who suggests a high CO_2 content is essential to development of a strongly alkaline magma. The high salinity of stage 1 fluid is indicative of a magmatic origin.

The abundance of highly differentiated alkaline intrusive-volcanic rocks in the district indicates prolonged differentiation of a deeper magmatic source. Volatile content of the fluids and the explosive forces associated with early development of the complex are further indications of an alkaline magma association. Although alkaline rocks tend to have low relative gold abundances (Boyle, 1979), some workers report enrichment in gold as potassium content in rocks increases by differentiation (Volarovich and Shilin, 1971). The high chlorine ion

content of early stage Ajax ore fluid provides an excellent mechanism for metal scavenging from the melt.

While not conclusive without isotopic data, evidence suggests a magmatic source for the ore-forming components of the Ajax vein system.

C. Recommendations for Exploration

Lack of zoning, vertically continuous boiling, and occurrence of high grade gold-telluride mineralization on the deepest level developed, indicate the Ajax vein system is continuous below levels currently being mined. Vertical continuity of the system may be limited by increasing temperature of vein deposition. The trend observed in fluid inclusion results (Fig. 41) from the 2600 level to the 3350 level indicates increasing proximity to a heat source. If this trend continues, an increase in base metals and a decrease in precious metal values can be expected. Other mines in the district not so deeply developed as the Ajax possibly contain vertically continuous veins. Exploration for vein targets should be concentrated near major shear zones and in mines that closed due to flooding prior to construction of the Carlton tunnel.

The possibility for lower grade, higher tonnage, disseminated mineralization exists in the "sediments" and fine grained breccias of the district and merits investigation. Exploration for disseminated mineralization should be concentrated in areas adjacent to vein systems that may have served as feeders.

Negative magnetic and gravity anomalies have been identified two miles northwest of the Golden Cycle mine (Kleinkopf, et al., 1970). Geophysical response of this unexplored area is similar to the response

over the central complex. This area may be a blind "breccia pipe" offshoot from the main complex.

D. Recommended Reading

Telluride-dominated vein systems associated with Tertiary volcanism are scarce. However, interesting similarities exist between Cripple Creek and some deposits of the Philippines and Fiji. Common features to both include: explosion-intrusion breccias -- commonly with evidence of convection, predominately vein-hosted mineralization, close spatial relationship to intrusive rocks, evidence of magmatic differentiation, and occurrence of gold tellurides. Deposits of interest in the Philippines are the Acupan and Antamok mines (Callow and Worley, 1965; Sawkins, O'Neil, and Thompson, 1979). In Fiji, mines of the Vatukoula township are of interest (Denholm, 1967).

REFERENCES

- Berry, L.G., (ed.), 1974, Selected powder diffraction data for minerals, joint committee on powder diffraction standards, pub. DBM-1-23, Swarthmore, Pennsylvania.
- Bodnar, R.J., and Kuehn, C.A., 1982, Effect of dissolved CO₂ on the estimated depths of formation of epithermal gold-silver deposits as calculated from fluid inclusion data: unpublished, 49 p.
- Bonorino, F.G., 1959, Hydrothermal alteration in the Front Range mineral belt, Colorado: Geol. Soc. America Bull., v. 70, p. 53-90.
- Boyle, R.W., 1969, Discussion: Hydrothermal transport and deposition of gold: Econ. Geol., v. 64, p. 112-113.
- _____, 1979, The geochemistry of gold and its deposits: Canada Geol. Survey, Bull. 280, 584 p.
- Bryner, L., 1969, Ore deposits of the Philippines -- an introduction to their geology: Econ. Geol., v. 64, p. 644-666.
- Buchanan, L.G., 1980, Ore controls of vertically stacked deposits, Guanajuato, Mexico: A.I.M.E. preprint 80-82, SME-AIME meeting Las Vegas, Feb., 1980, 26 p.
- _____, 1981, Precious metal deposits associated with volcanic environments in the southwest: in, Relations of Tectonics to Ore Deposits: Arizona Geol. Soc. Digest, v. XIV, p. 237-262.
- Callow, K.J., and Worley, B.W., 1965, The occurrence of telluride minerals at the Acupan gold mine, Mountain province, Philippines: Econ. Geol., v. 60, p. 251-268.
- Casadevall, T., and Ohmoto, H., 1977, Sunnyside mine, Eureka mining district, San Juan County, Colorado: Geochemistry of gold and base metal ore deposition in a volcanic environment: Econ. Geol., v. 72, p. 1285-1320.
- Chapin, C.E., and Epis, R.C., 1964, Some stratigraphic and structural features of the Thirtynine mile volcanic field, central Colorado: The Mountain Geologist, v. 1, p. 145-160.
- Colburn, E.A., Jr., 1913a, Replacement deposits in the Ajax mine: Eng. and Min. Jour., v. 95, p. 739-741.

- _____, 1913b, Influence of a flat dike on ore formation: Eng. and Min. Jour., v. 96, p. 599-600.
- Collins, P.L.F., 1979, Gas hydrates in CO₂-bearing fluid inclusions and the use of freezing data for estimation of salinity: Econ. Geol., v. 74, p. 1435-1444.
- Cross, W., and Penrose, R.A.F., Jr., 1895, Sixteenth Annual Report, U.S. Geol. Surv., Part II, p. 1-207.
- Denholm, L.S., 1967, Lode structures and ore shoots at Vatukoula, Fiji: Proc. Australasian Inst. Mining and Met., no. 222, p. 73-84.
- Erwood, R.J., Keslar, S.E., Cloke, P.L., 1979, Compositionally distinct, saline hydrothermal solutions, Naica mine, Chihuahua, Mexico: Econ. Geol., v. 74, p. 95-108.
- Fisher, J.R., 1976, The volumetric properties of H₂O -- a graphical portrayal: U.S. Geol. Surv. J. Res., no. 4, p. 189-193.
- Gittins, J. 1979, The feldspathoidal alkaline rocks, in, The evolution of the igneous rocks: Fiftieth anniversary perspectives, Princeton, Princeton Univ. Press, p. 352-389.
- Gott, G.B., McCarthy, J.H., Van Sickle, G.H., Jr., and McHugh, J.B., 1967, Distribution of gold and other metals in the Cripple Creek district, Colorado: U.S. Geol. Surv. Prof. Paper 625A, p. A1-A17.
- Graton, L.G., 1905, Consanguinity in the eruptive rocks of Cripple Creek: Science, v. 21, 1905, p. 391.
- Haas, J.L., Jr., 1971, The effect of salinity on the maximum thermal gradient of a hydrothermal system at hydrostatic pressure: Econ. Geol., v. 66, p. 940-946.
- Heinrich, E.W., and Levinson, A.A., 1955, Studies in the mica group; X-ray data on roscoelite and barium-muscovite: American Jour. of Sci., v. 253, p. 39-43.
- Helgeson, H.C., and Garrels, R.M., 1968, Hydrothermal transport and deposition of gold: Econ. Geol., v. 63, p. 622-635.
- Hemley, J.J., and Jones, W.R., 1964, Chemical aspects of hydrothermal alteration with emphasis on hydrogen metasomatism: Econ. Geol., v. 59, p. 538-569.
- Henderson, C.W., 1926, Mining in Colorado: A history of discovery, development, and production: U.S. Geol. Surv. Prof. Paper 138, p. 56-60.
- Henley, R.W., 1973, Solubility of gold in hydrothermal chloride solutions: Chem. Geol., v. 11, p. 73-87.

- Kamilli, R.J., and Ohmoto, H., 1977, Paragenesis, zoning, fluid inclusion, and isotopic studies of the Finlandia vein, Colquib district, central Peru: *Econ. Geol.*, v. 72, p. 950-982.
- Kelly, W.C., and Goddard, E.N., 1969, Telluride ores of Boulder County, Colorado: *Geol. Soc. America Mem.* 109, 237 p.
- Kleinkopf, M.D., Peterson, D.L., and Gott, G., 1970, Geophysical studies of the Cripple Creek mining district, Colorado: *Geophysics*, v. 35, p. 490-500.
- Koschmann, A.H., 1949, Structural control of the gold deposits of the Cripple Creek district, Teller County, Colorado: *U.S. Geol. Surv. Bull.* 955-B, p. 19-58.
- Krauskopf, K.B., 1951, The solubility of gold: *Econ. Geol.*, v. 46, p. 858-870.
- Lane, C.A., 1976, Geology, mineralogy, and fluid inclusion geothermometry of the El Paso gold mine, Cripple Creek, Colorado: Unpub. M.Sc. thesis, Univ. of Missouri-Rolla, 103 p.
- Lindgren, W., and Ransome, R.I., 1906, Geology and gold deposits of the Cripple Creek district, Colorado: *U.S. Geol. Surv. Prof. Paper* 54, 516 p.
- Loughlin, G.F., 1927, Ore at deep levels in the Cripple Creek district, Colorado: *American Inst. of Mining and Met. Eng.*, Tech. Pub. no. 13, 32 p.
- _____, and Koschmann, A.H., 1935, Geology of the ore deposits of the Cripple Creek district, Colorado: *Colo. Scientific Soc. Proc.*, v. 13, no. 6, p. 217-435.
- _____, Koschmann, A.H., Tunell, G., and Kasnda, C.J.A., 1940, Paragenetic study of hypogene gold and silver telluride ores of Cripple Creek, Colorado, (abs.): *Pan American Geologist*, v. 74, p. 36-37.
- Lovering, T.S., and Goddard, E.N., 1950, Geology and ore deposits of the Front Range, Colorado: *U.S. Geol. Surv. Prof. Paper* 223, 319 p.
- Marakushev, A.A., 1977, Geochemical properties of gold and conditions of its endogenic concentration: *Min. Dep.*, v. 12, p. 123-141.
- Mayo, E.B., 1976, after Cloos, H., 1941, Intrusive fragmental rocks directly or indirectly of igneous origin: in, *Tectonic Digest: Arizona Geol. Soc. Digest*, v. X, p. 347-430.
- McDowell, F.W., 1971, and Obradovich, J.D., 1973, age date information; in, 1974 *Isochron/west*, no. 11, 41 p.

- Nash, J.T., 1976, Fluid inclusion petrology -- data from porphyry copper deposits and applications to exploration: U.S. Geol. Surv. Prof. Paper 907-D, 16 p.
- Ramdohr, P., 1980, The Ore Minerals and Their Intergrowths, 2nd. ed., Pergamon Press Ltd., Elmsford, New York, v. 2, p. 801.
- Rickard, T.A., 1899-1900, The Cripple Creek gold field: Inst. of Min. and Met. (London), Transactions, v. 8, p. 49-111.
- _____, 1902, The Lodes of Cripple Creek: A.I.M.E. Trans., v. 33, p. 579-618.
- Roedder, E., 1962, Studies of fluid inclusions I: Low temperature application of a dual-purpose freezing and heating stage: Econ. Geol., v. 57, p. 1045-1061.
- _____, 1963, Studies of fluid inclusions II: Freezing data and their interpretation: Econ. Geol., v. 58, p. 167-211.
- _____, 1967, Fluid inclusions as samples of ore fluids; in, Barnes, H.L., ed., Geochemistry of hydrothermal ore deposits: New York, Holt, Rinehart, and Winston, p. 515-574.
- _____, 1972, Composition of fluid inclusions: U.S. Geol. Surv. Prof. Paper 440 JJ, 178 p.
- _____, 1979, Fluid inclusions as samples of ore fluids; in, Barnes, H.L., ed., Geochemistry of hydrothermal ore deposits, 2nd ed.: New York, Wiley-Interscience, p. 684-737.
- _____, 1982, Fluid inclusion evidence bearing on the environments of gold deposition: unpublished, 68 p.
- _____, and Bodnar, R.J., 1980, Geologic pressure determinations from fluid inclusion studies: Ann. Rev. Earth Planet. Sci., v. 8, p. 263-301.
- Romberger, S.B., 1982, Geology and geochemistry of precious metal deposits: unpublished short course notes, 128 p.
- Rose, A.W., and Burt, D.M., 1979, Hydrothermal alteration; in, Barnes, H.L., ed., Geochemistry of hydrothermal ore deposits, 2nd ed.: New York, Wiley-Interscience, p. 173-235.
- Sawkins, F.J., O'Neil, J.R., and Thompson, J.M., 1979, Fluid inclusion and geochemical studies of the Baguio district, Philippines: Econ. Geol., v. 74, p. 1420-1434.
- Seward, T.M., 1973, Thiocomplexes of gold and the transport of gold in hydrothermal ore solutions: Geochim. Cosmochim. A., v. 37, p. 379-399.

- Tweto, O., 1979, The Rio Grande rift system in Colorado; in, Rieker, R.I., ed: Rio Grande Rift: Tectonics and Magmatism: American Geophysical Union, Washington, D.C., p. 33-56.
- U.S. Bureau of Mines, 1934-1979, Minerals yearbook: Washington, D.C.
- Uytenbogaardt, W. and Burke, E.A.J., 1971, Tables for Microscopic Identification of Ore Minerals: Elsevier Publishing Co., New York, 430 p.
- Volarovich, G.P., and Shilin, N.G., 1971, Gold behavior during crystallization of granitoid magma on the example of miocene gabbro-granodiorite formation in central Kamchatka: Int. Geochem. Congr., Moscow, USSR, Abstracts of Reports II, p. 664-665.
- Weast, R.C., ed., 1981-1982, CRC Handbook of Chemistry and Physics, 62nd ed.: CRC Press Inc., Boca Raton, Florida.
- Weissburg, B.G., 1970, Solubility of gold in hydrothermal alkaline sulfide solutions: Econ. Geol. v. 65, p. 551-556.